FUNCTIONAL ANALYSIS OF LIVER RECEPTOR HOMOLOG-1 AND

FARNESOID X RECEPTOR IN ENTEROHEPATIC PHYSIOLOGY

APPROVED BY SUPERVISORY COMMITTEE

Steven A. Kliewer, Ph.D.

Robert E. Hammer, Ph.D.

David W. Russell, Ph.D.

Raymond J. MacDonald, Ph.D.

Dedicated to My Family

FUNCTIONAL ANALYSIS OF LIVER RECEPTOR HOMOLOG-1 AND

FARNESOID X RECEPTOR IN ENTEROHEPATIC PHYSIOLOGY

by

YOUN-KYOUNG LEE

DISSERTATION

Presented to the Faculty of the Graduate School of Biomedical Sciences

The University of Texas Southwestern Medical Center at Dallas

In Partial Fulfillment of the Requirements

For the Degree of

DOCTOR OF PHILOSOPHY

The University of Texas Southwestern Medical Center at Dallas

Dallas, Texas

March 2008

ACKNOWLEDGEMENTS

brother, Dong-Min. I really doubt I could have accomplished my Ph.D. without their

endless love and support.

FUNCTIONAL ANALYSIS OF LIVER RECEPTOR HOMOLOG-1 AND FARNESOID X RECEPTOR IN ENTEROHEPATIC PHYSIOLOGY

Youn-Kyoung Lee, Ph.D.

The University of Texas Southwestern Medical Center at Dallas, 2008

Supervising Professor: **Steven A. Kliewer, Ph.D.**

Liver receptor homolog-1 (LRH-1), an orphan nuclear receptor, and farnesoid X receptor (FXR), a bile acid receptor, are both highly expressed in liver and intestine, where they regulate bile acid homeostasis. To gain further insight into their biological actions, we investigated their function *in vivo* using gain-of-function and loss-of-function strategies. For LRH-1, three different experimental approaches were used. First, we generated and analyzed mice deficient for LRH-1 in either hepatocytes or intestinal epithelium. These tissue-specific knockout mice had altered expression of a large number of genes involved in bile acid metabolism. Furthermore, there was a marked

change in the composition of the bile acid pool in mice lacking LRH-1 in hepatocytes. In a second experimental approach, a constitutively-active form of LRH-1 (VP16LRH-1) was expressed in the intestine of transgenic mice. The intestines of these mice were profoundly enlarged due to alterations in pathways controlling proliferation and apoptosis. In a third experimental approach, the effect of LRH-1 on early developmental decisions was examined in *Xenopus laevis*. In animal cap explant assays, LRH-1 induced early molecular markers of endoderm differentiation. Taken together, the *Xenopus laevis* and mouse studies reveal the diverse roles that LRH-1 plays during development and in adult physiology, including effects on endoderm formation, intestinal proliferation, and bile acid homeostasis.

FXR regulates bile acid homeostasis through actions in both liver and intestine. In studies designed to probe for additional actions, we found that FXR has an important role in preventing the overgrowth of bacteria in the small intestine.

In summary, these studies reveal the diverse processes regulated by the nuclear receptors LRH-1 and FXR and their profound impact on enterohepatic physiology.

TABLE OF CONTENTS

CHAPTER 1. Nuclear Hormone Receptors

CHAPTER 2. Liver Receptor Homolog-1 and Farnesoid X Receptor

CHAPTER 3. LRH-1 in Bile Acid Homeostasis

PRIOR PUBLICATIONS

Xu BE, Stippec S, Lenertz L, Lee BH, Zhang W, **Lee YK**, and Cobb MH. (2004) WNK1 activates ERK5 by an MEKK2/3-dependent mechanism. *J. Biol. Chem.* 279: 7826-7831

Inagaki T, Moschetta A, **Lee YK**, Peng L, Zhao G, Downes M, Yu RT, Shelton JM, Richardson JA, Repa JJ, Mangelsdorf DJ, and Kliewer SA. (2006) Regulation of antibacterial defense in the small intestine by the nuclear bile acid receptor. *Proc Natl Acad Sci* 103: 3920-3925.

Lee YK, Schmidt DR, Cummins CL, Choi M, Peng L, Zhang Y, Goodwin B, Hammer RE, Mangelsdorf DJ, and Kliewer SA. (2008) Liver Receptor Homolog-1 Regulates Bile Acid Homeostasis But is Not Essential for Feedback Regulation of Bile Acid Synthesis. *Mol Endo* (In press)

LIST OF FIGURES

LIST OF TABLES

LIST OF ABBREVIATIOINS

ABC	ATP-Binding Cassette transporter
AFP	a1-Fetoprotein
APAF1	Apoptotic Peptidase Activating Factor 1
ASBT	Apical Sodium-dependant Bile acid Transporter
BDL	Bile Duct Ligation
BSEP	Bile Salt Export pump
CA	Cholic Acid
CAR	Constitutive Adrostane Receptor
CDCA	Chenodeoxycholic Acid
ChIP	Chromatin Immunoprecipitation
CYP	Cytochrome P450
CYP7A1	Cholesterol 7a-hydroxylase
CYP8B1	Sterol 12a-hydroxylase
DBD	DNA Binding Domain
DCA	Deoxycholic Acid
EMSA	Electrophoretic Mobility Shift Assay
FXR	Farnesoid X receptor
HMG-CoA Red	β-hydroxy-β-methylglutaryl-CoA reductase
HMG-CoA Syn	β-hydroxy-β-methylglutaryl-CoA synthase
HNF1	Hepatic Nuclear Factor 1

HNF4	Hepatocyte Nuclear Factor 4
HRE	Hormone Response Element
IBABP	Ileal Bile Acid Binding Protein
IR1	Inverted Repeat with one nucleotide spacer
LBD	Ligand Binding Domain
LC/MS	Liquid Chromatography Mass Spectrometry
LCA	Lithocholic Acid
LRH-1	Liver Receptor Homolog 1
LXR	Liver X Receptor
Ly6D	Lymphocyte Antigen 6 complex D
m/z	Mass/Charge
N-CoR	Nuclear receptor Co-Repressor
NTCP	Sodium Taurocholate Cotransporter
OSTα/β	Organic Solute Transporters
PPAR	Peroxisome Proliferator-Activated Receptor
PTTG1	Pituitary Tumor-Transforming 1
PXR	Pregnane X Receptor
RDH1	Retinol Dehydrogenase 1
RORα/β	Retinoid-related Orphan Receptors
RT-qPCR	Real-Time quantitative PCR
RXR	Retinoid X Receptor
SHP	Small Heterodimer Partner

SMAD	Sma and Mad Related Proteins
SMRT	Silencing Mediator for RARs and TRs
SR-BI	Scavenger Receptor class B type I
SRC	Steroid Receptor Coactivators
StAR	Steroidogenic Acute Regulatory protein
TERT	Telomerase Reverse Transcriptase
TOR	Target of Rapamycin

CHAPTER 1

NUCLEAR HORMONE RECEPTORS

1.1 Classification of Nuclear Hormone Receptors

Nuclear hormone receptors are members of a large superfamily of ligand-regulated transcription factors. Since the first family member—the glucocorticoid receptor—was cloned in 1988 (Giguere et al., 1988), there has been a vigorous search for new nuclear hormone receptors and their ligands. This search has been driven by the crucial roles the nuclear hormone receptors play in development, homeostasis, and disease. As a consequence of these efforts, we now know that there are 48 nuclear receptors in human and 49 nuclear receptors in mouse. A unified nomenclature system for the nuclear receptors has been established wherein they are classified into seven groups according to a molecular phylogeny comparison (Table 1-1) (Aranda and Pascual, 2001; Laudet, 1997). The nuclear hormone receptors also can be grouped into endocrine receptors, adopted orphan receptors, and orphan receptors based on the identity of their natural ligands and the binding affinity of the ligand for the receptor (Chawla et al., 2001). Androgen receptor (AR), estrogen receptors (ER), progesterone receptor (PR), glucocorticoid receptor (GR), mineralocorticoid receptor (MR), vitamin D receptor (VDR), retinoic acid receptors (RAR), and thyroid hormone receptors (TR) are endocrine receptors that bind to endogenous ligands with high affinity. Adopted orphan receptors include the retinoid X receptors (RXR), liver X receptors (LXR), farnesoid X receptors (FXR), peroxisome proliferator-activated receptors (PPAR), pregnane X

	Receptor	Subtype	Denomination	Ligand	Response Element	Monomer, Homodimer, or Heterodimer
Class I	TR	α, β	Thyroid hormone receptor	Thyroid hormone (T₃)	Pal, DR-4, IP	H
	RAR	α, β, γ	Retinoic acid receptor	Retinoic acid	DR-2, DR-5 Pal, IP	H
	VDR		Vitamin D receptor	1-25(OH)₂ vitamin D₃	DR-3, IP-9	H
	PPAR	α, β, γ	Peroxisome proliferator activated receptor	Benzotriene B4; Wy 14.643 Eicosanoids; thiazolidinediones (TZD₃); 15-deoxy-12,41-prostaglandin J₂; polyunsaturated fatty acids	DR-1	H
	PXR		Pregnane X receptor	Pregnanes; C21 steroids	DR-3	H
	CAR/MB67	α, β	Constitutive androstane receptor	Androstanes; 1,4-bis[2-(3,5-dichloropyridyloxy)]benzene	DR-5	H
	LXR	α, β	Liver X receptor	Oxysterols	DR-4	H
	FXR		Farnesoid X receptor	Bile acids	DR-4, IR-1	H
	RevErb	α, β	Reverse ErbA	Unknown	DR-2, Hemisite	M, D
	RZR/ROR	α, β, γ	Retinoid Z receptor/retinoic acid-related orphan receptor	Unknown	Hemisite	M
	UR		Ubiquitous receptor	Unknown	DR-4	H
Class II	RXR	α, β, γ	Retinoid X receptor	9-Cis-retinoic acid	Pal, DR-1	D
	COUP-TF	α, β, γ	Chicken ovalbumin upstream promoter transcription factor	Unknown	Pal, DR-5	D, H
	HNF-4	α, β, γ	Hepatocyte nuclear factor 4	Fatty acyl-CoA thioesters	DR-1, DR-2	D
	TLX		Tailles-related receptor	Unknown	DR-1, Hemisite	M, D
	PNR		Photoreceptor-specific nuclear receptor	Unknown	DR-1, Hemisite	M, D
	TR2	α, β	Testis receptor	Unknown	DR-1 to DR5	D, H
Class III	GR		Glucocorticoid receptor	Glucocorticoids	Pal	D
	AR		Androgen receptor	Androgens	Pal	D
	PR		Progesterone receptor	Progestins	Pal	D
	ER	α, β	Estrogen receptor	Estradiol	Pal	D
	ERR	α, β, γ	Estrogen-related receptor	Unknown	Pal, Hemisite	M, D
Class IV	NGFI-B	α, β, γ	NGF-induced clone B	Unknown	Pal, DR-5	M, D, H
Class V	SF-1/FTZ-F1	α, β	Steroidogenic factor 1 Fushi Tarazu factor 1	Oxysterols	Hemisite	M
Class VI	GCNF		Germ cell nuclear factor	Unknown	DR-0	D
Class 0	SHP		Small heterodimeric partner	Unknown		H
	DAX-1		Dosage-sensitive sex reversal	Unknown		

Table 1-1. Subfamilies of mammalian nuclear receptor

Evolutionary analysis of the receptors led to a subdivision in six different families. M, monomer; D,homodimer; H, heterodimer; NGF, nerve growth factor; DR, direct repeat; Pal, palindrom; IP, inverted palindrome**.** (Adapted with permission from Aranda, A. and Pascual, A. 2001).

receptor (PXR), and constitutive androstane receptor (AR). Whether other nuclear receptors, such as liver receptor homolog-1 (LRH-1), have endogenous ligands is uncertain, and thus they are designated as orphan receptors (Figure 1-1B).

1.2 Functional Modules and Regulation of Nuclear Hormone Receptors

Nuclear hormone receptors share common structural features. These include a ligand-independent AF-1 transactivation domain in the amino terminus, a centrally-located DNA-binding domain (DBD), and a ligand-binding domain (LBD) that includes a ligand-dependent AF-2 transactivation domain in the carboxy terminus (Figure 1-1A). The highly conserved DBD has two zinc fingers that recognize specific DNA sequences, referred to as hormone response elements containing one or two elements with the consensus sequence AGGTCA. The elements that comprise the HREs for receptors that bind to DNA as dimers can be configured as inverted, everted, or direct repeats with varied spacing between motifs. HREs for receptors that bind to DNA as monomers usually contain an A/T-rich region 5' of the AGGTCA motif (reviewed by (Aranda and Pascual, 2001; Mangelsdorf and Evans, 1995)). The precise sequence and organization of the HRE provides selectivity and specificity for nuclear receptor binding. Most of the nuclear receptors bind to DNA as either heterodimers (e.g., RXRs, PPARs, RARs, VDRs, LXRs, and FXR with RXRs as the common heterodimeric partner) or homodimers (e.g., COUP-TFs, HNF4s, GCNF, TR2, Rev-Erbs, and the steroid hormone receptors), and a few bind to DNA as monomers (e.g., LRH-1, SF-1, NGFI-B, ERRs, RORs, and TLX).

A

NH2 — AF1 | DNA | Ligand | AF2 — COOH

B

Endocrine	Adopted Orphan	Orphan
(Endocrine lipid sensors)	(Dietary & endogenous lipid sensors)	(Endogeous ligands unknown)

Endocrine (Endocrine lipid sensors):

GR	glucocorticoids
MR	mineralocorticoid
PR	progesterone
AR	androgens
ERα,β	estrogens

RARα,β,γ	retinoic acids
TRα,β	thyroid hormone
VDR	vitamin D, LCA

Adopted Orphan (Dietary & endogenous lipid sensors):

RXRα,β,γ	9-cis RA, DHA
PPARα,δ,γ	fatty acids
LXRα,β	oxysterols
FXR	bile acids
PXR	xenobiotics
CAR	xenobiotics

Orphan (Endogeous ligands unknown):

ERRα,β,γ	synthetic steroids
HNF-4α,γ	fatty acids?
RORα,β,γ	fatty acid, sterols?
SF-1	phospholipids?
LRH-1	phospholipids?
GCNF	?
PNR	?
TLX	?
TR2,4	?
NGFI-Bα,β,γ	?
COUP-TFα,β,γ	?
RVRα,β	?
DAX-1	?
SHP	?

Figure 1-1. Nuclear receptor superfamily

(A) Schematic structure of a typical nuclear receptor is shown. **(B)** Depending on the source and type of their ligand, nuclear receptors can be subdivided into three (or four) subgroups. (Adapted with permission from Chawla et al., 2001).

The LBD serves as a molecular switch for nuclear receptors in that ligand binding alters its conformation, causing dissociation from corepressors and recruitment of coactivators. Determining the structures of nuclear receptor LBDs has proven to be important for understanding the molecular basis for their regulation of transcription and for the design of pharmacologically active ligands. X-ray crystallography has revealed that nuclear receptor LBDs have similar structures that include 11-13 α-helices which fold into a three-layer antiparallel sandwich with the ligand-binding site buried within (reviewed by (Li et al., 2003)). The specificity and efficiency of ligand binding are determined by the size and shape of the ligand binding pocket.

The interaction of nuclear receptors with coregulators is crucial for transmitting the hormonal signal to the transcriptional machinery. Corepressors bind to nuclear receptor in their unliganded, basal state and recruit histone deacetylases (Glass and Rosenfeld, 2000). The first corepressors to be characterized, SMRT (Silencing mediator for RARs and TRs) and N-CoR (Nuclear receptor corepressor), were identified by yeast two-hybrid screening. Corepressors are rapidly dissociated from the receptor upon ligand binding, allowing the receptor to interact with a coactivator complex. Upon ligand binding, the AF2 domain in the carboxy terminus of nuclear receptors is stabilized in an active configuration in which it interacts with coactivators through the nuclear receptor binding sequence, LXXLL (Darimont et al., 1998). Coactivators can be divided into two groups: primary coactivators and secondary coactivators. Primary coactivators interact with nuclear receptors directly while secondary coactivators are constituents of multisubunit coactivator complexes (reviewed by (Lonard and O'Malley, 2006). During the past decade, ~300 nuclear receptor coregulators have been reported. These

coregulators function in a dynamic and combinatorial manner to modify chromatin and to recruit the basal transcriptional machinery to the target gene promoter, resulting in gene transcription.

1.3 Nuclear Hormone Receptors, Disease, and Clinical Implication

Nuclear hormone receptors regulate diverse physiological processes including development, metabolism, reproduction, inflammation, and the stress response. For instance, HNF4α was initially identified as a transcription factor required for liver-specific gene expression. It was subsequently shown to be involved in pancreatic β cell development and function. Oxysterols activate LXRs to control cholesterol metabolism, while bile acids activate FXR to control bile acid homeostasis. ERR regulates placental development and lipid metabolism, and DAX is involved in adrenal development and sex determination. PXR and CAR are activated by a variety of xenobiotic compounds including pregnenolone 16α-carbonitrile (PCN) and rifampicin to activate detoxification pathways in the body. ROR is involved in neuronal development and T cell selection. COUP-TFs control neurogenesis, angiogenesis, and heart development. Nurr1 and TLX have important roles in the central nervous system and are potential drug targets for treating neurodegenerative diseases. The biological actions of nuclear receptors are dictated to a large degree by their diverse expression patterns within tissues of the body (Figure 1-2) (Bookout et al., 2006).

The identification of synthetic ligands that are selective for specific nuclear receptors is an area of active research. These ligands are used as tools in the discovery of a variety of signaling pathways and have the potential to be used for the treatment of
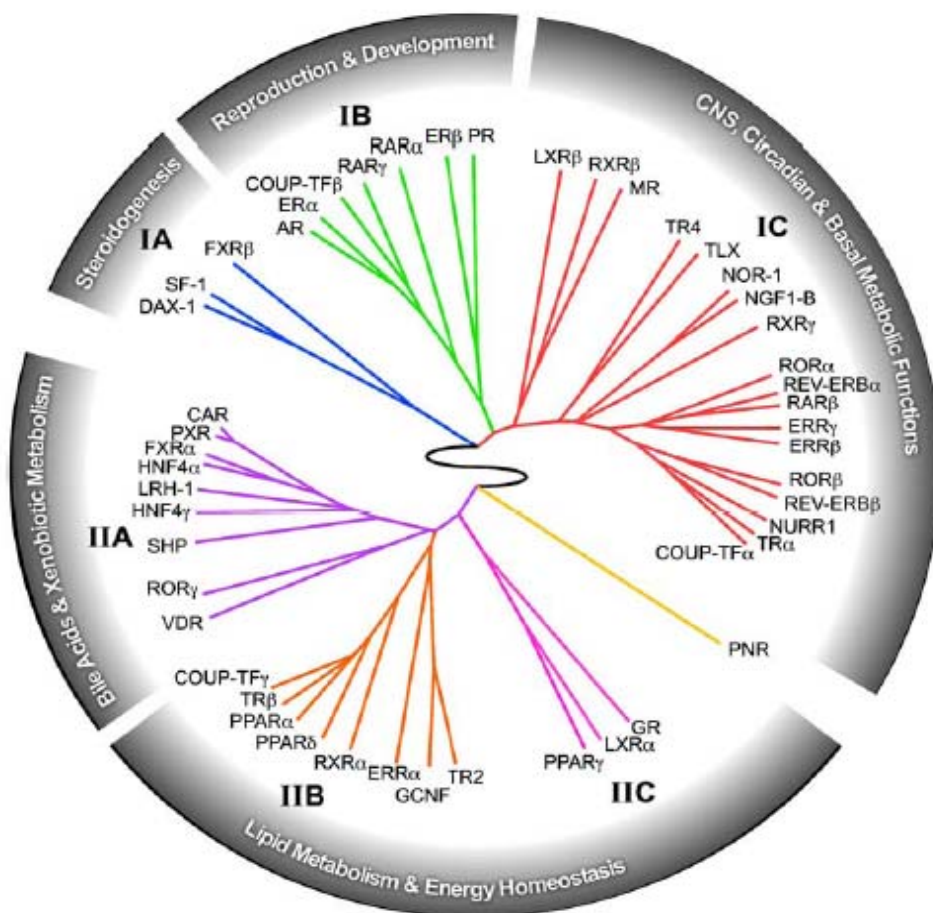
Figure 1-2. The nuclear receptor ring of physiology

From nuclear receptor tissue expression profiling and clustering analysis, the relationship between their expression, function, physiology is depicted as a circular dendrogram. Figure was adapted with permission from Bookout et al., 2006.

human diseases including diabetes, obesity, and neurodegeneration. Since their discovery, the PPARs have received significant attention as potential pharmacologic targets for the treatment of diabetes and obesity because of their important roles in the regulation of adipogenesis, fatty acid utilization, and the inflammatory response. They are activated by both natural ligands such as fatty acids and synthetic ligands such as thiazolidinediones (TZDs), which are widely used to treat type II diabetes. Ligands for other nuclear receptors are also used in the clinic. These include the estrogen receptor antagonist, tamoxifen, which is widely used to treat breast cancer, and retinoids such as 13-cis-retinoic acid, which are used for skin disorders.

1.4 References

Aranda, A., and Pascual, A. (2001). Nuclear hormone receptors and gene expression. Physiol Rev *81*, 1269-1304.

Bookout, A.L., Jeong, Y., Downes, M., Yu, R.T., Evans, R.M., and Mangelsdorf, D.J. (2006). Anatomical profiling of nuclear receptor expression reveals a hierarchical transcriptional network. Cell *126*, 789-799.

Chawla, A., Repa, J.J., Evans, R.M., and Mangelsdorf, D.J. (2001). Nuclear receptors and lipid physiology: opening the X-files. Science *294*, 1866-1870.

Darimont, B.D., Wagner, R.L., Apriletti, J.W., Stallcup, M.R., Kushner, P.J., Baxter, J.D., Fletterick, R.J., and Yamamoto, K.R. (1998). Structure and specificity of nuclear receptor-coactivator interactions. Genes Dev *12*, 3343-3356.

Giguere, V., Yang, N., Segui, P., and Evans, R.M. (1988). Identification of a new class of steroid hormone receptors. Nature *331*, 91-94.

Glass, C.K., and Rosenfeld, M.G. (2000). The coregulator exchange in transcriptional functions of nuclear receptors. Genes Dev *14*, 121-141.

Laudet, V. (1997). Evolution of the nuclear receptor superfamily: early diversification from an ancestral orphan receptor. J Mol Endocrinol *19*, 207-226.

Li, Y., Lambert, M.H., and Xu, H.E. (2003). Activation of nuclear receptors: a perspective from structural genomics. Structure *11*, 741-746.

Lonard, D.M., and O'Malley, B.W. (2006). The expanding cosmos of nuclear receptor coactivators. Cell *125*, 411-414.

Mangelsdorf, D.J., and Evans, R.M. (1995). The RXR heterodimers and orphan receptors. Cell *83*, 841-850.

CHAPTER 2

LIVER RECEPTOR HOMOLOG-1 AND FARNESOID X RECEPTOR

2.1 Introduction to LRH-1

2.1.1 Discovery of LRH-1

Liver receptor homolog-1 (LRH-1; also called NR5A2, α-fetoprotein transcription factor, FTZ-F1-related factor and CYP7A1 promoter binding factor) was isolated by several groups and given different names (Becker-Andre et al., 1993; Galarneau et al., 1996; Li et al., 1998; Nitta et al., 1999). In human, three different isoforms of LRH-1 are present (Zhang et al., 2001a), whereas only two isoforms are present in mouse (Gao et al., 2006). Spatial and temporal differences in the expression of these isoforms suggest that they may have distinct functions that have yet to be defined.

During development in mice, LRH-1 is first detected from E3.5 to E4 in the inner cell mass (ICM) and primitive endoderm of blastocysts and is subsequently expressed from E6.5 to E7 throughout the embryonic and extraembryonic regions, including the visceral endoderm and embryonic ectoderm (Gu et al., 2005). The broad expression pattern of LRH-1 suggests that it influences multiple developmental processes. In the adult, LRH-1 is highly expressed in endoderm-derived tissues such as liver, intestine, and exocrine pancreas, where it is implicated in the regulation of cholesterol and bile acid homeostasis. This receptor also is highly expressed in ovary and testis, suggesting possible roles in the control of reproduction and steroid hormone homeostasis.

2.1.2 Structure and activity of LRH-1

LRH-1 belongs to a nuclear receptor subfamily that includes steroidogenic factor 1 and fushi tarazu factor 1. Members of this subfamily regulate target gene transcription by binding as monomers to DNA response elements with the consensus sequence 5'-PyCAAGGPyCPu-3' (Fayard et al., 2004). It is widely accepted that LRH-1 is a constitutively active receptor whose activity is independent of ligand. This idea was supported by the crystal structure of the mouse LRH-1 LBD (Sablin et al., 2003), which showed the protein to contain a large hydrophobic pocket but to be in an active conformation even in the absence of bound ligand. Furthermore, substitution mutations that filled this pocket did not affect transcriptional activity. Interestingly, however, various phospholipids have been more recently shown to bind in the ligand binding pocket of human LRH-1 (Krylova et al., 2005; Ortlund et al., 2005; Wang et al., 2005b). Although the physiological relevance of these interactions remains uncertain, it has stimulated interest in the possibility that LRH-1 might be a tractable target for drug discovery. As a result, *cis*-bicyclo[3.3.0]-*oct*-2-ene was developed as an agonist of the NR5A receptors LRH-1 and SF-1 (Whitby et al., 2006).

Coregulators play a pivotal role in mediating the effects of nuclear receptors on transcription. Coactivators such as multiprotein bridging factor (MBF1) and steroid receptor coactivators (SRC) interact with LRH-1 with low affinity (reviewed by (Fayard et al., 2004)). Human LRH-1 is suppressed by the prospero-related homeobox transcription factor 1 (Prox1), which interacts with both the LBD and DBD of LRH-1 (Qin et al., 2004). The orphan nuclear receptor SHP also suppresses the transcriptional

activity of LRH-1 through direct interaction with the AF2 domain within the receptor's LBD (Lee and Moore, 2002).

LRH-1 activity is controlled by phosphorylation and sumoylation. Phosphorylation of serine residues 238 and 243 of human LRH-1 by ERK stimulates transactivation (Lee et al., 2006b). Sumoylated LRH-1 is sequestrated into promyelocytic leukemia protein nuclear bodies (PML-NBs) to prevent access to active chromatin domains (Chalkiadaki and Talianidis, 2005).

2.1.3 Physiological roles of LRH-1

LRH-1 regulates the expression of genes involved in early embryonic development including the POU homeodomain transcription factor, OCT4, fibroblast growth factor 4 (FGF4), Sry-related high mobility group box transcription factor 2 (SOX2), undifferentiated embryonic cell transcription factor 1 (UTF1), hepatocyte nuclear factors HNF1α, HNF3β, HNF4α, and α1-fetoprotein (AFP) (Gu et al., 2005; Pare et al., 2001). In addition, *Lrh-1*$^{-/-}$ mice die during early embryogenesis, indicating its important role in early animal development (Pare et al., 2004b).

LRH-1 also is implicated in the regulation of intestinal processes including epithelial cell renewal and the synthesis of glucocorticoids (Botrugno et al., 2004; Mueller et al., 2006). Heterozygous *Lrh-1*$^{+/-}$ mice have decreased epithelial cell proliferation and are susceptible to chemical-induced intestinal inflammation (Coste et al., 2007; Mueller et al., 2006).

LRH-1 is expressed in reproductive organs, where it controls genes including aromatase, which converts testicular androgens into estrogens (Pezzi et al., 2004), and

steroidogenic acute regulatory protein (StAR), which transports cholesterol into the inner mitochondrial membrane to initiate steroidogenesis (Kim et al., 2004). LRH-1 expression in the granulosa cells of the follicle and the corpus luteum in ovary suggests a role for the receptor in ovarian steroidogenesis (Hinshelwood et al., 2003), and its transient expression in germ and Sertoli cells in testes suggests a possible role in gonadal development (Hinshelwood et al., 2005).

LRH-1 is most studied in the context of reverse cholesterol transport, bile acid synthesis, and enterohepatic circulation. LRH-1 appears to regulate reverse cholesterol transport by controlling the expression of genes such as cholesteryl ester transfer protein (CETP), which remodels high density lipoproteins (HDL), and scavenger receptor type BI (SR-BI), which clears HDL in the liver (reviewed by (Fayard et al., 2004)). LRH-1 also is implicated in stimulating the basal expression of cholesterol 7α-hydroxylase (CYP7A1) and sterol 12α-hydroxylase (CYP8B1), which are key enzymes for bile acid biosynthesis, and in repressing their expression as part of the nuclear bile acid receptor (FXR)-small heterodimer partner (SHP) signaling cascade. Bile acids do not efficiently cross cell membranes on their own but are instead actively moved by protein transporters. *In vitro* studies suggest that LRH-1 regulates the transcription of several genes encoding bile acid transporters including the apical sodium-dependent bile acid transporter (ASBT) and the organic solute transporters (OSTα and β). LRH-1 also induces transcription of the genes encoding the cholesterol transporters ABCG5 and ABCG8.

2.2 Introduction to FXR

2.2.1 Discovery of FXR

Farnesoid X receptor (FXR; NR1H4) was first isolated from a rat liver cDNA library (Forman et al., 1995; Seol et al., 1995) and subsequently shown to serve as a bile acid senor. A related receptor, referred to as FXRβ, was identified later and shown to be activated by lanosterol, a precursor of cholesterol (Otte et al., 2003). FXR is mainly expressed in the liver, intestine, kidney, adrenals, and adipose tissue. There are four FXRα splice variants, although the physiological relevance of the isoforms remains to be determined (Figure 2-1A and B) (Huber et al., 2002).

2.2.2 Structure and activity of FXR

Like other nuclear receptors, FXR has a DBD and LBD. FXR binds to DNA as an RXR heterodimer and prefers HREs comprised of two hexanucleotide AGGTCA repeats organized in an inverted fashion and spaced by one nucleotide (IR1) (Figure 2-1C). The FXR/RXR heterodimer is activated by ligands for either FXR or RXR. There may be species differences in the bile acids that activate FXR: whereas cholic acid and its conjugated derivatives appear to be the most important FXR ligands in mice, chenodeoxycholic acid and its derivatives are likely to be the primary FXR agonists in humans (Cui et al., 2002). Several potent, synthetic FXR ligands have been identified including GW4064 (Maloney et al., 2000) and fexaramine (Downes et al., 2003). The binding of these agonists to FXR stabilizes the receptor and promotes recruitment of coactivators including steroid receptor coactivatoer-1 (SRC-1), PPARγ coactivator-1α (PGC-1α), protein arginine methyl transferase-1 (PRMT-1), coactivator-associated
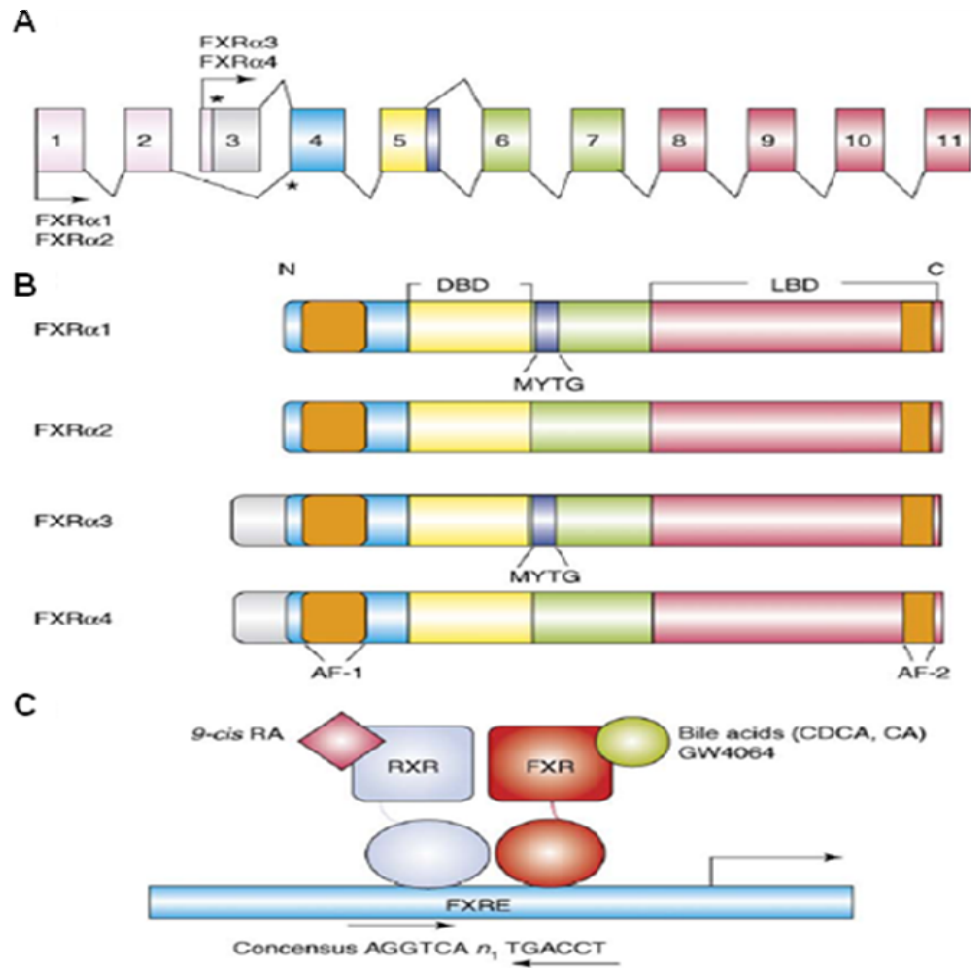
(Lee et al., 2006)

Figure 2-1. Genomic organization and protein isoforms of FXRα

(A) Structure of the human and mouse *Fxrα* gene. Two functional promoters are indicated. (B) The four FXR protein isoforms with the different domains color-coded. (C) FXR binds to response element (IR1) as a heterodimer with RXR. Figure was adapted with permission from Lee et al., 2006.

arginine methyl transferase-1 (CARM-1), and VDR-interacting protein-205 (DRIP-205) (reviewed by (Pellicciari et al., 2005)).

2.2.3 Physiological roles of FXR

Bile acids repress their synthesis via a negative feedback regulatory loop wherein transcription of the gene encoding cholesterol 7a-hydroxylase (CYP7A1), the first and rate-limiting step in the classic pathway for bile acid synthesis, is repressed. FXR regulates this process in two different ways. First, FXR induces expression of SHP, an atypical orphan nuclear receptor lacking a DNA binding domain that functions as a strong transcriptional repressor through interactions with other nuclear receptors and transcription factors (Seol et al., 1996). SHP, in turn, is recruited to the CYP7A1 promoter, where it represses gene transcription. In a second pathway, FXR induces transcription of the FGF15 gene in the small intestine. FGF15 is a hormone that cooperates with SHP in the liver to repress CYP7A1 through a mechanism that is not yet clearly defined (Inagaki et al., 2005). In addition to regulating this feedback mechanism, FXR also regulates the expression of a number of bile acids transporters including BSEP, NTCP, MRP2, ASBT, OSTα, and OSTβ (reviewed by (Lee et al., 2006a)).

Studies of $Fxr^{-/-}$ mice have demonstrated that FXR controls several metabolic pathways (Kok et al., 2003; Sinal et al., 2000). $Fxr^{-/-}$ mice have increased plasma triglycerides and cholesterol, especially high-density lipoprotein (HDL) cholesterol. Consistent with this observation, genes encoding apolipoproteins (ApoAI, ApoCII, and ApoCIII), PLTP, and SR-BI are dysregulated in $Fxr^{-/-}$ mice.

Several studies suggest that FXR regulates glucose metabolism. First, in the *db/db* diabetic mouse model, activated FXR lowers glucose and increases insulin sensitivity (Zhang et al., 2006). Second, $Fxr^{-/-}$ mice exhibit impaired glucose tolerance and blunted insulin signaling in skeletal muscle and liver (Ma et al., 2006). In both studies, hepatic expression of phosphoenolpyruvate carboxykinase (PEPCK) and glucose-6-phosphatase was reduced by FXR activation.

In addition to metabolic functions, FXR also plays a role in hepatoprotection and liver regeneration. Liu *et al.* demonstrated that activation of FXR by GW4064 protects against cholestatic liver damage (Liu et al., 2003), and Huang *et al.* showed that cholic acid promotes liver regeneration in wild type mice but not $Fxr^{-/-}$ mice that have undergone partial hepatectomy (Huang et al., 2006).

2.3 Description of research in thesis

This dissertation addresses several important questions regarding the biological actions of LRH-1 and FXR. The first is the role of LRH-1 in regulating bile acid homeostasis. Based on *in vitro* studies and *in vivo* experiments with either LRH-1 overexpression or $Lrh-1^{+/-}$ heterozygous mice, it was proposed that LRH-1 regulates genes involved in bile acid homeostasis and contributes to the feedback regulation of CYP7A1 and CYP8B1 via the FXR-SHP-LRH-1 cascade, however, the consequences of eliminating LRH-1 had not been evaluated *in vivo* because of the early embryonic lethality of $Lrh-1^{-/-}$ mice. The second is the function of LRH-1 in the intestine. Although LRH-1 has been shown to affect the proliferative capacity of the intestine, the mechanism underlying this effect was unknown. The third question is the role of LRH-1 in endoderm

formation. While LRH-1 deficient mice die during early development and LRH-1 regulates genes involved in endoderm differentiation, no direct evidence has been provided that LRH-1 regulates endoderm formation. Finally, FXR is highly expressed in intestine, where it regulates genes involved in bile acids homeostasis. However, it remained unclear what other processes might be affected by FXR in intestine.

In Chapter 3, the role of LRH-1 in bile acid homeostasis is examined using mice deficient for LRH-1 in either intestine or liver.

In Chapter 4, LRH-1 function in intestine is studied using transgenic mice selectively expressing a constitutively active form of the receptor (VP16LRH-1) in intestinal epithelium.

In Chapter 5, the role of LRH-1 in endoderm formation is examined using the *Xenopus* model system.

Chapter 6 presents the antibacterial actions of FXR in the small intestine.

2.4 References

Aranda, A., and Pascual, A. (2001). Nuclear hormone receptors and gene expression. Physiol Rev *81*, 1269-1304.

Becker-Andre, M., Andre, E., and DeLamarter, J.F. (1993). Identification of nuclear receptor mRNAs by RT-PCR amplification of conserved zinc-finger motif sequences. Biochem Biophys Res Commun *194*, 1371-1379.

Bookout, A.L., Jeong, Y., Downes, M., Yu, R.T., Evans, R.M., and Mangelsdorf, D.J. (2006). Anatomical profiling of nuclear receptor expression reveals a hierarchical transcriptional network. Cell *126*, 789-799.

Botrugno, O.A., Fayard, E., Annicotte, J.S., Haby, C., Brennan, T., Wendling, O., Tanaka, T., Kodama, T., Thomas, W., Auwerx, J.*, et al.* (2004). Synergy between LRH-1 and beta-catenin induces G1 cyclin-mediated cell proliferation. Mol Cell *15*, 499-509.

Chalkiadaki, A., and Talianidis, I. (2005). SUMO-dependent compartmentalization in promyelocytic leukemia protein nuclear bodies prevents the access of LRH-1 to chromatin. Mol Cell Biol *25*, 5095-5105.

Chawla, A., Repa, J.J., Evans, R.M., and Mangelsdorf, D.J. (2001). Nuclear receptors and lipid physiology: opening the X-files. Science *294*, 1866-1870.

Coste, A., Dubuquoy, L., Barnouin, R., Annicotte, J.S., Magnier, B., Notti, M., Corazza, N., Antal, M.C., Metzger, D., Desreumaux, P.*, et al.* (2007). LRH-1-mediated glucocorticoid synthesis in enterocytes protects against inflammatory bowel disease. Proc Natl Acad Sci U S A *104*, 13098-13103.

Cui, J., Heard, T.S., Yu, J., Lo, J.L., Huang, L., Li, Y., Schaeffer, J.M., and Wright, S.D. (2002). The amino acid residues asparagine 354 and isoleucine 372 of human farnesoid X receptor confer the receptor with high sensitivity to chenodeoxycholate. J Biol Chem *277*, 25963-25969.

Darimont, B.D., Wagner, R.L., Apriletti, J.W., Stallcup, M.R., Kushner, P.J., Baxter, J.D., Fletterick, R.J., and Yamamoto, K.R. (1998). Structure and specificity of nuclear receptor-coactivator interactions. Genes Dev *12*, 3343-3356.

Downes, M., Verdecia, M.A., Roecker, A.J., Hughes, R., Hogenesch, J.B., Kast-Woelbern, H.R., Bowman, M.E., Ferrer, J.L., Anisfeld, A.M., Edwards, P.A.*, et al.* (2003). A chemical, genetic, and structural analysis of the nuclear bile acid receptor FXR. Mol Cell *11*, 1079-1092.

Fayard, E., Auwerx, J., and Schoonjans, K. (2004). LRH-1: an orphan nuclear receptor involved in development, metabolism and steroidogenesis. Trends Cell Biol *14*, 250-260.

Forman, B.M., Goode, E., Chen, J., Oro, A.E., Bradley, D.J., Perlmann, T., Noonan, D.J., Burka, L.T., McMorris, T., Lamph, W.W.*, et al.* (1995). Identification of a nuclear receptor that is activated by farnesol metabolites. Cell *81*, 687-693.

Galarneau, L., Pare, J.F., Allard, D., Hamel, D., Levesque, L., Tugwood, J.D., Green, S., and Belanger, L. (1996). The alpha1-fetoprotein locus is activated by a nuclear receptor of the Drosophila FTZ-F1 family. Mol Cell Biol *16*, 3853-3865.

Gao, D.M., Wang, L.F., Liu, J., Kong, Y.Y., Wang, Y., and Xie, Y.H. (2006). Expression of mouse liver receptor homologue 1 in embryonic stem cells is directed by a novel promoter. FEBS Lett *580*, 1702-1708.

Giguere, V., Yang, N., Segui, P., and Evans, R.M. (1988). Identification of a new class of steroid hormone receptors. Nature *331*, 91-94.

Glass, C.K., and Rosenfeld, M.G. (2000). The coregulator exchange in transcriptional functions of nuclear receptors. Genes Dev *14*, 121-141.

Gu, P., Goodwin, B., Chung, A.C., Xu, X., Wheeler, D.A., Price, R.R., Galardi, C., Peng, L., Latour, A.M., Koller, B.H.*, et al.* (2005). Orphan nuclear receptor LRH-1 is required to maintain Oct4 expression at the epiblast stage of embryonic development. Mol Cell Biol *25*, 3492-3505.

Hinshelwood, M.M., Repa, J.J., Shelton, J.M., Richardson, J.A., Mangelsdorf, D.J., and Mendelson, C.R. (2003). Expression of LRH-1 and SF-1 in the mouse ovary: localization in different cell types correlates with differing function. Mol Cell Endocrinol *207*, 39-45.

Hinshelwood, M.M., Shelton, J.M., Richardson, J.A., and Mendelson, C.R. (2005). Temporal and spatial expression of liver receptor homologue-1 (LRH-1) during embryogenesis suggests a potential role in gonadal development. Dev Dyn *234*, 159-168.

Huang, W., Ma, K., Zhang, J., Qatanani, M., Cuvillier, J., Liu, J., Dong, B., Huang, X., and Moore, D.D. (2006). Nuclear receptor-dependent bile acid signaling is required for normal liver regeneration. Science *312*, 233-236.

Huber, R.M., Murphy, K., Miao, B., Link, J.R., Cunningham, M.R., Rupar, M.J., Gunyuzlu, P.L., Haws, T.F., Kassam, A., Powell, F.*, et al.* (2002). Generation of multiple farnesoid-X-receptor isoforms through the use of alternative promoters. Gene *290*, 35-43.

Inagaki, T., Choi, M., Moschetta, A., Peng, L., Cummins, C.L., McDonald, J.G., Luo, G., Jones, S.A., Goodwin, B., Richardson, J.A.*, et al.* (2005). Fibroblast growth factor 15 functions as an enterohepatic signal to regulate bile acid homeostasis. Cell Metab *2*, 217-225.

Kim, J.W., Peng, N., Rainey, W.E., Carr, B.R., and Attia, G.R. (2004). Liver receptor homolog-1 regulates the expression of steroidogenic acute regulatory protein in human granulosa cells. J Clin Endocrinol Metab *89*, 3042-3047.

Kok, T., Hulzebos, C.V., Wolters, H., Havinga, R., Agellon, L.B., Stellaard, F., Shan, B., Schwarz, M., and Kuipers, F. (2003). Enterohepatic circulation of bile salts in farnesoid X receptor-deficient mice: efficient intestinal bile salt absorption in the absence of ileal bile acid-binding protein. J Biol Chem *278*, 41930-41937.

Krylova, I.N., Sablin, E.P., Moore, J., Xu, R.X., Waitt, G.M., MacKay, J.A., Juzumiene, D., Bynum, J.M., Madauss, K., Montana, V.*, et al.* (2005). Structural analyses reveal phosphatidyl inositols as ligands for the NR5 orphan receptors SF-1 and LRH-1. Cell *120*, 343-355.

Laudet, V. (1997). Evolution of the nuclear receptor superfamily: early diversification from an ancestral orphan receptor. J Mol Endocrinol *19*, 207-226.

Lee, F.Y., Lee, H., Hubbert, M.L., Edwards, P.A., and Zhang, Y. (2006a). FXR, a multipurpose nuclear receptor. Trends Biochem Sci *31*, 572-580.

Lee, Y.K., Choi, Y.H., Chua, S., Park, Y.J., and Moore, D.D. (2006b). Phosphorylation of the hinge domain of the nuclear hormone receptor LRH-1 stimulates transactivation. J Biol Chem *281*, 7850-7855.

Lee, Y.K., and Moore, D.D. (2002). Dual mechanisms for repression of the monomeric orphan receptor liver receptor homologous protein-1 by the orphan small heterodimer partner. J Biol Chem *277*, 2463-2467.

Li, M., Xie, Y.H., Kong, Y.Y., Wu, X., Zhu, L., and Wang, Y. (1998). Cloning and characterization of a novel human hepatocyte transcription factor, hB1F, which binds and activates enhancer II of hepatitis B virus. J Biol Chem *273*, 29022-29031.

Li, Y., Lambert, M.H., and Xu, H.E. (2003). Activation of nuclear receptors: a perspective from structural genomics. Structure *11*, 741-746.

Liu, Y., Binz, J., Numerick, M.J., Dennis, S., Luo, G., Desai, B., MacKenzie, K.I., Mansfield, T.A., Kliewer, S.A., Goodwin, B.*, et al.* (2003). Hepatoprotection by the farnesoid X receptor agonist GW4064 in rat models of intra- and extrahepatic cholestasis. J Clin Invest *112*, 1678-1687.

Lonard, D.M., and O'Malley, B.W. (2006). The expanding cosmos of nuclear receptor coactivators. Cell *125*, 411-414.

Ma, K., Saha, P.K., Chan, L., and Moore, D.D. (2006). Farnesoid X receptor is essential for normal glucose homeostasis. J Clin Invest *116*, 1102-1109.

Maloney, P.R., Parks, D.J., Haffner, C.D., Fivush, A.M., Chandra, G., Plunket, K.D., Creech, K.L., Moore, L.B., Wilson, J.G., Lewis, M.C.*, et al.* (2000). Identification of a chemical tool for the orphan nuclear receptor FXR. J Med Chem *43*, 2971-2974.

Mangelsdorf, D.J., and Evans, R.M. (1995). The RXR heterodimers and orphan receptors. Cell *83*, 841-850.

Mueller, M., Cima, I., Noti, M., Fuhrer, A., Jakob, S., Dubuquoy, L., Schoonjans, K., and Brunner, T. (2006). The nuclear receptor LRH-1 critically regulates extra-adrenal glucocorticoid synthesis in the intestine. J Exp Med *203*, 2057-2062.

Nitta, M., Ku, S., Brown, C., Okamoto, A.Y., and Shan, B. (1999). CPF: an orphan nuclear receptor that regulates liver-specific expression of the human cholesterol 7alpha-hydroxylase gene. Proc Natl Acad Sci U S A *96*, 6660-6665.

Ortlund, E.A., Lee, Y., Solomon, I.H., Hager, J.M., Safi, R., Choi, Y., Guan, Z., Tripathy, A., Raetz, C.R., McDonnell, D.P.*, et al.* (2005). Modulation of human nuclear receptor LRH-1 activity by phospholipids and SHP. Nat Struct Mol Biol *12*, 357-363.

Otte, K., Kranz, H., Kober, I., Thompson, P., Hoefer, M., Haubold, B., Remmel, B., Voss, H., Kaiser, C., Albers, M., *et al.* (2003). Identification of farnesoid X receptor beta as a novel mammalian nuclear receptor sensing lanosterol. Mol Cell Biol *23*, 864-872.

Pare, J.F., Malenfant, D., Courtemanche, C., Jacob-Wagner, M., Roy, S., Allard, D., and Belanger, L. (2004). The fetoprotein transcription factor (FTF) gene is essential to embryogenesis and cholesterol homeostasis, and regulated by a DR4 element. J Biol Chem *279*, 21206-21216.

Pare, J.F., Roy, S., Galarneau, L., and Belanger, L. (2001). The mouse fetoprotein transcription factor (FTF) gene promoter is regulated by three GATA elements with tandem E box and Nkx motifs, and FTF in turn activates the Hnf3beta, Hnf4alpha, and Hnf1alpha gene promoters. J Biol Chem *276*, 13136-13144.

Pellicciari, R., Costantino, G., and Fiorucci, S. (2005). Farnesoid X receptor: from structure to potential clinical applications. J Med Chem *48*, 5383-5403.

Pezzi, V., Sirianni, R., Chimento, A., Maggiolini, M., Bourguiba, S., Delalande, C., Carreau, S., Ando, S., Simpson, E.R., and Clyne, C.D. (2004). Differential expression of steroidogenic factor-1/adrenal 4 binding protein and liver receptor homolog-1 (LRH-1)/fetoprotein transcription factor in the rat testis: LRH-1 as a potential regulator of testicular aromatase expression. Endocrinology *145*, 2186-2196.

Qin, J., Gao, D.M., Jiang, Q.F., Zhou, Q., Kong, Y.Y., Wang, Y., and Xie, Y.H. (2004). Prospero-related homeobox (Prox1) is a corepressor of human liver receptor homolog-1 and suppresses the transcription of the cholesterol 7-alpha-hydroxylase gene. Mol Endocrinol *18*, 2424-2439.

Sablin, E.P., Krylova, I.N., Fletterick, R.J., and Ingraham, H.A. (2003). Structural basis for ligand-independent activation of the orphan nuclear receptor LRH-1. Mol Cell *11*, 1575-1585.

Seol, W., Choi, H.S., and Moore, D.D. (1995). Isolation of proteins that interact specifically with the retinoid X receptor: two novel orphan receptors. Mol Endocrinol *9*, 72-85.

Seol, W., Choi, H.S., and Moore, D.D. (1996). An orphan nuclear hormone receptor that lacks a DNA binding domain and heterodimerizes with other receptors. Science *272*, 1336-1339.

Sinal, C.J., Tohkin, M., Miyata, M., Ward, J.M., Lambert, G., and Gonzalez, F.J. (2000). Targeted disruption of the nuclear receptor FXR/BAR impairs bile acid and lipid homeostasis. Cell *102*, 731-744.

Wang, W., Zhang, C., Marimuthu, A., Krupka, H.I., Tabrizizad, M., Shelloe, R., Mehra, U., Eng, K., Nguyen, H., Settachatgul, C., *et al.* (2005). The crystal structures of human

steroidogenic factor-1 and liver receptor homologue-1. Proc Natl Acad Sci U S A *102*, 7505-7510.

Whitby, R.J., Dixon, S., Maloney, P.R., Delerive, P., Goodwin, B.J., Parks, D.J., and Willson, T.M. (2006). Identification of small molecule agonists of the orphan nuclear receptors liver receptor homolog-1 and steroidogenic factor-1. J Med Chem *49*, 6652-6655.

Zhang, C.K., Lin, W., Cai, Y.N., Xu, P.L., Dong, H., Li, M., Kong, Y.Y., Fu, G., Xie, Y.H., Huang, G.M.*, et al.* (2001). Characterization of the genomic structure and tissue-specific promoter of the human nuclear receptor NR5A2 (hB1F) gene. Gene *273*, 239-249.

Zhang, Y., Lee, F.Y., Barrera, G., Lee, H., Vales, C., Gonzalez, F.J., Willson, T.M., and Edwards, P.A. (2006). Activation of the nuclear receptor FXR improves hyperglycemia and hyperlipidemia in diabetic mice. Proc Natl Acad Sci U S A *103*, 1006-1011.

CHAPTER 3

LRH-1 IN BILE ACID HOMEOSTASIS

3.1 Abstract

LRH-1 is highly expressed in liver and intestine, where it is implicated in the regulation of cholesterol, bile acid and steroid hormone homeostasis. Cholesterol 7α-hydroxylase (CYP7A1) and sterol 12α-hydroxylase (CYP8B1), which catalyze key steps in bile acid synthesis, are proposed target genes of LRH-1 in liver. *In vitro* studies suggest that LRH-1 may be involved both in stimulating basal CYP7A1 and CYP8B1 transcription and in repressing their expression as part of the nuclear bile acid receptor (FXR)-small heterodimer partner (SHP) signaling cascade, which culminates in SHP binding to LRH-1 to repress gene transcription. However, *in vivo* analysis of the effects of LRH-1 on CYP7A1, CYP8B1 and other genes has been hampered by the early embryonic lethality of *Lrh*$^{-/-}$ mice. To overcome this obstacle, mice were generated in which *Lrh-1* was selectively disrupted in either hepatocytes or intestinal epithelium. To test the FXR-SHP-LRH-1 negative feedback mechanism, *Lrh-1*$^{flox/flox}$*;Alb-cre* and control *Lrh-1*$^{flox/flox}$*;+* mice were administered the potent, selective FXR agonist GW4064 and mRNA levels of CYP7A1 and CYP8B1 were measured. LRH-1 deficiency in either of these tissues changed mRNA levels of a number of genes involved in cholesterol and bile acid homeostasis. Surprisingly, disrupting *Lrh-1* in liver had no significant effect on basal CYP7A1 expression or its repression by FXR. While CYP8B1 repression by FXR was also intact in the liver-specific *Lrh*$^{-/-}$ mice, basal CYP8B1 mRNA levels were

24

significantly decreased and there were corresponding changes in the composition of the bile acid pool. Taken together, these data reveal a broad role for LRH-1 in regulating bile acid homeostasis but demonstrate that LRH-1 is not essential for feedback regulation of bile acid synthesis.

3.2 Introduction

3.2.1 Synthesis of Bile Acids

Bile acids play crucial roles in the maintenance of cholesterol homeostasis, dietary lipid absorption, and activation of several signaling pathways. Bile acids are synthesized in liver, where they stimulate biliary excretion of cholesterol, and are released into the small intestine after the ingestion of food (Russell, 2003). Their amphipatic nature and ability to form mixed micelles permit bile acids possible to facilitate the uptake of dietary cholesterol, lipids, and lipophilic vitamins in small intestine (Hofmann, 1999). Bile acids are also recognized as signaling molecules since bile acids can activate the mitogen-activated protein kinase (MAPK) pathway (Gupta et al., 2001; Qiao et al., 2003), the G-protein-coupled receptor, TGR5 (Watanabe et al., 2006), and the nuclear hormone receptor, FXR.

Bile acids are derived from cholesterol. This process involves many different enzymes including cytochrome P450 enzymes which introduce a hydroxyl group into the molecule (Russell, 2003). There are two major pathways for bile acid synthesis: the neutral (classic) and acidic (alternative) pathways as shown in Figure 3-1. The neutral pathway is initiated with 7α-hydroxylation of cholesterol by cholesterol 7α-hydroxylase (CYP7A1), which is a rate limiting enzyme for bile acid biosynthesis. Subsequently,
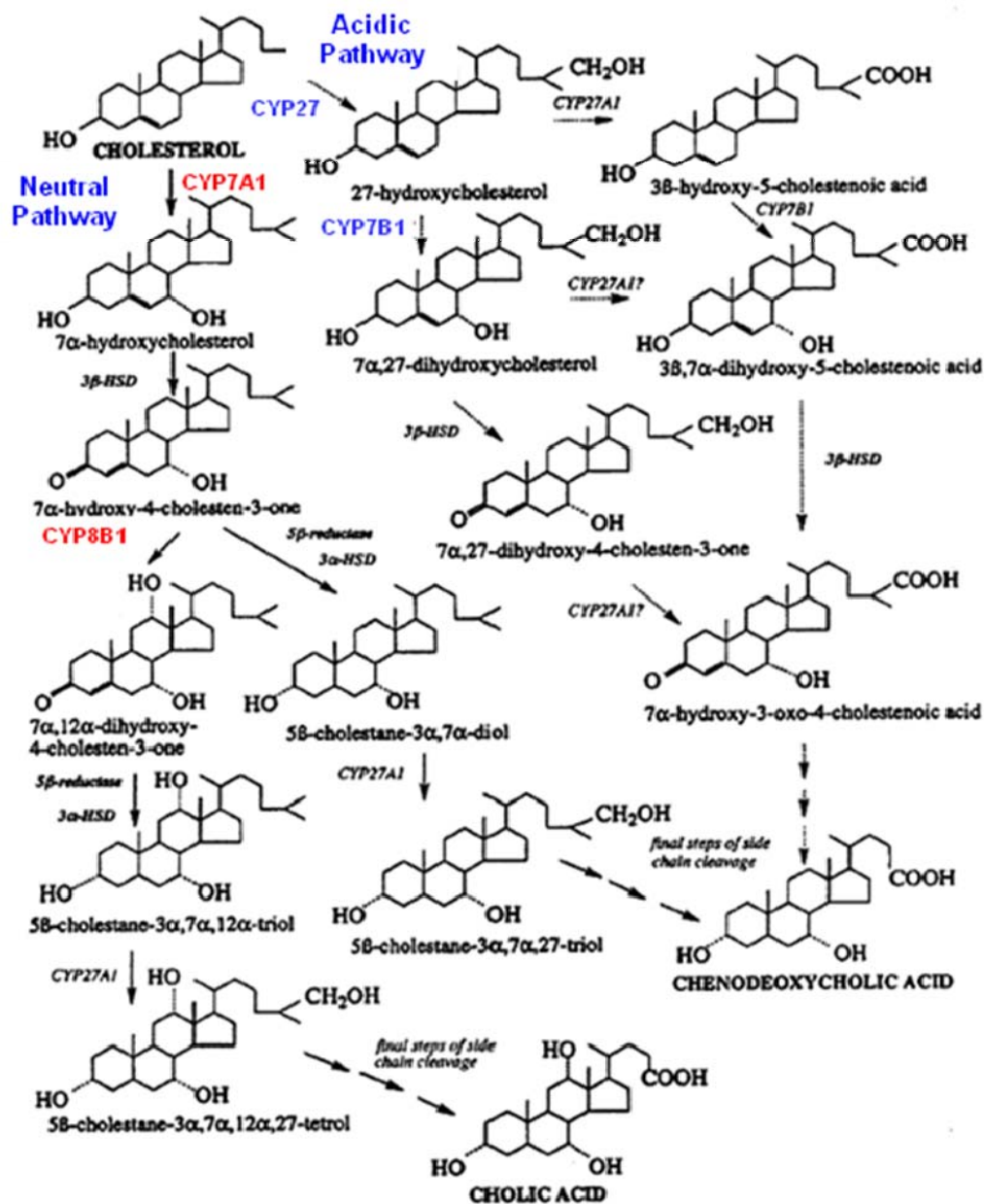
Figure 3-1. Bile acid biosynthesis pathways:

The neutral and acidic pathways. Adapted with permission from Norlin M and Wikvall K, 2007.

Figure 3-1. Bile acid biosynthesis pathways:

The neutral and acidic pathways. Adapted with permission from Norlin M and Wikvall K, 2007.

12α-hydroxylation is catalyzed by sterol 12α-hydroxylase (CYP8B1) to form cholic acids (CA). In the acidic pathway, sterol 27-hydroxylase (CYP27A1) initiates side chain oxidation and introduces a hydroxyl group in the 27-position. The major product of this pathway is chenodeoxycholic acid (CDCA). Most of primary bile acids are conjugated to glycine or taurine and can be further metabolized to secondary bile acids such as deoxycholic acid and lithocholic acid by microbial enzymes in intestine (Chiang, 2002). Approximately 95% of bile acids are reabsorbed in the ileum and returned to the liver via the portal blood, which completes the cycle referred to as enterohepatic circulation.

3.2.2 Regulation of Enterohepatic Bile Acids

Maintaining adequate concentrations of bile acids is crucial. Several clinically important diseases such as cholestasis, cholesterol gallstones and lipid malabsorption are the consequence of disturbances in bile acid homeostasis. At the transcriptional level, this is achieved mainly by the regulation of genes involved in bile acid biosynthesis and transport (Figure 3-2).

LRH-1 binding sites have been identified in the regulatory regions of many genes involved in cholesterol and bile acid homeostasis in liver (Fayard et al., 2004). Among these are the genes encoding CYP7A1 and CYP8B1, which catalyzes a step in the conversion of chenodeoxycholic acid to cholic acid (Russell, 2003). *In vitro* studies have suggested that LRH-1 has dual effects on *CYP7A1* and *CYP8B1* expression (Goodwin et al., 2000; Lu et al., 2000). First, it enhances basal transcription of these genes. Second, it is involved in the feedback repression of *CYP7A1* and *CYP8B1* through a signaling cascade involving the farnesoid X receptor (FXR), a nuclear bile acid
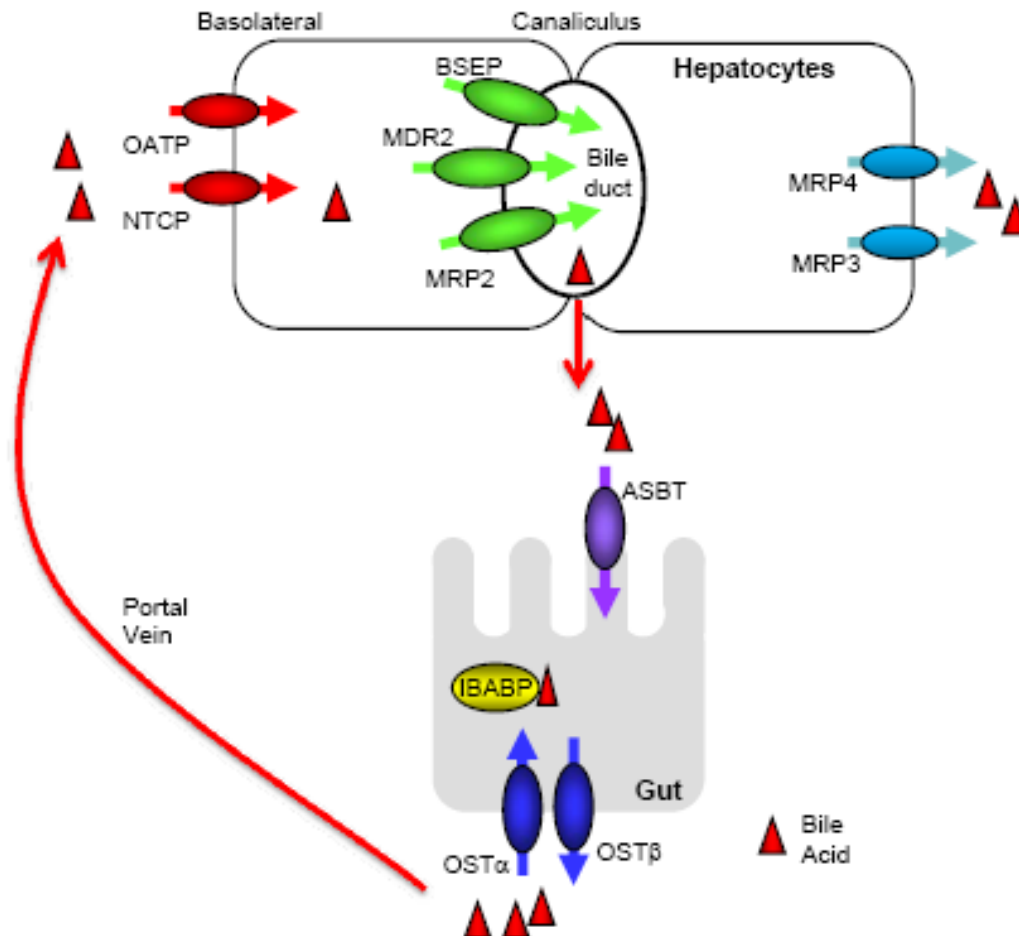
Figure 3-2. Regulation of enterohepatic bile acids

Bile acids efflux across the basolateral membrane of hepatocytes occurs via MRP3 and MRP4. Secretion across the canalicular membrane occurs via BSEP, MDR2, and MRP2. Bile acids are delivered in intestine where they aid in emlsifying dietary lipids. Most of bile acids are efficiently absorbed via ASBT, transported across the enterocytes by IBABP, and efflux through OSTα/β. Bile acids re-enter the portal blood and are transported to hepatocytes via NTCP and OATP to complete their enterohepatic circulation.

receptor, and small heterodimer partner (SHP) (Goodwin et al., 2000; Lu et al., 2000). Activation of FXR by bile acids induces expression of SHP, an atypical orphan nuclear receptor lacking a DNA binding domain that functions as a strong transcriptional repressor through interactions with other nuclear receptors and transcription factors (Seol et al., 1996)(reviewed in (Lee et al., 2007)). Since SHP binds efficiently to LRH-1 and inhibits its transcriptional activity *in vitro*, it was proposed that this interaction causes *CYP7A1* and *CYP8B1* repression (Goodwin et al., 2000; Lu et al., 2000). While the roles of FXR and SHP in this signaling cascade have been demonstrated *in vivo* using gene knockout mice (Kerr et al., 2002; Sinal et al., 2000; Wang et al., 2002), *Lrh-1$^{-/-}$* mice die during early embryogenesis, precluding their use in the analysis of LRH-1 function in adult tissues (Pare et al., 2004b). Interestingly, heterozygous *Lrh-1$^{+/-}$* mice have elevated CYP7A1 and CYP8B1 mRNA levels (del Castillo-Olivares et al., 2004; Pare et al., 2004b), suggesting that the dominant effect of LRH-1 on *Cyp7a1* and *Cyp8b1* transcription is the recruitment of SHP, not the induction of their basal activity. LRH-1 overexpression studies in mice have yielded contrasting outcomes: whereas CYP7A1 mRNA levels were increased in LRH-1 transgenic mice (Pare et al., 2004b), overexpression of LRH-1 using an adenoviral delivery system caused a strong decrease in CYP7A1 and CYP8B1 mRNA levels (del Castillo-Olivares et al., 2004). Given these mixed results, the precise role of LRH-1 in the regulation of bile acid synthesis remains unclear.

In the intestine, LRH-1 also regulates genes involved in cholesterol and bile acid homeostasis, including those encoding the ATP-binding cassette (ABC) transporters ABCG5 and ABCG8, the organic solute transporters (Postic et al.) α and β and the ileal

apical sodium-dependent bile acid transporter (ASBT; also known as solute carrier family 10, member A2) (Chen et al., 2003; Frankenberg et al., 2006; Freeman et al., 2004).

In this study, we describe the generation and characterization of mice deficient for LRH-1 in either hepatocytes or the intestinal epithelium. These studies demonstrate roles for LRH-1 in regulating bile acid homeostasis in both tissues. However, they also unexpectedly show that LRH-1 is not essential for FXR-mediated feedback repression of bile acid synthesis.

3.3 Materials and Methods

Animal Procedures

All animal experiments were approved by the Institutional Animal Care and Research Advisory Committee of the University of Texas Southwestern Medical Center. Animals were housed in a pathogen-free and a temperature-controlled environment with 12 hour light/dark cycles. Animals were housed in a pathogen-free and a temperature-controlled environment with 12 hour light/dark cycles and fed standard irradiated rodent chow (TD7913, Harlan Teklad, Madison, WI) and water *ad libitum*. All animal experiments were done with 8 to 12 week-old male mice killed between 10 am and 12 pm. Body weight and liver weight were measured in all animals and the length of small intestine was measured in intestine-specific $Lrh-1^{-/-}$ mice. For measurement of bile acid pool size and composition, mice were fasted 4 hours prior to sacrifice. For experiments with GW4064, control and liver and intestine-specific $Lrh-1^{-/-}$ mice were administrated GW4064 (100 mg/kg, in 1% methylcellulose, 1% Tween80) or vehicle by oral gavage and killed 14 hours later. Tissues were snap-frozen in liquid nitrogen and stored at -80°C

until RNA was prepared. Small intestine was removed and cut into three segments of equal length representing the duodenum, jejunum and ileum. Then, they were cut open longitudinally and gently scraped after flushing with ice cold phosphate buffered saline. Liver was powdered before mechanical homogenizing.

Generation of LRH-1 Deficient Mice

High-fidelity PCR amplification of 129SvEv genomic DNA was used to generate a ~3.7 kb long arm including exons 3 and 4, a ~0.8 kb targeting arm including exon 5, and a ~1.6 kb short arm including intron 5. These fragments were assembled in the pMC1neo PolyA vector (Stratagene) containing a neomycin resistance cassette and loxP and FRT sites. AatII-linearized DNA was electroporated into 129SvEv-derived ES cells. ES cells were screened for targeted recombination by Southern blot analysis using 5' and 3' probes as shown Figure 3-3A and DNA digested with NheI or NdeI, respectively. Probes were generated by PCR amplication using the following primers: 5' probe forward primer: CCATGGTGGATTTGGTTCTC; reverse primer: TGTAGCATAAGTTGGTCCGG; 3' probe forward primer: GGCTGTTCTTGCTACTTGAG; reverse primer: CAGGTGCACTGTATGTAGCT. Two independently derived ES cell clones were injected into C57BL/6J blastocysts to produce chimeric mice that transmitted the modified *Lrh-1* locus. The neomycin resistance cassette was removed by crossing *Lrh-1*^flox/+ mice with R26::FLPe transgenic mice (Farley et al., 2000). Hepatocyte and intestinal epithelium-specific LRH-1 deletion was achieved by breeding LRH-1^flox/flox mice with albumin-cre (Postic et al., 1999) or villin-cre (Madison et al., 2002) transgenic mice. To confirm homologous recombination and tissue-specific deletion of exon 5 of *Lrh-1*, genomic DNA was extracted from tail,

liver and intestine, and PCR analysis was performed using the following primers: forward primer1: CGATGTCCCTACTGTCGA; reverse primer1: CGCAGCATTCTTCGGCAG; forward primer2: CATAAGGGCTCAGTGGCAC; reverse primer2: CTTCACTGGCTGCCAAGCTG.

RT-PCR and Sequencing

Total RNA was extracted from liver and small intestine of *Lrh-1$^{flox/flox}$;+* , *Lrh-1$^{flox/flox}$;Alb-Cre*, and *Lrh-1$^{flox/flox}$;Vil-Cre* mice. Reaction for reverse-transcription includes 5 ug of total RNA, 250 ng of Oligo dT$_{20}$, 250 ng of random hexamers, 10 mM each dNTP, 40 unit of RNaseOUT (Invitrogen), and SuperScript II (Invitrogen). PCR amplication was done using primers as follows: LRH exon 4 forward primer: CTGGAAGAGCTATGTCCTGTGTG; LRH exon 6 reverse primer: GCTAATGGGAGATGTGACAAAGGG. PCR products were purified by Qiagen PCR purification kit and sequenced.

Immunoblot Analysis

Nuclear extract was prepared from homogenized liver using hypotonic buffer (10 mM HEPES pH 7.5, 1.5 mM MgCl$_2$, 10 mM KCl, 1.5 mM DTT, Complete Protease Inhibitor Cocktail (Roche Diagnostic)) and nuclear lysis buffer (50 mM TrisHCl pH 7.5, 150 mM NaCl, 0.5% Triton X-100, Complete Protease Inhibitor Cocktail (Roche Diagnostic)) following a standard procedure. The 50 ug of nuclear extract was resolved on a 10% SDS-polyacrylamide gel and transferred to a PVDF membrane (Amersham). The membrane was probed with guinea pig polyclonal anti-mouse LRH-1 antibody against residues 318-560 (Li et al., 2005b) at a dilution of 1:5000 at 4 °C overnight followed by a secondary horseradish peroxidase-conjugated antibody at a dilution of

1:10000. The membrane was reprobed with antibody against TATA-binding protein (Santa Cruz Biotechnology) as a loading control. Proteins were detected by Super Signal West Femto chemiluminescense substrate (Pierce).

Histological Procedures

Liver was sliced and ileum was cut transversely, fixed with 10% formalin, paraffin embedded, sectioned, and stained with hematoxylin and eosin. Sections were photographed using a Nikon DXM1200F camera and Nikon Eclipse 80i microscope at 20X or 40X magnification.

RT-qPCR Analysis

Total RNA was extracted from liver and scraped intestinal using RNA STAT-60 (Tel-Test, Inc.). After DNase I (Roche Molecular Biochemicals) treatment, RNA was reverse transcribed into cDNA with random hexamers using the SuperScript II First-Strand Synthesis System (Invitrogen). Primers for each gene were designed using Primer Express Software (Applied Biosystems, Foster City, CA) and were validated as previously described (Bookout and Mangelsdorf, 2003). Primer sequences are shown in Table 3-1. RT-qPCR reactions contained 25 ng of cDNA, 150 nM of each primer, and 5 μl of SYBR GreenER PCR Master Mix (Invitrogen), and were carried out in triplicate using an Applied Biosystems Prism 7900HT instrument. Relative mRNA levels were calculated using either the comparative C_T or standard curve methods normalized to cyclophilin or 18S RNA, respectively.

Table 3-1. RT-qPCR primer sequences

Genes	Accession number	Forward Primer	Reverse Primer
ABCG5	AF312713	TCAATGAGTTTTACGGCCTGAA	GCACATCGGGTGATTTAGCA
ABCG8	AF324495	TGCCCACCTTCCACATGTC	ATGAAGCCGGCAGTAAGGTAGA
APOA1	NM_009692	TCCTCCTTGGGCCAACA	GAACCCAGAGTGTCCCAGTTT
ASBT	NM_011388	TGACTCGGGAACGATTGTG	GGAATAACAAGAGCAACCAGAGAA
BSEP	NM_021022	AAGCTACATCTGCCTTAGACACAGAA	CAATACAGGTCCGACCCTCTCT
CYP27A1	NM_024264	GCCTCACCTATGGGATCTTCA	TCAAAGCCTGACGCAGATG
CYP7A1	L23754	AGCAACTAAACAACCTGCCAGTACTA	GTCCGGATATTCAAGGATGCA
CYP7B1	NM_007825	TAGCCCTCTTTCCTCCACTCATA	GAACCGATCGAACCTAAATTCCT
CYP8B1	AF090317	GCCTTCAAGTATGATCGGTTCCT	GATCTTCTTGCCCGACTTGTAGA
FGF15	NM_008003	ACGGGCTGATTCGCTACTC	TGTAGCCTAAACAGTCCATTTCCT
FXR	NM_009108	TCCGGACATTCAACCATCAC	TCACTGCACATCCCAGATCTC
HMGCR	XM_127496	CTTGTGGAATGCCTTGTGATTG	AGCCGAAGCAGCACATGAT
HMGCS1	NM_145942	GCCGTGAACTGGGTCGAA	GCATATATAGCAATGTCTCCTGCAA
HNF4α	NM_008261	ACCAAGAGGTCCATGGTGTTT	GTGCCGAGGGACGATGTAG
IBABP	NM_008375	TTGAGAGTGAGAAGAATTACGATGAGT	TTTCAATCACGTCTCCTGGAA
LRH-1ex 5	NM_030676	GAACTGTCCAAAACCAAAAAAGG	CGTTTTCTCTGCGTTTTGTCA
MDR2	NM_008830	CTTGAGGCAGCGAGAAATG	GGTTGCTGATGCTGCCTAGT
MRP2	AF282773	GCTGGGAGAAATGGAGAATGT	ACTGCTGAGGGACGTAGGCTAT
MRP3	NM_029600	AGCTGGGCTCCAAGTTCTG	GTGTGAGGTCCGGAGTGTTG
NTCP	U95131	GAAGTCCAAAAGGCCACACTATGT	ACAGCCACAGAGAGGGAGAAAG
OSTα	NM_145932	AACAGAACATGGGATCCAAGTTT	CAGGGCGGTCAGGATGA
OSTβ	NM_178933	GACAAGCATGTTCCTCCTGAGA	TGTCTTGTGGCTGCTTCTTTC

SHP	NM_011850	CGATCCTCTTCAACCCAGATG	AGGGCTCCAAGACTTCACACA
SR-B1	BC004656	TCCCCATGAACTGTTCTGTGAA	TGCCCGATGCCCTTGA
18S	M10098	ACCGCAGCTAGGAATAATGGA	GCCTCAGTTCCGAAAACCA
Cyclophilin	NM_011149	GGAGATGGCACAGGAGGAA	GCCCGTAGTGCTTCAGCTT

LC/MS Analysis of Bile Acids

Gall bladder, liver and intestines were removed together and placed into 50 mL of EtOH. The tissues in solution were spiked with 50 µg of chenodeoxycholic acid- D_4 (C/D/N Isotopes, Pointe-Claire, Canada) and extracted. Samples were minced and boiled for 1hr to reduce the EtOH volume to ~30 mL.   Samples were filtered through #2 Whatman paper and the volume was brought to 50 mL using a volumetric flask. One mL of the extract was centrifuge filtered using a PVDF membrane (Millipore) prior to analysis. Dr. Carolyn L. Cummins, a post-doctoral fellow and Daniel R. Schmidt, a graduate student in the laboratory of Dr. David J. Mangelsdorf, performed LC/MS work together. Bile acids were quantitated by LC/MS (Agilent Technologies, Palo Alto, CA) with electrospray ionization in negative ion mode by modification of a published procedure (Burkard et al., 2005).   Briefly, samples were loaded onto a pre-column (Zorbax C8, 4.6 x 12.5 mm, 5 µm, Agilent) at 1 mL/min for 1 min with water containing 5 mM NH_4Ac and then backflushed onto the analytical column at 0.4 mL/min (Eclipse XDB-C18, 4.6 x 50 mm, 5 µm, Agilent).   The mobile phase consisted of methanol/0.024% formic acid (A) and water/10 mM NH_4Ac/0.024% formic acid (B). The following gradient was run for a total run time of 30 minutes: 0-15 min, 70 to 80% (A), 15-17 min 80% (A), 17-20 min 80 to 95% (A), 20-26 min 95%. MS parameters were set

as follows: gas temperature 350°C, nebulizer pressure 30 psig, drying gas (nitrogen) 12 L/min, capillary voltage 4000 V, fragmentor voltage 200 V. Selective ion monitoring was used to detect the conjugated and unconjugated bile acids (Table 3-2). Quantification was performed based on peak areas using external calibration curves of standards prepared in methanol. CDCA-D$_4$ was used to calculate the recovery of bile acids after extraction relative to a blank control.

Compound	Retention Time (min)	Ion Monitored [M-H]-(m/z)
Taurine-Conjugates		
tLCA	10.8	482
tUDCA	4.1	498
tHDCA	4.4	498
tCDCA	7.3	498
tDCA	8	498
t-MCA	3.5	514
tHCA	4.1	514
tCA	5.2	514
tLCA-3-SO4	4	562
Unconjugated		
LCA	22.4	375
MCA	7.8	391
UDCA	9.1	391
HDCA	10.7	391
CDCA / CDCA-D4	17.3	391
DCA	18	391
b-MCA	6.9	407
a-MCA	7.4	407
CA	11.8	407
LCA-3-SO4	10.8	455

Table 3-2. Summary of LC/MS parameters used to measure bile acids

Fecal Bile Acid Excretion

Fecal excrement was collected from mice individually housed for 72 hr. Bile acids were extracted and 3α-dehydroxysteroid dehydrogenase (3HSD) assays performed to quantify bile acid excretion as described previously (Turley et al., 1998). Briefly, feces were dried in an 80°C vacuum oven, weighed, ground, and filtered with mesh to have the final fine powder. A [Carboxyl- ^{14}C] cholate was added in 1 g of stool as an internal control and treated with 10 ml sodium borohydride. After alkaline hydrolysis at 100°C for 12 hours, samples were eluted with methanol using C18 Bond Elute column (Varian). Extracts were incubated with 3HSD for enzymatic assay. Daily excretion was expressed as umol/day/100 g body weight.

Hepatic Lipids

Liver lipids were extracted by the method of Folch (Folch et al., 1957). Liver tissue (100 mg) was homogenized in 2:1 chloroform/methanol then washed once with 50 mM NaCl and twice with 0.36 M $CaCl_2$/Methanol. The organic phase was separated by centrifugation at 2100 rpm between washes and chloroform was added to a final volume of 5 ml. Ten micrometer of Triton-X 100/chloroform(1:1,v/v) was added to duplicate of 100 μl aliquots of each extract, which were dried under nitrogen. Colorimetric enzymatic assays were performed to measure cholesterol (Roche) and triglyceride (Trinity Biotech).

Plasma Parameters

Vena cava blood was collected and transferred into Li-heparin tubes (Sarstedt). Samples were centrifuged at 4000 rpm at 4 °C for 10 min, and total plasma cholesterol, triglycerides, glucose, aspartate aminotransferase, and alanine aminotransferase were

measured using a Vitros 250 automated analyzer at phenotyping core facility at UT Southwestern Medical Center. Plasma free fatty acids were measured with colorimetric assay kits (Roche). Total plasma bile acids were measured using enzymatic assay kits (Diagnostic Chemicals Limited).

FGF15 promoter subcloning and mutagenesis

Potential LRH-1 response element (LRH-RE) were searched by Nubiscan program (http://www.nubiscan.unibas.ch/) and amplified from mouse genomic DNA. One or two copies of LRH-RE were inserted into pCMX-tk-luciferase at BamH1site. Site-directed mutagenesis was done with the QuikChange kit (Stratagene) according to the manufacturer's instructions. All constructs and mutants were confirmed by sequencing. FGF15LRH-RE BamH1: forward primer CGGATCCGCCCGGCAACATCTTTC; reverse primer GGATCCCCTGGGGCCATCACTTTACG: FGF15LRH-RE mutant: forward primer AAGGAACTTCGAGGGCAACCTACCAATGATAGT; reverse primer CCCACTATCATTGGTAGTTGGCCCTCGAAGTTC.

Transient transfection

COS7 and HEK293 cells were cultured in Dulbecco's modified Eagle's medium (Gibco) containing 10% fetal bovine serum (Gibco) and 1% penicillin/streptomycin (Invitrogen) at 37 °C, 5% CO_2 incubator. Cells were plated in 96-well plates and grown to 70% confluence. Transient transfection was carried out with 50 ng of reporter plasmid, 15 ng of receptor expression plasmid, 30 ng of pCMX-β-galactosidase and pGEM carrier DNA to give 120 ng of DNA total per well of a 96-well plate using Fugene 6 (Roche). Sixteen hours after transfection, cells were harvested for measuring luciferase and β-

galactosidase activity using a Dynex Technologies, Inc. MLX microtiter plate luminometer and a Fisher Scientific, Inc. Opsys MR spectrophotometer, respectively. Luciferase data were normalized to an internal β-galactosidase control and represent the mean (± standard deviation) of triplicate assays.

Electrophoretic Mobility Shift Assay (EMSA)

Receptor proteins were *in vitro* translated with the TNT Quick Coupled Transcription/Translation System (Promega). Double-stranded oligonucleotides with overhangs were end-filling labeled with $\alpha[^{32}P]$-dCTP following standard procedure. Oligonucleotides sequences are follows: FGF15LRH-RE1: forward primer GCGATTGCCATCAAGGACGTCAG; reverse primer GCTGCTGACGTCCTTGATGGCAA; FGF15LRH-RE1 mutant: forward primer: GCGATTGCCATCAACCACGTCAG; reverse primer: GCTGCTGACGTGGTTGATGGCAA. Briefly, 1 uM of double-stranded oligonucleotides, 10 mM each dATP, dGTP, dTTP, Klenow polymerase were incubated at 37°C for 2 hr then, 65°C for 5 min. Oligonucleoties were purified with G-25 sephadex columns (Roche) and diluted to 200,000 cpm. Binding reactions were performed in a total volume of 20 μl consisting of binding buffer (150 mM KCl, 40 mM HEPES at pH 7.8, 4 mM DTT, 15 % glycerol, 0.2% NP-40), 2 μg of poly[d(I-C)] (Pharmacia), 20 pmol of a nonspecific single-stranded oligonucleotide to remove nonspecific binding, and 2 μl of LRH-1 protein. Reactions containing competing oligonucleotides were incubated for 30 min on ice, followed by the addition of 1 ul of labeled LRH-RE oligos and further incubation at room temperature for 30 min. Samples were then analyzed on 5%

polyacrylamide gels run at 275 V for 90 min in 0.5 × TBE buffer and were dried and visualized by autoradiography.

Statistical Analyses

Statistical analyses were performed using Minitab Release 14 software (Minitab Inc, State College, PA). Values are expressed as mean ± SEM. Significant differences of two groups were evaluated using a two-tailed, unpaired Student's T-test. Multiple groups were analyzed by one-way ANOVA followed by Fisher's least significant difference test.

3.4 Result

Generation of tissue-specific LRH-1 deficient mice. To circumvent the early embryonic lethality caused by disruption of *Lrh-1*, mice were generated in which exon 5 of the LRH-1 gene, which includes the region encoding the second zinc finger of the DNA binding domain, was flanked by loxP sites (Figure 3-3A). Southern Blot analysis demonstrated the homologous recombination in ES cells (Figure 3-3B), which were injected into C57BL/6J blastocyst to produce chimeric mice. The resulting *Lrh-1$^{flox/flox}$* mice were crossed against either albumin-cre or villin-cre to generate *Lrh-1$^{flox/flox}$;Alb-cre* and *Lrh-1$^{flox/flox}$;Vil-cre* mice lacking an intact LRH-1 gene in either hepatocytes or intestinal epithelium, respectively (Figure 3-3C-F). The residual LRH-1 mRNA in liver of *Lrh-1$^{flox/flox}$;Alb-cre* mice (Figure 3-3E) is likely due to LRH-1 expression in non-hepatocytes. While an LRH-1 transcript was detected by RT-qPCR in intestines of *Lrh-1$^{flox/flox}$;Vil-cre* and livers of *Lrh-1$^{flox/flox}$;Alb-cre* mice using primers directed against sequences downstream of exon 5, cloning and sequencing of this transcript revealed a stop codon created by deletion of the floxed region that precludes production of
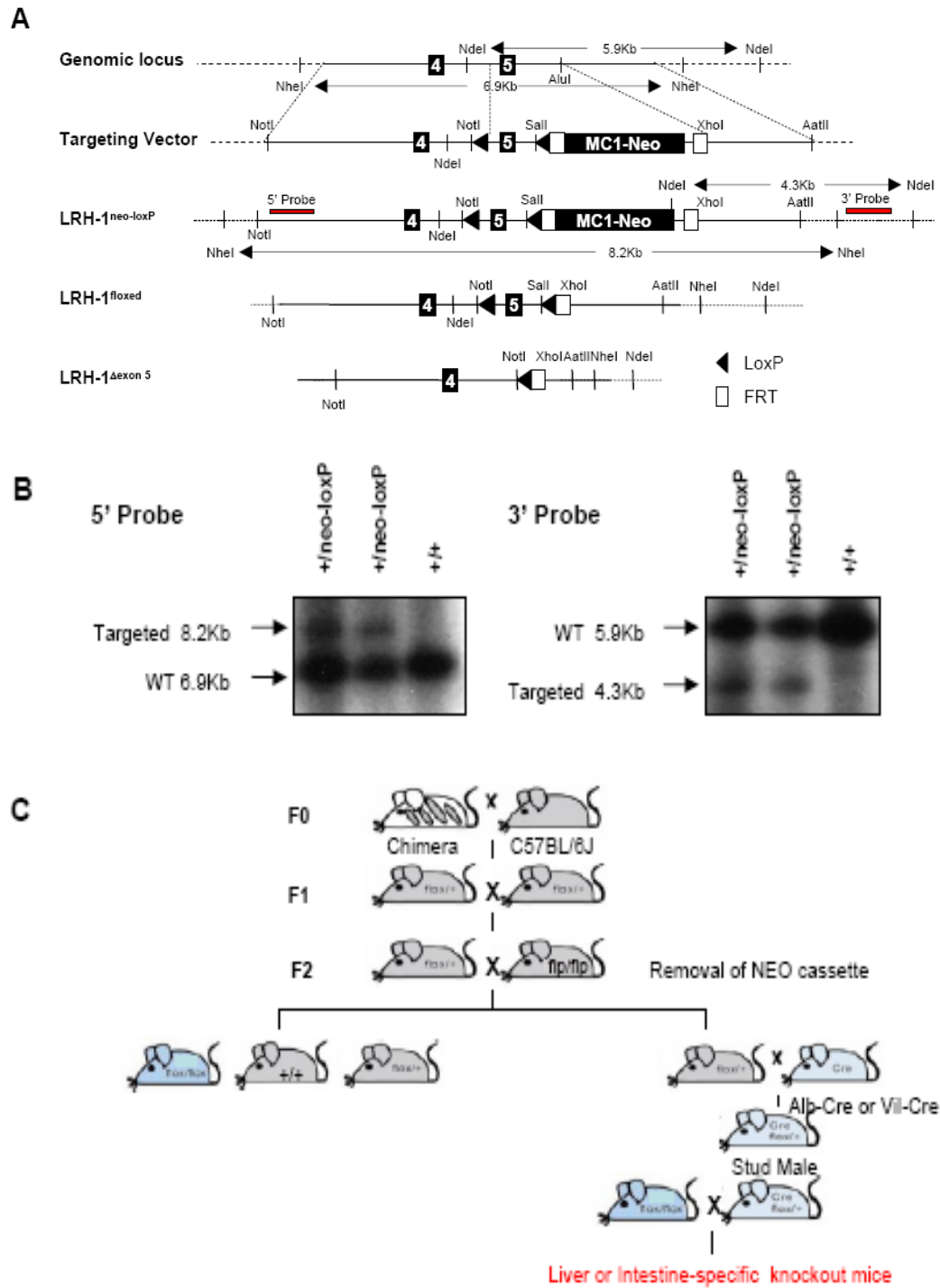
Figure 3-3. Generation of mice deficient for LRH-1 in liver or intestine

(A) Schematic representation of the targeting strategy to inactivate the *Lrh-1* gene. The scheme shows exons 4 and 5 of the *Lrh-1* gene, the targeting vector, and the targeted *Lrh-1* allele both before and after successive removal of the MC1-neo cassette with FLPe recombinase and Exon 5 with cre recombinase. LoxP sites (solid arrowheads), FLPe recombinase target sites (Frt) and selected restriction enzyme sites are indicated. **(B)** Homologous recombination in ES cells was screened by Southern blot analysis using both 5' and 3' probe as shown figure 3-1A after digestion of NheI and NdeI. Expected alleles and sizes are shown on the top and left side, respectively. **(C)** Breeding strategy for generation of mice deficient for LRH-1 in liver or intestine. After removal of neo cassette, albumine-cre or villin-cre mice were crossed with *Lrh-1*$^{\text{flox/flox}}$ mice to achieve the exon 5 deletion.
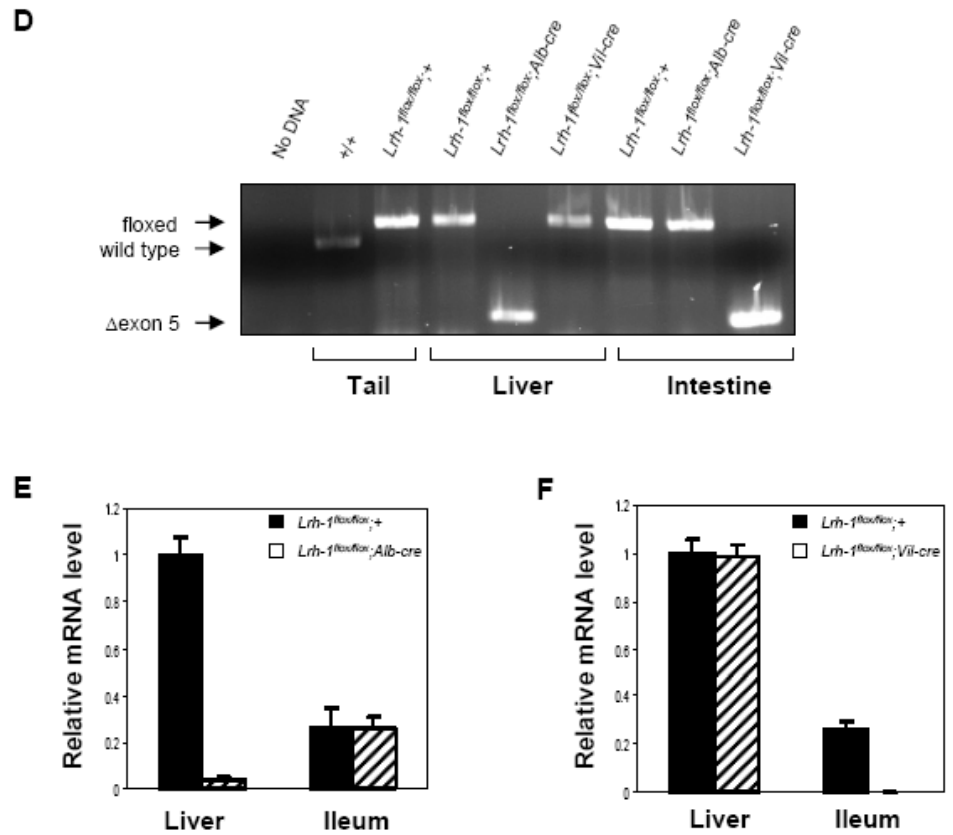
Figure 3-3. Generation of mice deficient for LRH-1 in liver or intestine

(D) PCR analysis of *Lrh-1* alleles using cDNA prepared from liver and intestine of *Lrh-1^{flox/flox}*;+, *Lrh-1^{flox/flox}*;*Alb-cre* or *Lrh-1^{flox/flox}*;*Villin-cre*. PCR products from wild type (+/+) and *Lrh-1^{flox/flox}* (floxed) mice are shown on the left. The positions of the PCR products generated by the wild type (WT) *Lrh-1* allele and the *Lrh-1^{flox/flox}* (floxed) and deleted exon 5 *Lrh-1* (Δexon 5) alleles are indicated. **(E and F)** RT-qPCR analysis done using a primer set that recognizes *Lrh*-1 exon 5 and cDNA from liver and ileum of either *Lrh-1^{flox/flox}*;+ and *Lrh-1^{flox/flox}*;*Alb-cre* mice **(E)** or *Lrh-1^{flox/flox}*;+ and *Lrh-1^{flox/flox}*;*Vil-cre* mice **(F)**.

G

H

```
atgtctgctagtttggatactggagattttcaagaatttcttaagcatggacttacagct
 M  S  A  S  L  D  T  G  D  F  Q  E  F  L  K  H  G  L  T  A
attgcgtctgcaccagggtcagagactcgccactcccccaaacgtgaggaacaactccgg
 I  A  S  A  P  G  S  E  T  R  H  S  P  K  R  E  E  Q  L  R
gaaaaacgtgctgggcttccggaccgacaccgacgccccattcccgcccgcagccgcctt
 E  K  R  A  G  L  P  D  R  H  R  R  P  I  P  A  R  S  R  L
gtcatgctgcccaaagtggagacggaagccccaggactggtccgatcgcatggggaacag
 V  M  L  P  K  V  E  T  E  A  P  G  L  V  R  S  H  G  E  Q
gggcagatgccagaaaacatgcaagtgtctcaatttaaaatggtgaattactcctatgat
 G  Q  M  P  E  N  M  Q  V  S  Q  F  K  M  V  N  Y  S  Y  D
gaagatctggaagagctatgtcctgtgtgtggcgataaagtgtctgggtaccattacggt
 E  D  L  E  E  L  C  P  V  C  G  D  K  V  S  G  Y  H  Y  G
ctcctcacgtgcgaaagctgcaagccgtaagagccgaccgcatgcgaggggggcagaaata
 L  L  T  C  E  S  C  K  P  *
```

Figure 3-3. Generation of mice deficient for LRH-1 in liver or intestine

(G) RNA was prepared from liver and ileum of *Lrh-1^flox/flox^;Alb-cre* and *Lrh-1^flox/flox^;Vil-cre* mice, and corresponding flox/flox control mice. RT-PCR was done using primers in exon 4 (forward) and exon 6 (reverse). Positions of the *Lrh-1* ^flox/flox^ and deleted exon 5 (Δexon5) RT-PCR products are indicated. **(H)** Nucleotide sequence of the Δexon5 product derived from either liver or ileum of *Lrh-1^flox/flox^;Alb-cre* and *Lrh-1^flox/flox^;Vil-cre* mice, respectively. The recombination event introduces a stop codon at the junction formed by deletion of exon 5. **(I)** Immunoblot analysis using *in vitro* translated LRH-1 (IVT) or nuclear extracts prepared from livers of *Lrh-1^flox/flox^;+* and *Lrh-1^flox/flox^;Alb-cre* mice (n=3 male mice/group, pooled) with antibodies against LRH-1 or TATA-binding protein (TBP). The LRH-1 band migrates at ~62 kD.

functional protein (Figure 3-3G and H). Consistent with the mRNA data, there was a marked decrease in LRH-1 protein in liver extracts prepared from *Lrh-1^flox/flox^;Alb-cre* mice (Figure 3-I). For unknown reasons, we were unable to detect LRH-1 protein in intestinal extracts prepared from either control or *Lrh-1^flox/flox^;Vil-cre* mice. Based on these data, we conclude that LRH-1 is efficiently eliminated in hepatocytes and intestinal epithelium of *Lrh-1^flox/flox^;Alb-cre* and *Lrh-1^flox/flox^;Vil-cre* mice, respectively.

There were no overt abnormalities in the *Lrh-1^flox/flox^;Alb-cre* (Figure 3-4A and B) and *Lrh-1^flox/flox^;Vil-cre* mice (Figure 3-5A and B) in terms of body weight and liver weight or length of small intestine nor were there changes in tissue morphology seen in hematoxylin and eosin-stained sections of liver (Figure 3-4C and D) or small intestine (Figure 3-5C and D). Analysis of plasma parameters did not reveal significant changes in triglyceride, free fatty acid, glucose, bile acid or alanine aminotransferase concentrations in *Lrh-1^flox/flox^;Alb-cre* or *Lrh-1^flox/flox^;Vil-cre* mice (Table 3-3). Plasma cholesterol and aspartate aminotransferase levels were modestly but significantly decreased *in Lrh-1^flox/flox^;Alb-cre* and *Lrh-1^flox/flox^;Vil-cre* mice, respectively (Table 3-3). Hepatic cholesterol and triglyceride concentrations were not significantly decreased in either the *Lrh-1^flox/flox^;Alb-cre* and *Lrh-1^flox/flox^;Vil-cre* mice (Table 3-3). The differences in basal plasma cholesterol and triglyceride concentrations in the control *Lrh-1^flox/flox^;+* mice may reflect the slight difference in their genetic backgrounds.

Effects of LRH-1 deficiency in hepatocytes. The consequences of eliminating LRH-1 in hepatocytes on the expression of genes involved in bile acid and cholesterol homeostasis were examined. mRNA was prepared from livers of *Lrh-1^flox/flox^;Alb-cre* and control *Lrh-1^flox/flox^;+* mice. Although CYP7A1 mRNA levels trended upwards in
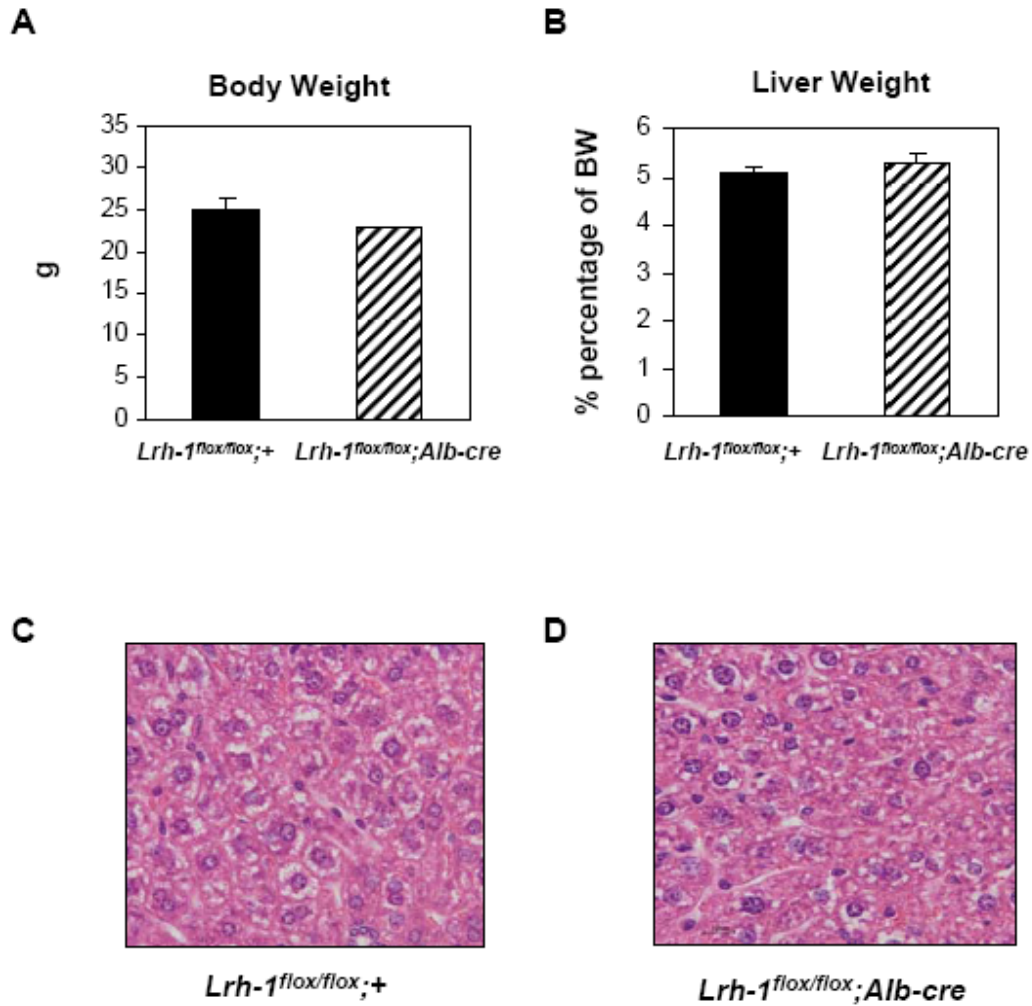
Figure 3-4. Phenotype of mice deficient for LRH-1 in liver

(**A**) Body weight of *Lrh-1^{flox/flox}* and *Lrh-1^{flox/flox};Alb-cre* mice. (**B**) Liver weight from *Lrh-1^{flox/flox}* and *Lrh-1^{flox/flox};Alb-cre*. Liver weights were normalized with body weight. n=6-7 male mice/group, 8-10 week old of age. (**C and D**) Liver sections from *Lrh-1^{flox/flox}* and *Lrh-1^{flox/flox};Alb-cre* mice were stained with hemotoxylin/eosin (40X magnification).
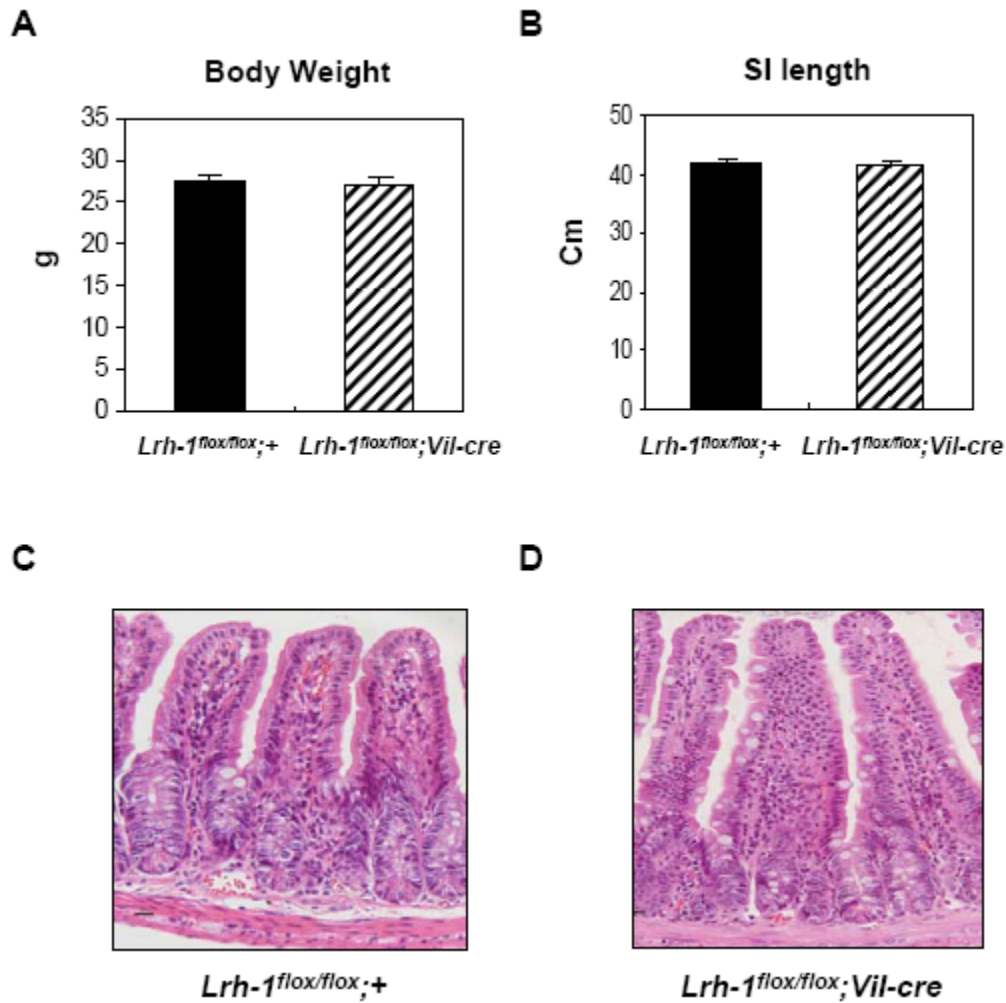
Figure 3-5. Phenotype of mice deficient for LRH-1 in intestine

(A) Body weight of *Lrh-1$^{flox/flox}$* and *Lrh-1$^{flox/flox}$;Vil-Cre* mice. **(B)** Length of small intestine from *Lrh-1*$^{flox/flox}$ and *Lrh-1$^{flox/flxo}$;Vil-Cre*. n=7 male mice/group, 8 week old of age. **(C and D)** Transverse sections of ileum from *Lrh-1$^{flox/flox}$* and *Lrh-1$^{flox/flox}$;Vil-Cre* mice were stained with hemotoxylin and eosin (20X magnification).

Parameter	LRH-1$^{flox/flox}$	LRH-1^{HepKO}	P value	LRH-1$^{flox/flox}$	LRH-1^{IeKO}	P value
Cholesterol (mg/dl)	156 ± 4.0	125 ± 2.4	0.033	109 ± 3.5	115 ± 6.3	0.70
Triglycerides (mg/dl)	140 ± 6.8	122 ± 4.4	0.42	90.8 ± 2.4	97.8 ± 5.2	0.57
Free fatty acids (mmol/L)	0.71 ± 0.01	0.74 ± 0.02	0.64	0.58 ± 0.01	0.57 ± 0.02	0.81
Bile acids (μmol/L)	5.5 ± 0.5	5.3 ± 0.1	0.88	4.2 ± 0.2	4.5 ± 0.2	0.61
Glucose (mmol/L)	17.1 ± 0.5	16.1 ± 0.4	0.57	17.6 ± 0.3	19.7 ± 0.8	0.27
Aspartate aminotransferase (U/L)	43 ± 0.8	37.8 ± 0.5	0.055	44 ± 0.2	41.3 ± 0.4	0.033
Alanine aminotransferase (U/L)	40.3 ± 1.5	38.4 ± 0.9	0.69	34.6 ± 0.4	33.3 ± 0.7	0.46
Hepatic cholesterol (mg/g)	2.8 ± 0.1	2.7 ± 0.1	0.34	2.1 ± 0.15	2.5 ± 0.15	0.080
Hepatic triglyceride (mg/g)	10.3 ± 1.7	7.0 ± 0.6	0.092	9.8 ± 1.5	9.0 ± 1.5	0.73

Table 3-3. Plasma and liver parameters in LRH-1-deficient mice

Plasma parameters were measured in mice fasted for 4 hours, n=4-6/group. Data are shown SEM.

Lrh-1$^{flox/flox}$;Alb-cre mice, this difference was not statistically significant (Table 3-4). In

contrast, CYP8B1 mRNA levels were decreased >10-fold in the Lrh-1$^{flox/flox}$;Alb-cre mice,

demonstrating differential effects of LRH-1 on CYP7A1 and CYP8B1. There was also a

dramatic decrease in SHP mRNA in Lrh-1$^{flox/flox}$;Alb-cre mice (Table 3-4). Significant

decreases were also seen in the mRNAs encoding FXR, the bile acid biosynthetic enzyme

CYP27A1, the scavenger receptor B1, and the transporters ABCG5, ABCG8, bile salt

export pump (BSEP), multi-drug resistance transporter 2 (MDR2; also known as

ABCB4), multidrug resistance protein (MRP2; also known as ABCC2), MRP3 (also

known as ABCC3), and the sodium-dependent bile acid cotransporter (NTCP; also

known as SLC10A1) (Table 3-4). Thus, LRH-1 has widespread effects on genes

involved in cholesterol and bile acid homeostasis. There were no significant changes in

the mRNA levels of apolipoprotein A1, CYP7B1, HMG-CoA synthase 1, HMG-CoA

reductase, and hepatocyte nuclear factor 4α (HNF4α).

We also examined the effect of LRH-1 deficiency in hepatocytes on gene

expression in ileum. There were significant increases in mRNAs encoding FXR and

decreases of fibroblast growth factor 15 (FGF15), a hormone secreted from the small

intestine that is required for FXR-mediated feedback repression of CYP7A1 (Inagaki et

al., 2005; Kim et al., 2007) (Table 3-5). There were also trends towards increased mRNA

levels of ABCG8, OSTα, and SR-B1.

Effects of LRH-1 deficiency in intestinal epithelium. We next examined the

effect of eliminating LRH-1 in the intestinal epithelium on the expression of genes

involved in bile acid and cholesterol homeostasis. mRNA was prepared from the ileal

epithelium of Lrh-1$^{flox/flox}$;Vil-Cre and control Lrh-1$^{flox/flox}$;+ mice. SHP mRNA was

Gene	$Lrh-1^{flox/flox};Alb\text{-}Cre\,/Lrh-1^{flox/flox}$ ±SEM	P value	
ABCG5	0.41 ± 0.05	0.001	↓
ABCG8	0.38 ± 0.03	0.001	↓
APOA1	0.88 ± 0.07	0.21	
BSEP	0.71 ± 0.08	0.037	↓
CYP27A1	0.82 ± 0.03	0.030	↓
CYP7A1	1.6 ± 0.2	0.14	
CYP7B1	1.6 ± 0.4	0.15	
CYP8B1	0.090 ± 0.012	0.002	↓
FXR	0.53 ± 0.010	0.031	↓
HMGCR	0.80 ± 0.16	0.38	
HMGCS1	0.71 ± 0.09	0.25	
HNF4α	0.92 ± 0.07	0.61	
MDR2	0.46 ± 0.03	<0.000	↓
MRP2	0.60 ± 0.05	< 0.000	↓
MRP3	0.15 ± 0.03	< 0.000	↓
NTCP	0.42 ± 0.03	< 0.000	↓
SHP	0.033 ± 0.006	< 0.000	↓
SR-B1	0.50 ± 0.02	< 0.000	↓

Table 3-4. Liver gene expression in mice deficient for LRH-1 in liver

Data are shown ± SEM, n=6-7 mice/group. Significant changes are indicated by arrows. HMGCR, HMG-CoA reductase; HMGCS1, HMG-CoA synthase 1.

Gene	$Lrh-1^{flox/flox}$;$Alb-Cre$ /$Lrh-1^{flox/flox}$ ±SEM	P value	
ABCG5	1.0 ± 0.03	0.63	
ABCG8	1.5 ± 0.2	0.080	
ASBT	2.3 ± 0.7	0.17	
FGF15	0.49 ± 0.13	0.047	↓
FXR	2.0 ± 0.2	0.002	↑
HNF4α	1.2 ± 0.1	0.18	
IBABP	1.0 ± 0.1	0.84	
OSTα	1.6 ± 0.2	0.058	
OSTβ	0.74 ± 0.02	0.15	
SHP	0.65 ± 0.26	0.52	
SR-B1	1.8 ± 0.3	0.077	

Table 3-5. Intestinal gene expression in mice deficient for LRH-1 in liver

Data are shown ± SEM, n=6-7 mice/group. Significant changes are indicated by arrows

reduced ~10-fold in ilea of *Lrh-1^{flox/flox};Vil-Cre* mice (Table 3-6). The absence of LRH-1 also caused significant reductions in the mRNA levels of ileal bile acid binding protein (IBABP) and FGF15 (Table 3-6), which have not been previously described as LRH-1 target genes. Trends toward decreased expression were also observed for the mRNAs encoding ASBT, OSTα and OSTβ, which have been shown to be regulated directly by LRH-*1 in vitro* (Chen et al., 2003; Frankenberg et al., 2006).

No significant changes were seen in hepatic gene expression in *Lrh-1^{flox/flox};Vil-Cre* mice although there was a strong trend towards decreased FXR mRNA (Table 3-7). Although there was a 2-fold decrease in FGF15 mRNA in the intestine of *Lrh-1^{flox/flox};Vil-Cre* mice, there was no corresponding increase in CYP7A1 expression (Table 3-7).

Effects of LRH-1 deficiency on the bile acid pool. The effect of LRH-1 deficiency on bile acid pool size and composition was analyzed. In *Lrh-1^{flox/flox};Alb-Cre* mice, there was no change in the bile acid pool size but a marked change in its composition (Figure 3-7A and B). Compared to control *Lrh-1^{flox/flox};+* mice, bile from *Lrh-1^{flox/flox};Alb-Cre* mice contained significantly higher concentrations of tauro-β-muricholic acid (tBMCA) and tauro-chenodeoxycholic acid (tCDCA) and lower taurocholic acid (tCA) concentrations (Figure 3-7B). This altered profile is consistent with the decreased levels of CYP8B1 mRNA levels in *Lrh-1^{flox/flox};Alb-Cre* mice (Table 3-4). *Lrh-1^{flox/flox};Vil-Cre* mice had no significant changes in either bile acid pool size or composition (Figure 3-7C and D). No change was seen in fecal bile acid excretion in either the *Lrh-1^{flox/flox};Alb-Cre* or *Lrh-1^{flox/flox};Vil-Cre* mice (Figure 3-7E and F).

Gene	*Lrh-1*$Lrh\text{-}1^{flox/flox};Vil\text{-}Cre\,/Lrh\text{-}1^{flox/flox}$ ±SEM	P value	
ABCG5	1.2 ± 0.1	0.39	
ABCG8	1.2 ± 0.5	0.49	
ASBT	0.55 ± 0.14	0.073	
FGF15	0.49 ± 0.08	0.041	↓
FXR	1.2 ± 0.1	0.30	
HNF4α	1.2 ± 0.1	0.16	
IBABP	0.19 ± 0.05	0.010	↓
OSTα	0.56 ± 0.09	0.098	
OSTβ	0.60 ± 0.09	0.058	
SHP	0.10 ± 0.04	0.002	↓
SR-B1	0.78 ± 0.18	0.37	

Table 3-6. Intestinal gene expression in mice deficient for LRH-1 in intestine

Data are shown ± SEM, n=7-8 mice/group. Significant changes are indicated by arrows.

Gene	*Lrh-1$^{flox/flox}$;Vil-Cre /Lrh-1$^{flox/flox}$* ±SEM	P value
ABCG5	1.1 ± 0.2	0.75
ABCG8	1.0 ± 0.2	0.99
APOA1	1.0 ± 0.2	0.87
BSEP	1.3 ± 0.1	0.062
CYP27A1	0.90 ± 0.17	0.60
CYP7A1	0.75 ± 0.21	0.56
CYP7B1	1.2 ± 0.4	0.69
CYP8B1	1.0 ± 0.1	0.88
FXR	0.79 ± 0.11	0.053
HMGCR	1.4 ± 0.5	0.48
HMGCS1	0.85 ± 0.14	0.61
HNF4α	1.2 ± 0.1	0.21
MDR2	1.1 ± 0.2	0.41
MRP2	1.1 ± 0.2	0.75
MRP3	0.84 ± 0.11	0.37
NTCP	1.1 ± 0.1	0.64
SHP	0.81 ± 0.12	0.20
SR-B1	1.2 ± 0.2	0.38

Table 3-7. Liver gene expression in mice deficient for LRH-1 in intestine

Data are shown ± SEM, n=7-8 mice/group. HMGCR, HMG-CoA reductase; HMGCS1, HMG-CoA synthase 1.
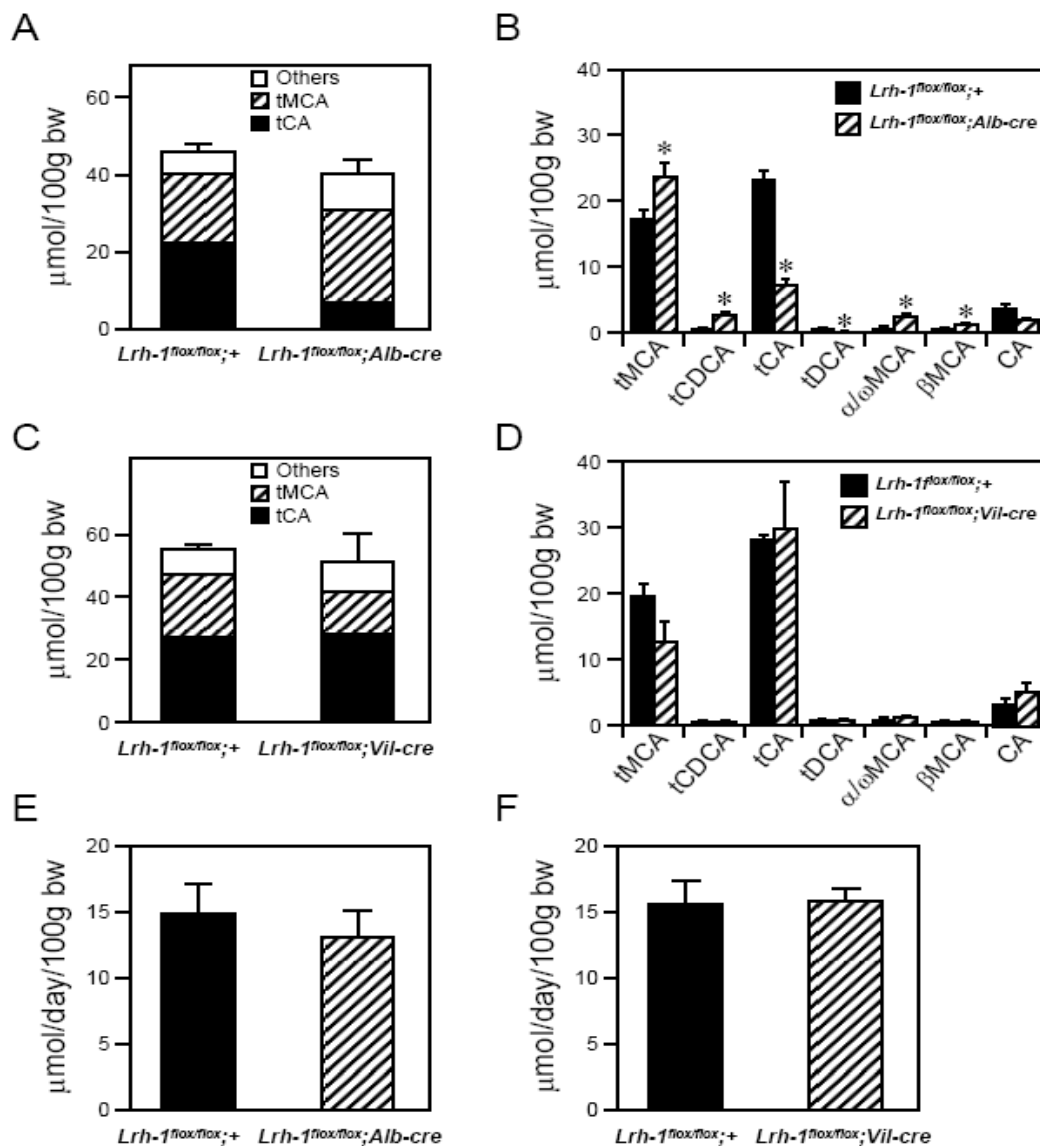
Figure 3-6. Effects of LRH-1 deficiency in liver or intestine on bile acid pool size and composition. **(A-D)** Bile acid pool size and composition were measured in either *Lrh-1flox/flox;Alb-Cre* **(panels A and B)** or *Lrh-1flox/flox;Vil-Cre* mice **(panels C and D)** and corresponding *Lrh-1*flox/flox mice. All bile acid species shown in Table 3-1 were measured but only those at concentration >1 μmol/100 g body weight (bw) are shown. **(E and F)** Fecal bile acid excretion was measured in either *Lrh-1flox/flox;Alb-Cre* **(panel E)** or *Lrh-1flox/flox;Vil-Cre* mice **(panel F)** and corresponding *Lrh-1*flox/flox mice. Data are the mean ± SEM (n=4-6 male mice/group).

Effects of activating FXR on gene expression in *Lrh-1^flox/flox^;Alb-Cre* and *Lrh-1^flox/flox^;Vil-Cre* mice. It is proposed that hepatic LRH-1 plays a central role in FXR-mediated repression of CYP7A1 and CYP8B1 (Goodwin et al., 2000; Lu et al., 2000). To address this hypothesis directly, *Lrh-1^flox/flox^;Alb-cre* and control *Lrh-1^flox/flox^;+* mice were administered the potent, selective FXR agonist GW4064 for 14 hours, at which point the mice were killed and CYP7A1 and CYP8B1 mRNA levels measured by RT-qPCR. Surprisingly, CYP7A1 was repressed as efficiently in *Lrh-1^flox/flox^;Alb-cre* mice as in *Lrh-1^flox/flox^;+* control mice (Figure 3-8A). CYP8B1 was also repressed by GW4064 in *Lrh-1^flox/flox^;Alb-cre* mice, although the fold repression was reduced relative to that seen in control mice due to the decrease in basal mRNA levels in the *Lrh-1^flox/flox^;Alb-cre* mice (Figure 3-8B). GW4064 also efficiently repressed CYP7A1 and CYP8B1 expression in livers of *Lrh-1^flox/flox^;Vil-Cre* mice (Figure 3-8D and E).

The efficient repression of CYP7A1 by GW4064 in *Lrh-1^flox/flox^;Alb-cre* and *Lrh-1^flox/flox^;Vil-Cre* mice was particularly surprising in light of the decreased expression of hepatic SHP in the *Lrh-1^flox/flox^;Alb-cre* mice and intestinal FGF15 in the *Lrh-1^flox/flox^;Vil-Cre* mice (Tables 3-4 and 3-6). However, GW4064 administration caused marked increases in hepatic SHP mRNA in *Lrh-1^flox/flox^;Alb-cre* and *Lrh-1^flox/flox^;Vil-Cre* mice (Figure 3-8C and F) and intestinal FGF15 in *Lrh-1^flox/flox^;Alb-cre* and *Lrh-1^flox/flox^;Vil-Cre* mice (Figure 3-9A and B). IBABP was also efficiently induced in ilea of *Lrh-1^flox/flox^;Vil-Cre* mice (Figure 3-9C). Thus, although LRH-1 contributes to the basal expression of SHP, IBABP and FGF15, it is not required for their efficient induction by FXR.
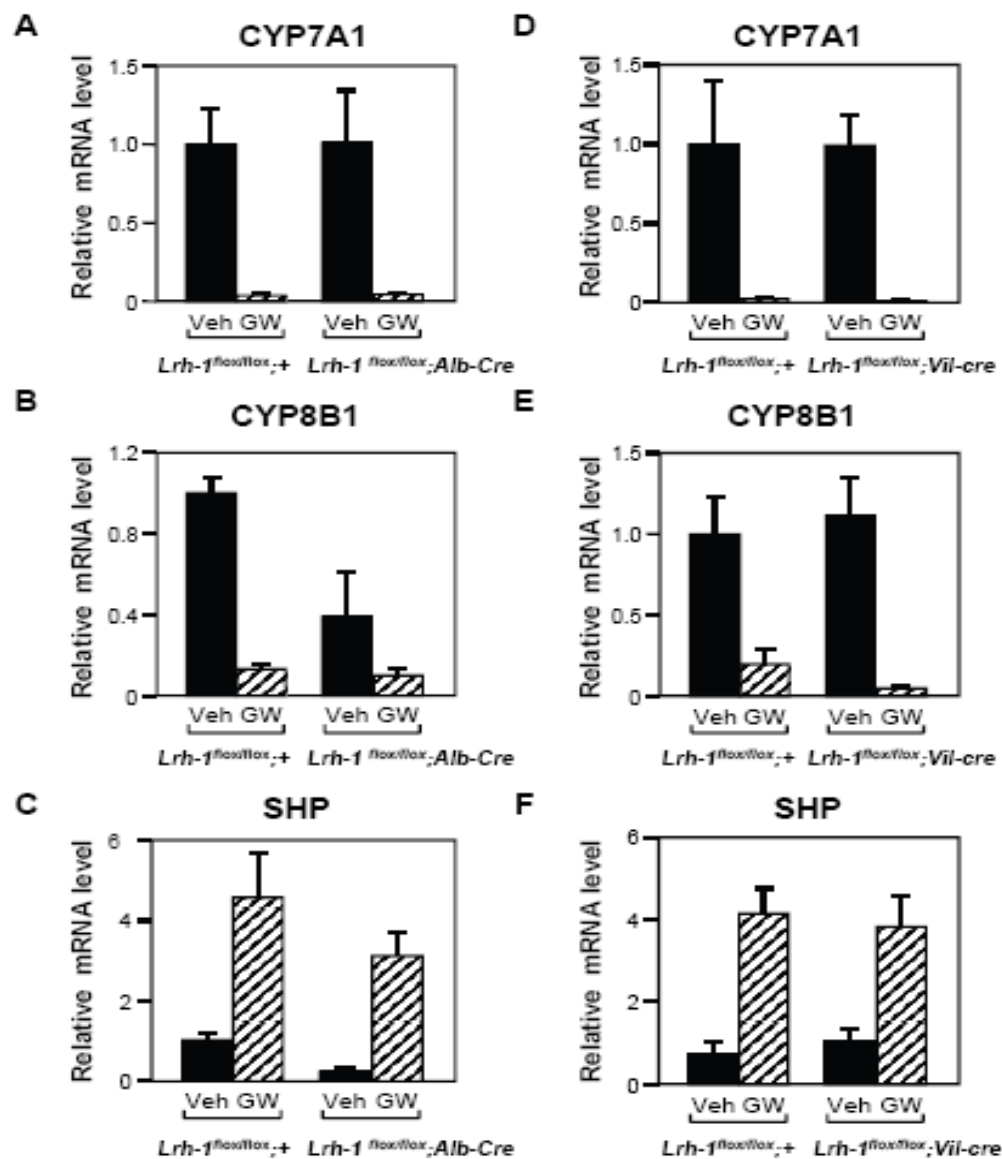
Figure 3-7. **Effect of FXR activation on gene expression in tissue-specific LRH-1 deficient mice in liver.** *Lrh-1$^{flox/flox}$;Alb-cre*, *Lrh-1$^{flox/flox}$;Vil-cre*, and corresponding *Lrh-1*$^{flox/flox}$ mice were treated with vehicle (Veh) or GW4064 (GW) for 14 hours and RNA was prepared from liver and ileum. RT-qPCR was used to measure mRNA levels of CYP7A1 **(panels A and D)**, CYP8B1 **(panel B and E)** , and SHP **(panel C and F)**. Data are the mean ± SEM (n=3-4 male mice/group).
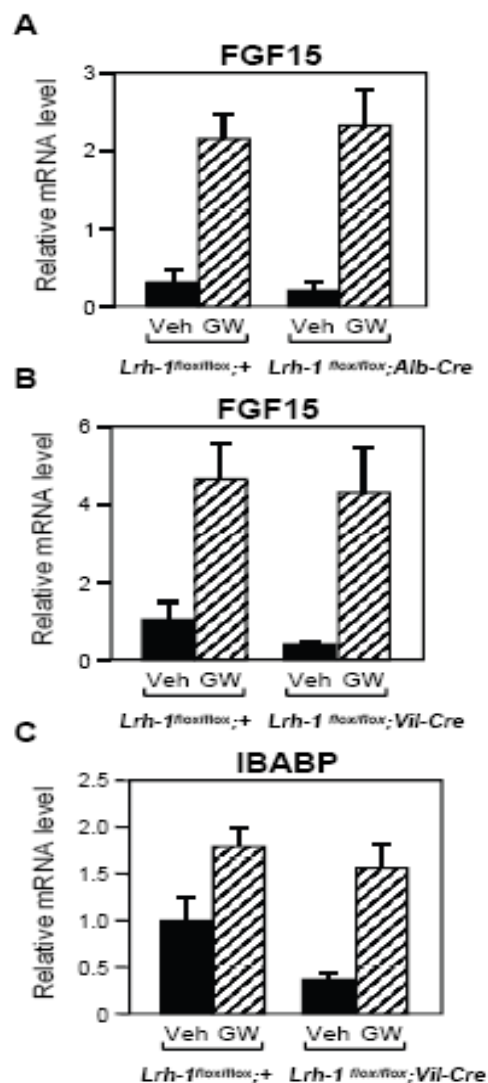
Figure 3-8. Effect of FXR activation on gene expression in tissue-specific LRH-1 deficient mice in intestine. **(A-C)** *Lrh-1^{flox/flox};Alb-cre*, *Lrh-1^{flox/flox};Vil-cre*, and corresponding *Lrh-1*^{flox/flox} mice were treated with vehicle (Veh) or GW4064 (GW) for 14 hours and RNA prepared from liver and ileum. RT-qPCR was used to measure mRNA levels of FGF15 in *Lrh-1^{flox/flox};Alb-cre* **(panel A)** and FGF15 and IBABP *Lrh-1^{flox/flox};Vil-cre* **(panel B and C)**. Data are the mean ± SEM (n=3-4 male mice/group).

LRH-1 activation of FGF15 expression. The absence of LRH-1 in hepatocytes and intestinal epithelium caused a 2-fold reduction in the mRNA levels of FGF15 (Tables 3-5 and 3-6), which has not been previously described as a LRH-1 target gene. To determine whether LRH-1 regulates FGF15 transcription directly, a candidate LRH-1 response element (FGF15LRHRE) located in the second exon of the FGF15 gene was cloned and inserted into a luciferase reporter plasmid driven by the SV40 promoter. Results from cotransfection assays performed with VP16LRH-1 or LRH-1 expression plasmids demonstrated that LRH-1 induced reporter expression (Figure 3-10A). The induction in promoter activity was even greater when two copies of the FGF15LRHRE were inserted into the reporter plasmid. This response was decreased by either co-transfecting SHP or muatating the LRHRE (Figure 3-10B). To test whether LRH-1 binds directly to the FGF15LRHRE, electrophoretic mobility-shift assays (EMSA) were performed. *In vitro* translated LRH-1 bound to radiolabeled FGF15LRHRE. This complex was competed by wild type unlabeled FGF15LRHE oligonucleotide but not by a mutated derivative (Figure 3-11). These results suggest that LRH-1 regulates FGF15 transcription directly.
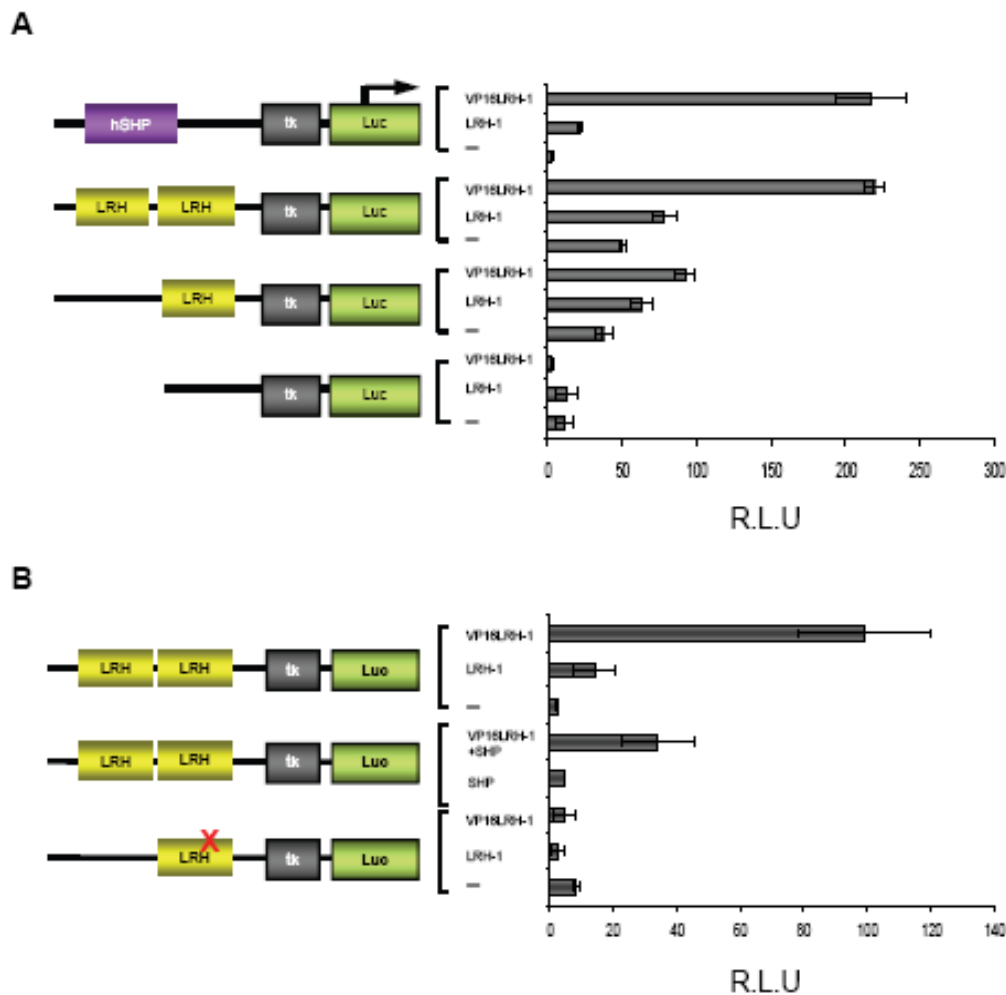
Figure 3-10. LRH-1 activates *Fgf15* promoter.

(A and B) Transfection assays were performed using the tk-luc reporters shown on the left. Reporter plasmids were transfected into either COS7 cells **(panel A)** or HEK293 cells **(panel B)** and luciferase activities were measured. SHP reporter was used as a positive control in the assay. Data are the mean of assays performed in triplicate ± SD.
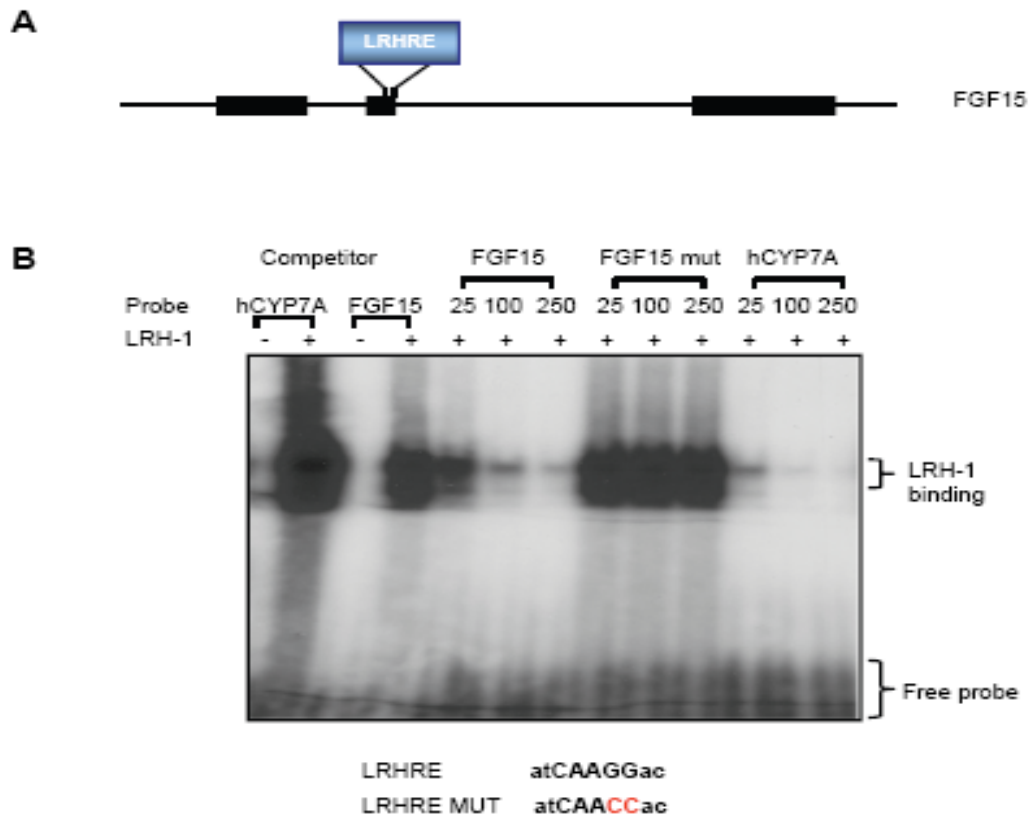
Figure 3-11. LRH-1 binds to *Fgf15* promoter

(**A**) Schematic repesentation of the FGF15 gene. The three exons are indicated as black rectangles. The position of LRHRE motif in exon 2 are shown. (**B**) EMSAs were done using [^{32}P]-labeled *Fgf15* LRHRE oligonucleotide as probe and *in vitro* synthesized mouse LRH-1 as indicated. The position of LRH-1 binding is indicated on the right. Competition reactions were done using 25-fold, 100-fold, or 500-fold excess of unlabeled *CYP7A1*, *Fgf15*, or mutant *Fgf15* LRHRE. Mutated sequences in LRHRE oligonucleotides are shown by red.

3.5 Discussion

LRH-1 is implicated in the regulation of many genes involved in cholesterol and bile acid homeostasis (Fayard et al., 2004). On the *CYP7A1* gene, LRH-1 is proposed to serve both as a positive-acting basal transcription factor and as a docking site for the transcriptional repressor SHP, which is induced by bile acids through an FXR-dependent mechanism (Goodwin et al., 2000; Lu et al., 2000). The role of SHP in repressing *Cyp7a1* has been validated *in vivo* using *Shp* knockout mice (Kerr et al., 2002; Wang et al., 2002). While LRH-1 was identified in an unbiased screen as a major transcription factor bound to the *CYP7A1* promoter (Nitta et al., 1999) and several studies have shown that LRH-1 can regulate *CYP7A1* either *in vitro* or *in vivo* (del Castillo-Olivares et al., 2004; del Castillo-Olivares and Gil, 2000; Goodwin et al., 2000; Lu et al., 2000; Pare et al., 2004b), a comprehensive analysis of LRH-1 function *in vivo* has been hampered by the lack of *Lrh-1* knockout mice. In this study, we show the generation and characterization of mice deficient for LRH-1 in hepatocytes and intestinal epithelium.

A surprising outcome of this study was that LRH-1 deficiency in hepatocytes had no significant effect on either basal *Cyp7a1* expression or its repression by FXR. This was unexpected given that LRH-1 binds to the murine *Cyp7a1* promoter as measured by chromatin immunoprecipitation assays (Boulias et al., 2005), and LRH-1 haploinsufficiency or overexpression affects hepatic CYP7A1 mRNA levels in mice (del Castillo-Olivares et al., 2004; Pare et al., 2004b). There are at least two possible explanations for these data. First, LRH-1 may not regulate *Cyp7a1* or play a relatively minor role. Alternatively, there may be a redundant factor or compensatory response in the *Lrh-1^{flox/flox};Alb-cre* mice that maintains *Cyp7a1* regulation in the absence of LRH-1.

One possible candidate for mediating a compensatory response is HNF4α, which binds to the same composite response element in the *CYP7A1* promoter as LRH-1 and, like LRH-1, is repressed by SHP *in vitro* (Lee et al., 2000). Mice deficient for HNF4α in liver have decreased CYP7A1 mRNA and protein levels during the dark cycle (Inoue et al., 2006). Although no significant changes in HNF4α mRNA levels were seen in *Lrh-1$^{flox/flox}$;Alb-cre* mice, additional studies will be needed to determine the role of HNF4α and its relationship with LRH-1 in regulating both basal expression and FXR-mediated repression of *CYP7A1*. Additional studies will also be required to determine whether our findings in mice are relevant in other species, including humans. There are well established species differences in the regulation of *CYP7A1*, especially with regard to its modulation by cholesterol metabolites (Agellon et al., 2002; Chiang et al., 2001; Goodwin et al., 2003; Horton et al., 1995; Jelinek et al., 1990; Pandak et al., 1991; Rudel et al., 1994; Xu et al., 1995). Thus, LRH-1 may be important for the regulation of *CYP7A1* in other species.

In contrast to CYP7A1, basal CYP8B1 mRNA levels were significantly reduced in mice deficient for LRH-1 in liver. The change in CYP8B1 expression was accompanied by a corresponding increase in the fraction of tBMCA in the bile acid pool. Like CYP7A1, FXR-mediated repression of CYP8B1 still occurred in the *Lrh-1$^{flox/flox}$;Alb-cre* mice. These data demonstrate an important role for LRH-1 in determining the composition of the bile acid pool through effects on CYP8B1 expression. They also reveal marked differences in the regulation of CYP7A1 and CYP8B1. The differential regulation of CYP7A1 and CYP8B1 was also recently highlighted by Kim et al. (Kim et

al., 2007), who showed that CYP7A1 is repressed more efficiently than CYP8B1 by FGF15.

In the *Lrh-1^{flox/flox};Alb-cre* mice, there were significant decreases in the hepatic mRNA levels of SHP, CYP27A1, SR-B1, ABCG5, ABCG8, BSEP, MDR2, MRP2, MRP3 and NTCP. Several different mechanisms may contribute to their decreased expression. First, LRH-1 may regulate these genes directly. In the case of SHP, MRP3, ABCG5, ABCG8 and SR-B1, binding sites for LRH-1 have been identified in the gene regulatory regions (Freeman et al., 2004; Goodwin et al., 2000; Inokuchi et al., 2001; Lu et al., 2000; Schoonjans et al., 2002). The decreased expression of a subset of these genes may be due also to changes in the activity of FXR, which directly regulates the SHP, BSEP, and MRP2 genes (Ananthanarayanan et al., 2001; Goodwin et al., 2000; Kast et al., 2002; Lu et al., 2000). FXR mRNA levels were decreased ~2 fold in livers of *Lrh-1^{flox/flox};Alb-cre* mice. Furthermore, it was previously shown that cholic acid is an important endogenous agonist for FXR in mice (Li-Hawkins et al., 2002). In *Lrh-1^{flox/flox};Alb-cre* mice, the reduction in CYP8B1 mRNA and resulting decrease in biliary cholic acid may contribute to the reduced hepatic expression of genes that are regulated by FXR. Thus, decreases in both FXR levels and its endogenous ligands could contribute to the altered hepatic gene expression in *Lrh-1^{flox/flox};Alb-cre* mice.

LRH-1 also appears to have both direct and indirect effects on gene expression in ileum. In *Lrh-1^{flox/flox};Vil-Cre* mice, SHP, IBABP and FGF15 mRNA levels were significantly decreased in ileum, and there were trends towards decreased expression of OSTα, OSTβ, and ASBT. Whereas SHP, OSTα, OSTβ and ASBT have been shown previously to be regulated directly by LRH-1 *in vitro* (Chen et al., 2003; Frankenberg et

al., 2006; Goodwin et al., 2000; Lu et al., 2000), IBABP and FGF15 have not. Notably, FGF15 mRNA was also decreased in ilea of mice deficient for LRH-1 in liver. The results from transient transfection and EMSA experiments with a candidate LRHRE in the FGF15 gene suggest that LRH-1 controls FGF15 expression directly at the transcriptional level. However, chromatin immunoprecipitation assays (ChIP) are required to determine definitively whether LRH-1 associates with the FGF15 promoter *in vivo*. Since FGF15 is also regulated strongly by FXR (Inagaki et al., 2005; Li et al., 2005a), its reduced expression in *Lrh-1^{flox/flox};Alb-Cre* mice may be due to the aforementioned reduction in FXR agonist activity. However, since SHP and IBABP are also FXR target genes (Goodwin et al., 2000; Grober et al., 1999; Lu et al., 2000), it is surprising that their mRNA levels were not also significantly decreased in the *Lrh-1^{flox/flox};Alb-Cre* mice.

Mataki et al. reported the characterization of mice in which exons 4 and 5 of the LRH-1 gene were deleted in hepatocytes using a tamoxifen-inducible cre (Mataki et al., 2007). While their findings are similar in many respects to ours with the *Lrh-1^{flox/flox};Alb-Cre* mice, they did not investigate the effect of LRH-1 deficiency on feedback regulation of bile acid synthesis nor did they generate mice lacking LRH-1 in the intestinal epithelium. Notably, they reported significant increases in fecal bile acid excretion in their LRH-1-deficient mice that were not seen in the current study. Moreover, they did not see the modest decrease in plasma cholesterol that we observed in the *Lrh-1^{flox/flox};Alb-Cre* mice. The basis for these differences is not clear but could relate to either the different strategies used to disrupt *Lrh-1* or the different background strains.

In summary, this study revealed that hepatic LRH-1 plays a major role in determining the composition of the bile acid pool through effects on CYP8B1 expression but that, surprisingly, it is not essential for FXR-mediated feedback regulation of CYP7A1.

3.6 Reference

Agellon, L.B., Drover, V.A., Cheema, S.K., Gbaguidi, G.F., and Walsh, A. (2002). Dietary cholesterol fails to stimulate the human cholesterol 7alpha-hydroxylase gene (CYP7A1) in transgenic mice. J Biol Chem *277*, 20131-20134.

Alrefai, W.A. and Gill, R.K. (2007). Bile acid transporters: Structure, function, regulation and pathopysiological implication. Pharmaceutical Res *24*, 1803-1823.

Alican, I., and Kubes, P. (1996). A critical role for nitric oxide in intestinal barrier function and dysfunction. Am J Physiol *270*, G225-237.

Ananthanarayanan, M., Balasubramanian, N., Makishima, M., Mangelsdorf, D.J., and Suchy, F.J. (2001). Human bile salt export pump promoter is transactivated by the farnesoid X receptor/bile acid receptor. J Biol Chem *276*, 28857-28865.

Ang, S.L., Wierda, A., Wong, D., Stevens, K.A., Cascio, S., Rossant, J., and Zaret, K.S. (1993). The formation and maintenance of the definitive endoderm lineage in the mouse: involvement of HNF3/forkhead proteins. Development *119*, 1301-1315.

Annicotte, J.S., Fayard, E., Swift, G.H., Selander, L., Edlund, H., Tanaka, T., Kodama, T., Schoonjans, K., and Auwerx, J. (2003). Pancreatic-duodenal homeobox 1 regulates expression of liver receptor homolog 1 during pancreas development. Mol Cell Biol *23*, 6713-6724.

Aranda, A., and Pascual, A. (2001). Nuclear hormone receptors and gene expression. Physiol Rev *81*, 1269-1304.

Batlle, E., Henderson, J.T., Beghtel, H., van den Born, M.M., Sancho, E., Huls, G., Meeldijk, J., Robertson, J., van de Wetering, M., Pawson, T.*, et al.* (2002). Beta-catenin and TCF mediate cell positioning in the intestinal epithelium by controlling the expression of EphB/ephrinB. Cell *111*, 251-263.

Becker-Andre, M., Andre, E., and DeLamarter, J.F. (1993). Identification of nuclear receptor mRNAs by RT-PCR amplification of conserved zinc-finger motif sequences. Biochem Biophys Res Commun *194*, 1371-1379.

Bennin, D.A., Don, A.S., Brake, T., McKenzie, J.L., Rosenbaum, H., Ortiz, L., DePaoli-Roach, A.A., and Horne, M.C. (2002). Cyclin G2 associates with protein phosphatase 2A catalytic and regulatory B' subunits in active complexes and induces nuclear aberrations and a G1/S phase cell cycle arrest. J Biol Chem *277*, 27449-27467.

Berg, R.D. (1995). Bacterial translocation from the gastrointestinal tract. Trends Microbiol *3*, 149-154.

Biet, F., Locht, C., and Kremer, L. (2002). Immunoregulatory functions of interleukin 18 and its role in defense against bacterial pathogens. J Mol Med *80*, 147-162.

Bookout, A.L., Jeong, Y., Downes, M., Yu, R.T., Evans, R.M., and Mangelsdorf, D.J. (2006). Anatomical profiling of nuclear receptor expression reveals a hierarchical transcriptional network. Cell *126*, 789-799.

Bookout, A.L., and Mangelsdorf, D.J. (2003). Quantitative real-time PCR protocol for analysis of nuclear receptor signaling pathways. Nucl Recept Signal *1*, e012.

Botrugno, O.A., Fayard, E., Annicotte, J.S., Haby, C., Brennan, T., Wendling, O., Tanaka, T., Kodama, T., Thomas, W., Auwerx, J.*, et al.* (2004). Synergy between LRH-1 and beta-catenin induces G1 cyclin-mediated cell proliferation. Mol Cell *15*, 499-509.

Boulias, K., Katrakili, N., Bamberg, K., Underhill, P., Greenfield, A., and Talianidis, I. (2005). Regulation of hepatic metabolic pathways by the orphan nuclear receptor SHP. Embo J *24*, 2624-2633.

Brakenhoff, R.H., Gerretsen, M., Knippels, E.M., van Dijk, M., van Essen, H., Weghuis, D.O., Sinke, R.J., Snow, G.B., and van Dongen, G.A. (1995). The human E48 antigen, highly homologous to the murine Ly-6 antigen ThB, is a GPI-anchored molecule apparently involved in keratinocyte cell-cell adhesion. J Cell Biol *129*, 1677-1689.

Burkard, I., von Eckardstein, A., and Rentsch, K.M. (2005). Differentiated quantification of human bile acids in serum by high-performance liquid chromatography-tandem mass spectrometry. J Chromatogr B Analyt Technol Biomed Life Sci *826*, 147-159.

Cahill, C.J. (1983). Prevention of postoperative renal failure in patients with obstructive jaundice--the role of bile salts. Br J Surg *70*, 590-595.

Cahill, C.J., Pain, J.A., and Bailey, M.E. (1987). Bile salts, endotoxin and renal function in obstructive jaundice. Surg Gynecol Obstet *165*, 519-522.

Chalkiadaki, A., and Talianidis, I. (2005). SUMO-dependent compartmentalization in promyelocytic leukemia protein nuclear bodies prevents the access of LRH-1 to chromatin. Mol Cell Biol *25*, 5095-5105.

Chawla, A., Repa, J.J., Evans, R.M., and Mangelsdorf, D.J. (2001). Nuclear receptors and lipid physiology: opening the X-files. Science *294*, 1866-1870.

Chen, F., Ma, L., Dawson, P.A., Sinal, C.J., Sehayek, E., Gonzalez, F.J., Breslow, J., Ananthanarayanan, M., and Shneider, B.L. (2003). Liver receptor homologue-1 mediates species- and cell line-specific bile acid-dependent negative feedback regulation of the apical sodium-dependent bile acid transporter. J Biol Chem *278*, 19909-19916.

Chesnokova, V., Kovacs, K., Castro, A.V., Zonis, S., and Melmed, S. (2005). Pituitary hypoplasia in Pttg-/- mice is protective for Rb+/- pituitary tumorigenesis. Mol Endocrinol *19*, 2371-2379.

Chiang, J.Y. (2002). Bile acid regulation of gene expression: roles of nuclear hormone receptors. Endocr Rev *23*, 443-463.

Chiang, J.Y., Kimmel, R., and Stroup, D. (2001). Regulation of cholesterol 7alpha-hydroxylase gene (CYP7A1) transcription by the liver orphan receptor (LXRalpha). Gene *262*, 257-265.

Clements, W.D., Parks, R., Erwin, P., Halliday, M.I., Barr, J., and Rowlands, B.J. (1996). Role of the gut in the pathophysiology of extrahepatic biliary obstruction. Gut *39*, 587-593.

Coste, A., Dubuquoy, L., Barnouin, R., Annicotte, J.S., Magnier, B., Notti, M., Corazza, N., Antal, M.C., Metzger, D., Desreumaux, P.*, et al.* (2007). LRH-1-mediated glucocorticoid synthesis in enterocytes protects against inflammatory bowel disease. Proc Natl Acad Sci U S A *104*, 13098-13103.

Cui, J., Heard, T.S., Yu, J., Lo, J.L., Huang, L., Li, Y., Schaeffer, J.M., and Wright, S.D. (2002). The amino acid residues asparagine 354 and isoleucine 372 of human farnesoid X receptor confer the receptor with high sensitivity to chenodeoxycholate. J Biol Chem *277*, 25963-25969.

Culjkovic, B., Topisirovic, I., and Borden, K.L. (2007). Controlling gene expression through RNA regulons: the role of the eukaryotic translation initiation factor eIF4E. Cell Cycle *6*, 65-69.

Darimont, B.D., Wagner, R.L., Apriletti, J.W., Stallcup, M.R., Kushner, P.J., Baxter, J.D., Fletterick, R.J., and Yamamoto, K.R. (1998). Structure and specificity of nuclear receptor-coactivator interactions. Genes Dev *12*, 3343-3356.

Deitch, E.A., Sittig, K., Li, M., Berg, R., and Specian, R.D. (1990). Obstructive jaundice promotes bacterial translocation from the gut. Am J Surg *159*, 79-84.

del Castillo-Olivares, A., Campos, J.A., Pandak, W.M., and Gil, G. (2004). The role of alpha1-fetoprotein transcription factor/LRH-1 in bile acid biosynthesis: a known nuclear receptor activator that can act as a suppressor of bile acid biosynthesis. J Biol Chem *279*, 16813-16821.

del Castillo-Olivares, A., and Gil, G. (2000). Role of FXR and FTF in bile acid-mediated suppression of cholesterol 7alpha-hydroxylase transcription. Nucleic Acids Res *28*, 3587-3593.

Ding, J.W., Andersson, R., Norgren, L., Stenram, U., and Bengmark, S. (1992). The influence of biliary obstruction and sepsis on reticuloendothelial function in rats. Eur J Surg *158*, 157-164.

Ding, J.W., Andersson, R., Soltesz, V., Willen, R., and Bengmark, S. (1993). The role of bile and bile acids in bacterial translocation in obstructive jaundice in rats. Eur Surg Res *25*, 11-19.

Ding, J.W., Andersson, R., Soltesz, V., Willen, R., and Bengmark, S. (1994). Obstructive jaundice impairs reticuloendothelial function and promotes bacterial translocation in the rat. J Surg Res *57*, 238-245.

Downes, M., Verdecia, M.A., Roecker, A.J., Hughes, R., Hogenesch, J.B., Kast-Woelbern, H.R., Bowman, M.E., Ferrer, J.L., Anisfeld, A.M., Edwards, P.A., *et al.* (2003). A chemical, genetic, and structural analysis of the nuclear bile acid receptor FXR. Mol Cell *11*, 1079-1092.

Dyer, K.D., and Rosenberg, H.F. (2005). The mouse RNase 4 and RNase 5/ang 1 locus utilizes dual promoters for tissue-specific expression. Nucleic Acids Res *33*, 1077-1086.

Edwards, C.M., and Chapman, S.J. (2007). Biomechanical modelling of colorectal crypt budding and fission. Bull Math Biol *69*, 1927-1942.

Edwards, P.A., Kast, H.R., and Anisfeld, A.M. (2002). BAREing it all: the adoption of LXR and FXR and their roles in lipid homeostasis. J Lipid Res *43*, 2-12.

Ellinger-Ziegelbauer, H., Glaser, B., and Dreyer, C. (1995). A naturally occurring short variant of the FTZ-F1-related nuclear orphan receptor xFF1rA and interactions between domains of xFF1rA. Mol Endocrinol *9*, 872-886.

Ellinger-Ziegelbauer, H., Hihi, A.K., Laudet, V., Keller, H., Wahli, W., and Dreyer, C. (1994). FTZ-F1-related orphan receptors in Xenopus laevis: transcriptional regulators differentially expressed during early embryogenesis. Mol Cell Biol *14*, 2786-2797.

Evans, H.J., Torrealba, V., Hudd, C., and Knight, M. (1982). The effect of preoperative bile salt administration on postoperative renal function in patients with obstructive jaundice. Br J Surg *69*, 706-708.

Farley, F.W., Soriano, P., Steffen, L.S., and Dymecki, S.M. (2000). Widespread recombinase expression using FLPeR (flipper) mice. Genesis *28*, 106-110.

Fayard, E., Auwerx, J., and Schoonjans, K. (2004). LRH-1: an orphan nuclear receptor involved in development, metabolism and steroidogenesis. Trends Cell Biol *14*, 250-260.

Folch, J., Lees, M., and Sloane Stanley, G.H. (1957). A simple method for the isolation and purification of total lipides from animal tissues. J Biol Chem *226*, 497-509.

Forman, B.M., Goode, E., Chen, J., Oro, A.E., Bradley, D.J., Perlmann, T., Noonan, D.J., Burka, L.T., McMorris, T., Lamph, W.W., *et al.* (1995). Identification of a nuclear receptor that is activated by farnesol metabolites. Cell *81*, 687-693.

Frankenberg, T., Rao, A., Chen, F., Haywood, J., Shneider, B.L., and Dawson, P.A. (2006). Regulation of the mouse organic solute transporter alpha-beta, Ostalpha-Ostbeta, by bile acids. Am J Physiol Gastrointest Liver Physiol *290*, G912-922.

Freeman, L.A., Kennedy, A., Wu, J., Bark, S., Remaley, A.T., Santamarina-Fojo, S., and Brewer, H.B., Jr. (2004). The orphan nuclear receptor LRH-1 activates the ABCG5/ABCG8 intergenic promoter. J Lipid Res *45*, 1197-1206.

Galarneau, L., Pare, J.F., Allard, D., Hamel, D., Levesque, L., Tugwood, J.D., Green, S., and Belanger, L. (1996). The alpha1-fetoprotein locus is activated by a nuclear receptor of the Drosophila FTZ-F1 family. Mol Cell Biol *16*, 3853-3865.

Gao, D.M., Wang, L.F., Liu, J., Kong, Y.Y., Wang, Y., and Xie, Y.H. (2006). Expression of mouse liver receptor homologue 1 in embryonic stem cells is directed by a novel promoter. FEBS Lett *580*, 1702-1708.

Garcia-Tsao, G. (2004). Bacterial infections in cirrhosis. Can J Gastroenterol *18*, 405-406.

Giguere, V., Yang, N., Segui, P., and Evans, R.M. (1988). Identification of a new class of steroid hormone receptors. Nature *331*, 91-94.

Glass, C.K., and Rosenfeld, M.G. (2000). The coregulator exchange in transcriptional functions of nuclear receptors. Genes Dev *14*, 121-141.

Goodwin, B., Jones, S.A., Price, R.R., Watson, M.A., McKee, D.D., Moore, L.B., Galardi, C., Wilson, J.G., Lewis, M.C., Roth, M.E., *et al.* (2000). A regulatory cascade of the nuclear receptors FXR, SHP-1, and LRH-1 represses bile acid biosynthesis. Mol Cell *6*, 517-526.

Goodwin, B., Watson, M.A., Kim, H., Miao, J., Kemper, J.K., and Kliewer, S.A. (2003). Differential regulation of rat and human CYP7A1 by the nuclear oxysterol receptor liver X receptor-alpha. Mol Endocrinol *17*, 386-394.

Grober, J., Zaghini, I., Fujii, H., Jones, S.A., Kliewer, S.A., Willson, T.M., Ono, T., and Besnard, P. (1999). Identification of a bile acid-responsive element in the human ileal bile acid-binding protein gene. Involvement of the farnesoid X receptor/9-cis-retinoic acid receptor heterodimer. J Biol Chem *274*, 29749-29754.

Gu, P., Goodwin, B., Chung, A.C., Xu, X., Wheeler, D.A., Price, R.R., Galardi, C., Peng, L., Latour, A.M., Koller, B.H.*, et al.* (2005). Orphan nuclear receptor LRH-1 is required to maintain Oct4 expression at the epiblast stage of embryonic development. Mol Cell Biol *25*, 3492-3505.

Gupta, S., Stravitz, R.T., Dent, P., and Hylemon, P.B. (2001). Down-regulation of cholesterol 7alpha-hydroxylase (CYP7A1) gene expression by bile acids in primary rat hepatocytes is mediated by the c-Jun N-terminal kinase pathway. J Biol Chem *276*, 15816-15822.

Halmi, P., Lehtonen, J., Waheed, A., Sly, W.S., and Parkkila, S. (2004). Expression of hypoxia-inducible, membrane-bound carbonic anhydrase isozyme XII in mouse tissues. Anat Rec A Discov Mol Cell Evol Biol *277*, 171-177.

Haramis, A.P., Begthel, H., van den Born, M., van Es, J., Jonkheer, S., Offerhaus, G.J., and Clevers, H. (2004). De novo crypt formation and juvenile polyposis on BMP inhibition in mouse intestine. Science *303*, 1684-1686.

Heaney, A.P., Singson, R., McCabe, C.J., Nelson, V., Nakashima, M., and Melmed, S. (2000). Expression of pituitary-tumour transforming gene in colorectal tumours. Lancet *355*, 716-719.

Henry, G.L., and Melton, D.A. (1998). Mixer, a homeobox gene required for endoderm development. Science *281*, 91-96.

Hinshelwood, M.M., Repa, J.J., Shelton, J.M., Richardson, J.A., Mangelsdorf, D.J., and Mendelson, C.R. (2003). Expression of LRH-1 and SF-1 in the mouse ovary: localization in different cell types correlates with differing function. Mol Cell Endocrinol *207*, 39-45.

Hinshelwood, M.M., Shelton, J.M., Richardson, J.A., and Mendelson, C.R. (2005). Temporal and spatial expression of liver receptor homologue-1 (LRH-1) during embryogenesis suggests a potential role in gonadal development. Dev Dyn *234*, 159-168.

Hofmann, A.F. (1999). Bile Acids: The Good, the Bad, and the Ugly. News Physiol Sci *14*, 24-29.

Holman, J.M., Jr., Rikkers, L.F., and Moody, F.G. (1979). Sepsis in the management of complicated biliary disorders. Am J Surg *138*, 809-813.

Hooper, L.V., Stappenbeck, T.S., Hong, C.V., and Gordon, J.I. (2003). Angiogenins: a new class of microbicidal proteins involved in innate immunity. Nat Immunol *4*, 269-273.

Horb, M.E., and Thomsen, G.H. (1997). A vegetally localized T-box transcription factor in Xenopus eggs specifies mesoderm and endoderm and is essential for embryonic mesoderm formation. Development *124*, 1689-1698.

Horne, M.C., Donaldson, K.L., Goolsby, G.L., Tran, D., Mulheisen, M., Hell, J.W., and Wahl, A.F. (1997). Cyclin G2 is up-regulated during growth inhibition and B cell antigen receptor-mediated cell cycle arrest. J Biol Chem *272*, 12650-12661.

Horton, J.D., Cuthbert, J.A., and Spady, D.K. (1995). Regulation of hepatic 7 alpha-hydroxylase expression and response to dietary cholesterol in the rat and hamster. J Biol Chem *270*, 5381-5387.

Howe, J.R., Bair, J.L., Sayed, M.G., Anderson, M.E., Mitros, F.A., Petersen, G.M., Velculescu, V.E., Traverso, G., and Vogelstein, B. (2001). Germline mutations of the gene encoding bone morphogenetic protein receptor 1A in juvenile polyposis. Nat Genet *28*, 184-187.

Howe, J.R., Roth, S., Ringold, J.C., Summers, R.W., Jarvinen, H.J., Sistonen, P., Tomlinson, I.P., Houlston, R.S., Bevan, S., Mitros, F.A.*, et al.* (1998). Mutations in the SMAD4/DPC4 gene in juvenile polyposis. Science *280*, 1086-1088.

Huang, W., Ma, K., Zhang, J., Qatanani, M., Cuvillier, J., Liu, J., Dong, B., Huang, X., and Moore, D.D. (2006). Nuclear receptor-dependent bile acid signaling is required for normal liver regeneration. Science *312*, 233-236.

Huber, R.M., Murphy, K., Miao, B., Link, J.R., Cunningham, M.R., Rupar, M.J., Gunyuzlu, P.L., Haws, T.F., Kassam, A., Powell, F.*, et al.* (2002). Generation of multiple farnesoid-X-receptor isoforms through the use of alternative promoters. Gene *290*, 35-43.

Hudson, C., Clements, D., Friday, R.V., Stott, D., and Woodland, H.R. (1997). Xsox17alpha and -beta mediate endoderm formation in Xenopus. Cell *91*, 397-405.

Inagaki, T., Choi, M., Moschetta, A., Peng, L., Cummins, C.L., McDonald, J.G., Luo, G., Jones, S.A., Goodwin, B., Richardson, J.A.*, et al.* (2005). Fibroblast growth factor 15 functions as an enterohepatic signal to regulate bile acid homeostasis. Cell Metab *2*, 217-225.

Inokuchi, A., Hinoshita, E., Iwamoto, Y., Kohno, K., Kuwano, M., and Uchiumi, T. (2001). Enhanced expression of the human multidrug resistance protein 3 by bile salt in

human enterocytes. A transcriptional control of a plausible bile acid transporter. J Biol Chem *276*, 46822-46829.

Inoue, Y., Yu, A.M., Yim, S.H., Ma, X., Krausz, K.W., Inoue, J., Xiang, C.C., Brownstein, M.J., Eggertsen, G., Bjorkhem, I.*, et al.* (2006). Regulation of bile acid biosynthesis by hepatocyte nuclear factor 4alpha. J Lipid Res *47*, 215-227.

Jelinek, D.F., Andersson, S., Slaughter, C.A., and Russell, D.W. (1990). Cloning and regulation of cholesterol 7 alpha-hydroxylase, the rate-limiting enzyme in bile acid biosynthesis. J Biol Chem *265*, 8190-8197.

Kalambaheti, T., Cooper, G.N., and Jackson, G.D. (1994). Role of bile in non-specific defence mechanisms of the gut. Gut *35*, 1047-1052.

Kanai-Azuma, M., Kanai, Y., Gad, J.M., Tajima, Y., Taya, C., Kurohmaru, M., Sanai, Y., Yonekawa, H., Yazaki, K., Tam, P.P.*, et al.* (2002). Depletion of definitive gut endoderm in Sox17-null mutant mice. Development *129*, 2367-2379.

Kaneko, Y., Sakakibara, S., Imai, T., Suzuki, A., Nakamura, Y., Sawamoto, K., Ogawa, Y., Toyama, Y., Miyata, T., and Okano, H. (2000). Musashi1: an evolutionarily conserved marker for CNS progenitor cells including neural stem cells. Dev Neurosci *22*, 139-153.

Kast, H.R., Goodwin, B., Tarr, P.T., Jones, S.A., Anisfeld, A.M., Stoltz, C.M., Tontonoz, P., Kliewer, S., Willson, T.M., and Edwards, P.A. (2002). Regulation of multidrug resistance-associated protein 2 (ABCC2) by the nuclear receptors pregnane X receptor, farnesoid X-activated receptor, and constitutive androstane receptor. J Biol Chem *277*, 2908-2915.

Kerr, T.A., Saeki, S., Schneider, M., Schaefer, K., Berdy, S., Redder, T., Shan, B., Russell, D.W., and Schwarz, M. (2002). Loss of nuclear receptor SHP impairs but does not eliminate negative feedback regulation of bile acid synthesis. Dev Cell *2*, 713-720.

Kim, I., Ahn, S.H., Inagaki, T., Choi, M., Ito, S., Guo, G.L., Kliewer, S.A., and Gonzalez, F.J. (2007). Differential regulation of bile acid homeostasis by the farnesoid X receptor in liver and intestine. J Lipid Res *48*, 2664-2672.

Kim, J.W., Peng, N., Rainey, W.E., Carr, B.R., and Attia, G.R. (2004). Liver receptor homolog-1 regulates the expression of steroidogenic acute regulatory protein in human granulosa cells. J Clin Endocrinol Metab *89*, 3042-3047.

Kleinert, H., Schwarz, P.M., and Forstermann, U. (2003). Regulation of the expression of inducible nitric oxide synthase. Biol Chem *384*, 1343-1364.

Kok, T., Hulzebos, C.V., Wolters, H., Havinga, R., Agellon, L.B., Stellaard, F., Shan, B., Schwarz, M., and Kuipers, F. (2003). Enterohepatic circulation of bile salts in farnesoid

X receptor-deficient mice: efficient intestinal bile salt absorption in the absence of ileal bile acid-binding protein. J Biol Chem *278*, 41930-41937.

Krylova, I.N., Sablin, E.P., Moore, J., Xu, R.X., Waitt, G.M., MacKay, J.A., Juzumiene, D., Bynum, J.M., Madauss, K., Montana, V.*, et al.* (2005). Structural analyses reveal phosphatidyl inositols as ligands for the NR5 orphan receptors SF-1 and LRH-1. Cell *120*, 343-355.

Laudet, V. (1997). Evolution of the nuclear receptor superfamily: early diversification from an ancestral orphan receptor. J Mol Endocrinol *19*, 207-226.

Lee, F.Y., Lee, H., Hubbert, M.L., Edwards, P.A., and Zhang, Y. (2006a). FXR, a multipurpose nuclear receptor. Trends Biochem Sci *31*, 572-580.

Lee, Y.K., Choi, Y.H., Chua, S., Park, Y.J., and Moore, D.D. (2006b). Phosphorylation of the hinge domain of the nuclear hormone receptor LRH-1 stimulates transactivation. J Biol Chem *281*, 7850-7855.

Lee, Y.K., Dell, H., Dowhan, D.H., Hadzopoulou-Cladaras, M., and Moore, D.D. (2000). The orphan nuclear receptor SHP inhibits hepatocyte nuclear factor 4 and retinoid X receptor transactivation: two mechanisms for repression. Mol Cell Biol *20*, 187-195.

Lee, Y.K., and Moore, D.D. (2002). Dual mechanisms for repression of the monomeric orphan receptor liver receptor homologous protein-1 by the orphan small heterodimer partner. J Biol Chem *277*, 2463-2467.

Lee, Y.S., Chanda, D., Sim, J., Park, Y.Y., and Choi, H.S. (2007). Structure and function of the atypical orphan nuclear receptor small heterodimer partner. Int Rev Cytol *261*, 117-158.

LeSueur, J.A., and Graff, J.M. (1999). Spemann organizer activity of Smad10. Development *126*, 137-146.

Levy, L., and Hill, C.S. (2005). Smad4 dependency defines two classes of transforming growth factor {beta} (TGF-{beta}) target genes and distinguishes TGF-{beta}-induced epithelial-mesenchymal transition from its antiproliferative and migratory responses. Mol Cell Biol *25*, 8108-8125.

Li-Hawkins, J., Gafvels, M., Olin, M., Lund, E.G., Andersson, U., Schuster, G., Bjorkhem, I., Russell, D.W., and Eggertsen, G. (2002). Cholic acid mediates negative feedback regulation of bile acid synthesis in mice. J Clin Invest *110*, 1191-1200.

Li, J., Pircher, P.C., Schulman, I.G., and Westin, S.K. (2005a). Regulation of complement C3 expression by the bile acid receptor FXR. J Biol Chem *280*, 7427-7434.

Li, M., Xie, Y.H., Kong, Y.Y., Wu, X., Zhu, L., and Wang, Y. (1998). Cloning and characterization of a novel human hepatocyte transcription factor, hB1F, which binds and activates enhancer II of hepatitis B virus. J Biol Chem *273*, 29022-29031.

Li, Y., Choi, M., Suino, K., Kovach, A., Daugherty, J., Kliewer, S.A., and Xu, H.E. (2005b). Structural and biochemical basis for selective repression of the orphan nuclear receptor liver receptor homolog 1 by small heterodimer partner. Proc Natl Acad Sci U S A *102*, 9505-9510.

Li, Y., Lambert, M.H., and Xu, H.E. (2003). Activation of nuclear receptors: a perspective from structural genomics. Structure *11*, 741-746.

Lieu, H.T., Simon, M.T., Nguyen-Khoa, T., Kebede, M., Cortes, A., Tebar, L., Smith, A.J., Bayne, R., Hunt, S.P., Brechot, C.*, et al.* (2006). Reg2 inactivation increases sensitivity to Fas hepatotoxicity and delays liver regeneration post-hepatectomy in mice. Hepatology *44*, 1452-1464.

Liu, Y., Binz, J., Numerick, M.J., Dennis, S., Luo, G., Desai, B., MacKenzie, K.I., Mansfield, T.A., Kliewer, S.A., Goodwin, B.*, et al.* (2003). Hepatoprotection by the farnesoid X receptor agonist GW4064 in rat models of intra- and extrahepatic cholestasis. J Clin Invest *112*, 1678-1687.

Lonard, D.M., and O'Malley, B.W. (2006). The expanding cosmos of nuclear receptor coactivators. Cell *125*, 411-414.

Lorenzo-Zuniga, V., Bartoli, R., Planas, R., Hofmann, A.F., Vinado, B., Hagey, L.R., Hernandez, J.M., Mane, J., Alvarez, M.A., Ausina, V.*, et al.* (2003). Oral bile acids reduce bacterial overgrowth, bacterial translocation, and endotoxemia in cirrhotic rats. Hepatology *37*, 551-557.

Lu, T.T., Makishima, M., Repa, J.J., Schoonjans, K., Kerr, T.A., Auwerx, J., and Mangelsdorf, D.J. (2000). Molecular basis for feedback regulation of bile acid synthesis by nuclear receptors. Mol Cell *6*, 507-515.

Lustig, K.D., Kroll, K.L., Sun, E.E., and Kirschner, M.W. (1996). Expression cloning of a Xenopus T-related gene (Xombi) involved in mesodermal patterning and blastopore lip formation. Development *122*, 4001-4012.

Ma, K., Saha, P.K., Chan, L., and Moore, D.D. (2006). Farnesoid X receptor is essential for normal glucose homeostasis. J Clin Invest *116*, 1102-1109.

Madison, B.B., Braunstein, K., Kuizon, E., Portman, K., Qiao, X.T., and Gumucio, D.L. (2005). Epithelial hedgehog signals pattern the intestinal crypt-villus axis. Development *132*, 279-289.

Madison, B.B., Dunbar, L., Qiao, X.T., Braunstein, K., Braunstein, E., and Gumucio, D.L. (2002). Cis elements of the villin gene control expression in restricted domains of the vertical (crypt) and horizontal (duodenum, cecum) axes of the intestine. J Biol Chem *277*, 33275-33283.

Makishima, M., Okamoto, A.Y., Repa, J.J., Tu, H., Learned, R.M., Luk, A., Hull, M.V., Lustig, K.D., Mangelsdorf, D.J., and Shan, B. (1999). Identification of a nuclear receptor for bile acids. Science *284*, 1362-1365.

Maloney, P.R., Parks, D.J., Haffner, C.D., Fivush, A.M., Chandra, G., Plunket, K.D., Creech, K.L., Moore, L.B., Wilson, J.G., Lewis, M.C.*, et al.* (2000). Identification of a chemical tool for the orphan nuclear receptor FXR. J Med Chem *43*, 2971-2974.

Mangelsdorf, D.J., and Evans, R.M. (1995). The RXR heterodimers and orphan receptors. Cell *83*, 841-850.

Manigold, T., Bocker, U., Traber, P., Dong-Si, T., Kurimoto, M., Hanck, C., Singer, M.V., and Rossol, S. (2000). Lipopolysaccharide/endotoxin induces IL-18 via CD14 in human peripheral blood mononuclear cells in vitro. Cytokine *12*, 1788-1792.

Martinez-Gac, L., Alvarez, B., Garcia, Z., Marques, M., Arrizabalaga, M., and Carrera, A.C. (2004a). Phosphoinositide 3-kinase and Forkhead, a switch for cell division. Biochem Soc Trans *32*, 360-361.

Martinez-Gac, L., Marques, M., Garcia, Z., Campanero, M.R., and Carrera, A.C. (2004b). Control of cyclin G2 mRNA expression by forkhead transcription factors: novel mechanism for cell cycle control by phosphoinositide 3-kinase and forkhead. Mol Cell Biol *24*, 2181-2189.

Mataki, C., Magnier, B.C., Houten, S.M., Annicotte, J.S., Argmann, C., Thomas, C., Overmars, H., Kulik, W., Metzger, D., Auwerx, J.*, et al.* (2007). Compromised intestinal lipid absorption in mice with a liver-specific deficiency of liver receptor homolog 1. Mol Cell Biol *27*, 8330-8339.

Montagne, J., Stewart, M.J., Stocker, H., Hafen, E., Kozma, S.C., and Thomas, G. (1999). Drosophila S6 kinase: a regulator of cell size. Science *285*, 2126-2129.

Mueller, M., Cima, I., Noti, M., Fuhrer, A., Jakob, S., Dubuquoy, L., Schoonjans, K., and Brunner, T. (2006). The nuclear receptor LRH-1 critically regulates extra-adrenal glucocorticoid synthesis in the intestine. J Exp Med *203*, 2057-2062.

Nathan, C. (1997). Inducible nitric oxide synthase: what difference does it make? J Clin Invest *100*, 2417-2423.

Nitta, M., Ku, S., Brown, C., Okamoto, A.Y., and Shan, B. (1999). CPF: an orphan nuclear receptor that regulates liver-specific expression of the human cholesterol 7alpha-hydroxylase gene. Proc Natl Acad Sci U S A *96*, 6660-6665.

Nolin, M., and Wikvall, K. (2007). Enzymes in the conversioin of cholesterol into bile acid. Curr Mol Med *7*, 199-218.

Ohanna, M., Sobering, A.K., Lapointe, T., Lorenzo, L., Praud, C., Petroulakis, E., Sonenberg, N., Kelly, P.A., Sotiropoulos, A., and Pende, M. (2005). Atrophy of S6K1(-/-) skeletal muscle cells reveals distinct mTOR effectors for cell cycle and size control. Nat Cell Biol *7*, 286-294.

Okano, H., Kawahara, H., Toriya, M., Nakao, K., Shibata, S., and Imai, T. (2005). Function of RNA-binding protein Musashi-1 in stem cells. Exp Cell Res *306*, 349-356.

Ortlund, E.A., Lee, Y., Solomon, I.H., Hager, J.M., Safi, R., Choi, Y., Guan, Z., Tripathy, A., Raetz, C.R., McDonnell, D.P.*, et al.* (2005). Modulation of human nuclear receptor LRH-1 activity by phospholipids and SHP. Nat Struct Mol Biol *12*, 357-363.

Otte, K., Kranz, H., Kober, I., Thompson, P., Hoefer, M., Haubold, B., Remmel, B., Voss, H., Kaiser, C., Albers, M.*, et al.* (2003). Identification of farnesoid X receptor beta as a novel mammalian nuclear receptor sensing lanosterol. Mol Cell Biol *23*, 864-872.

Pandak, W.M., Li, Y.C., Chiang, J.Y., Studer, E.J., Gurley, E.C., Heuman, D.M., Vlahcevic, Z.R., and Hylemon, P.B. (1991). Regulation of cholesterol 7 alpha-hydroxylase mRNA and transcriptional activity by taurocholate and cholesterol in the chronic biliary diverted rat. J Biol Chem *266*, 3416-3421.

Pare, J.F., Malenfant, D., Courtemanche, C., Jacob-Wagner, M., Roy, S., Allard, D., and Belanger, L. (2004a). The fetoprotein transcription factor (FTF) gene is essential to embryogenesis and cholesterol homeostasis and is regulated by a DR4 element. J Biol Chem *279*, 21206-21216.

Pare, J.F., Malenfant, D., Courtemanche, C., Jacob-Wagner, M., Roy, S., Allard, D., and Belanger, L. (2004b). The fetoprotein transcription factor (FTF) gene is essential to embryogenesis and cholesterol homeostasis, and regulated by a DR4 element. J Biol Chem *279*, 21206-21216.

Pare, J.F., Roy, S., Galarneau, L., and Belanger, L. (2001). The mouse fetoprotein transcription factor (FTF) gene promoter is regulated by three GATA elements with tandem E box and Nkx motifs, and FTF in turn activates the Hnf3beta, Hnf4alpha, and Hnf1alpha gene promoters. J Biol Chem *276*, 13136-13144.

Parks, R.W., Stuart Cameron, C.H., Gannon, C.D., Pope, C., Diamond, T., and Rowlands, B.J. (2000). Changes in gastrointestinal morphology associated with obstructive jaundice. J Pathol *192*, 526-532.

Pei, L., and Melmed, S. (1997). Isolation and characterization of a pituitary tumor-transforming gene (PTTG). Mol Endocrinol *11*, 433-441.

Pellicciari, R., Costantino, G., and Fiorucci, S. (2005). Farnesoid X receptor: from structure to potential clinical applications. J Med Chem *48*, 5383-5403.

Pende, M., Kozma, S.C., Jaquet, M., Oorschot, V., Burcelin, R., Le Marchand-Brustel, Y., Klumperman, J., Thorens, B., and Thomas, G. (2000). Hypoinsulinaemia, glucose intolerance and diminished beta-cell size in S6K1-deficient mice. Nature *408*, 994-997.

Pezzi, V., Sirianni, R., Chimento, A., Maggiolini, M., Bourguiba, S., Delalande, C., Carreau, S., Ando, S., Simpson, E.R., and Clyne, C.D. (2004). Differential expression of steroidogenic factor-1/adrenal 4 binding protein and liver receptor homolog-1 (LRH-1)/fetoprotein transcription factor in the rat testis: LRH-1 as a potential regulator of testicular aromatase expression. Endocrinology *145*, 2186-2196.

Porter, E.M., Bevins, C.L., Ghosh, D., and Ganz, T. (2002). The multifaceted Paneth cell. Cell Mol Life Sci *59*, 156-170.

Postic, C., Shiota, M., Niswender, K.D., Jetton, T.L., Chen, Y., Moates, J.M., Shelton, K.D., Lindner, J., Cherrington, A.D., and Magnuson, M.A. (1999). Dual roles for glucokinase in glucose homeostasis as determined by liver and pancreatic beta cell-specific gene knock-outs using Cre recombinase. J Biol Chem *274*, 305-315.

Potten, C.S., Booth, C., Tudor, G.L., Booth, D., Brady, G., Hurley, P., Ashton, G., Clarke, R., Sakakibara, S., and Okano, H. (2003). Identification of a putative intestinal stem cell and early lineage marker; musashi-1. Differentiation *71*, 28-41.

Preston, S.L., Wong, W.M., Chan, A.O., Poulsom, R., Jeffery, R., Goodlad, R.A., Mandir, N., Elia, G., Novelli, M., Bodmer, W.F.*, et al.* (2003). Bottom-up histogenesis of colorectal adenomas: origin in the monocryptal adenoma and initial expansion by crypt fission. Cancer Res *63*, 3819-3825.

Qiao, L., Han, S.I., Fang, Y., Park, J.S., Gupta, S., Gilfor, D., Amorino, G., Valerie, K., Sealy, L., Engelhardt, J.F.*, et al.* (2003). Bile acid regulation of C/EBPbeta, CREB, and c-Jun function, via the extracellular signal-regulated kinase and c-Jun NH2-terminal kinase pathways, modulates the apoptotic response of hepatocytes. Mol Cell Biol *23*, 3052-3066.

Qin, J., Gao, D.M., Jiang, Q.F., Zhou, Q., Kong, Y.Y., Wang, Y., and Xie, Y.H. (2004). Prospero-related homeobox (Prox1) is a corepressor of human liver receptor homolog-1 and suppresses the transcription of the cholesterol 7-alpha-hydroxylase gene. Mol Endocrinol *18*, 2424-2439.

Rausa, F.M., Galarneau, L., Belanger, L., and Costa, R.H. (1999). The nuclear receptor fetoprotein transcription factor is coexpressed with its target gene HNF-3beta in the developing murine liver, intestine and pancreas. Mech Dev *89*, 185-188.

Reichling, T., Goss, K.H., Carson, D.J., Holdcraft, R.W., Ley-Ebert, C., Witte, D., Aronow, B.J., and Groden, J. (2005). Transcriptional profiles of intestinal tumors in Apc(Min) mice are unique from those of embryonic intestine and identify novel gene targets dysregulated in human colorectal tumors. Cancer Res *65*, 166-176.

Repa, J.J., Lund, E.G., Horton, J.D., Leitersdorf, E., Russell, D.W., Dietschy, J.M., and Turley, S.D. (2000). Disruption of the sterol 27-hydroxylase gene in mice results in hepatomegaly and hypertriglyceridemia. Reversal by cholic acid feeding. J Biol Chem *275*, 39685-39692.

Reuter, B.K., and Pizarro, T.T. (2004). Commentary: the role of the IL-18 system and other members of the IL-1R/TLR superfamily in innate mucosal immunity and the pathogenesis of inflammatory bowel disease: friend or foe? Eur J Immunol *34*, 2347-2355.

Rosen, H., Reshef, A., Maeda, N., Lippoldt, A., Shpizen, S., Triger, L., Eggertsen, G., Bjorkhem, I., and Leitersdorf, E. (1998). Markedly reduced bile acid synthesis but maintained levels of cholesterol and vitamin D metabolites in mice with disrupted sterol 27-hydroxylase gene. J Biol Chem *273*, 14805-14812.

Rudel, L., Deckelman, C., Wilson, M., Scobey, M., and Anderson, R. (1994). Dietary cholesterol and downregulation of cholesterol 7 alpha-hydroxylase and cholesterol absorption in African green monkeys. J Clin Invest *93*, 2463-2472.

Russell, D.W. (2003). The enzymes, regulation, and genetics of bile acid synthesis. Annu Rev Biochem *72*, 137-174.

Ruvinsky, I., Sharon, N., Lerer, T., Cohen, H., Stolovich-Rain, M., Nir, T., Dor, Y., Zisman, P., and Meyuhas, O. (2005). Ribosomal protein S6 phosphorylation is a determinant of cell size and glucose homeostasis. Genes Dev *19*, 2199-2211.

Sablin, E.P., Krylova, I.N., Fletterick, R.J., and Ingraham, H.A. (2003). Structural basis for ligand-independent activation of the orphan nuclear receptor LRH-1. Mol Cell *11*, 1575-1585.

Sancho, E., Batlle, E., and Clevers, H. (2004). Signaling pathways in intestinal development and cancer. Annu Rev Cell Dev Biol *20*, 695-723.

Satoh, Y., Nagashima, Y., Oomori, Y., Ishikawa, K., Matoba, M., and Ono, K. (1985). Scanning electron microscopical observation on the isolated mucosa of rat small intestine: with special reference to the intestinal crypt. Anat Anz *159*, 305-309.

Schoonjans, K., Annicotte, J.S., Huby, T., Botrugno, O.A., Fayard, E., Ueda, Y., Chapman, J., and Auwerx, J. (2002). Liver receptor homolog 1 controls the expression of the scavenger receptor class B type I. EMBO Rep *3*, 1181-1187.

Schoonjans, K., Dubuquoy, L., Mebis, J., Fayard, E., Wendling, O., Haby, C., Geboes, K., and Auwerx, J. (2005). Liver receptor homolog 1 contributes to intestinal tumor formation through effects on cell cycle and inflammation. Proc Natl Acad Sci U S A *102*, 2058-2062.

Seol, W., Choi, H.S., and Moore, D.D. (1995). Isolation of proteins that interact specifically with the retinoid X receptor: two novel orphan receptors. Mol Endocrinol *9*, 72-85.

Seol, W., Choi, H.S., and Moore, D.D. (1996). An orphan nuclear hormone receptor that lacks a DNA binding domain and heterodimerizes with other receptors. Science *272*, 1336-1339.

Sinal, C.J., Tohkin, M., Miyata, M., Ward, J.M., Lambert, G., and Gonzalez, F.J. (2000). Targeted disruption of the nuclear receptor FXR/BAR impairs bile acid and lipid homeostasis. Cell *102*, 731-744.

Slocum, M.M., Sittig, K.M., Specian, R.D., and Deitch, E.A. (1992). Absence of intestinal bile promotes bacterial translocation. Am Surg *58*, 305-310.

Stennard, F., Carnac, G., and Gurdon, J.B. (1996). The Xenopus T-box gene, Antipodean, encodes a vegetally localised maternal mRNA and can trigger mesoderm formation. Development *122*, 4179-4188.

Trapani, J.A., and Smyth, M.J. (2002). Functional significance of the perforin/granzyme cell death pathway. Nat Rev Immunol *2*, 735-747.

Turley, S.D., Schwarz, M., Spady, D.K., and Dietschy, J.M. (1998). Gender-related differences in bile acid and sterol metabolism in outbred CD-1 mice fed low- and high-cholesterol diets. Hepatology *28*, 1088-1094.

Wallace, J.L., and Miller, M.J. (2000). Nitric oxide in mucosal defense: a little goes a long way. Gastroenterology *119*, 512-520.

Wang, L., Lee, Y.K., Bundman, D., Han, Y., Thevananther, S., Kim, C.S., Chua, S.S., Wei, P., Heyman, R.A., Karin, M.*, et al.* (2002). Redundant pathways for negative feedback regulation of bile acid production. Dev Cell *2*, 721-731.

Wang, L., Tang, Y., Rubin, D.C., and Levin, M.S. (2007). Chronically administered retinoic acid has trophic effects in the rat small intestine and promotes adaptation in a resection model of short bowel syndrome. Am J Physiol Gastrointest Liver Physiol *292*, G1559-1569.

Wang, S., Lan, F., Huang, L., Dong, L., Zhu, Z., Li, Z., Xie, Y., and Fu, J. (2005a). Suppression of hLRH-1 mediated by a DNA vector-based RNA interference results in cell cycle arrest and induction of apoptosis in hepatocellular carcinoma cell BEL-7402. Biochem Biophys Res Commun *333*, 917-924.

Wang, W., Zhang, C., Marimuthu, A., Krupka, H.I., Tabrizizad, M., Shelloe, R., Mehra, U., Eng, K., Nguyen, H., Settachatgul, C.*, et al.* (2005b). The crystal structures of human steroidogenic factor-1 and liver receptor homologue-1. Proc Natl Acad Sci U S A *102*, 7505-7510.

Wang, Z., Moro, E., Kovacs, K., Yu, R., and Melmed, S. (2003). Pituitary tumor transforming gene-null male mice exhibit impaired pancreatic beta cell proliferation and diabetes. Proc Natl Acad Sci U S A *100*, 3428-3432.

Wang, Z., Yu, R., and Melmed, S. (2001). Mice lacking pituitary tumor transforming gene show testicular and splenic hypoplasia, thymic hyperplasia, thrombocytopenia, aberrant cell cycle progression, and premature centromere division. Mol Endocrinol *15*, 1870-1879.

Wasan, H.S., Park, H.S., Liu, K.C., Mandir, N.K., Winnett, A., Sasieni, P., Bodmer, W.F., Goodlad, R.A., and Wright, N.A. (1998). APC in the regulation of intestinal crypt fission. J Pathol *185*, 246-255.

Watanabe, M., Houten, S.M., Mataki, C., Christoffolete, M.A., Kim, B.W., Sato, H., Messaddeq, N., Harney, J.W., Ezaki, O., Kodama, T.*, et al.* (2006). Bile acids induce energy expenditure by promoting intracellular thyroid hormone activation. Nature *439*, 484-489.

Whitby, R.J., Dixon, S., Maloney, P.R., Delerive, P., Goodwin, B.J., Parks, D.J., and Willson, T.M. (2006). Identification of small molecule agonists of the orphan nuclear receptors liver receptor homolog-1 and steroidogenic factor-1. J Med Chem *49*, 6652-6655.

Xu, G., Salen, G., Shefer, S., Ness, G.C., Nguyen, L.B., Parker, T.S., Chen, T.S., Zhao, Z., Donnelly, T.M., and Tint, G.S. (1995). Unexpected inhibition of cholesterol 7 alpha-hydroxylase by cholesterol in New Zealand white and Watanabe heritable hyperlipidemic rabbits. J Clin Invest *95*, 1497-1504.

Yu, Y., Sitaraman, S., and Gewirtz, A.T. (2004). Intestinal epithelial cell regulation of mucosal inflammation. Immunol Res *29*, 55-68.

Zhang, C.K., Lin, W., Cai, Y.N., Xu, P.L., Dong, H., Li, M., Kong, Y.Y., Fu, G., Xie, Y.H., Huang, G.M.*, et al.* (2001a). Characterization of the genomic structure and tissue-specific promoter of the human nuclear receptor NR5A2 (hB1F) gene. Gene *273*, 239-249.

Zhang, J., Houston, D.W., King, M.L., Payne, C., Wylie, C., and Heasman, J. (1998). The role of maternal VegT in establishing the primary germ layers in Xenopus embryos. Cell *94*, 515-524.

Zhang, M., Chen, W., Smith, S.M., and Napoli, J.L. (2001b). Molecular characterization of a mouse short chain dehydrogenase/reductase active with all-trans-retinol in intact cells, mRDH1. J Biol Chem *276*, 44083-44090.

Zhang, Y., Lee, F.Y., Barrera, G., Lee, H., Vales, C., Gonzalez, F.J., Willson, T.M., and Edwards, P.A. (2006). Activation of the nuclear receptor FXR improves hyperglycemia and hyperlipidemia in diabetic mice. Proc Natl Acad Sci U S A *103*, 1006-1011.

CHAPTER 4

LRH-1 IN INTESTINAL CELL PROLIFERATION

4.1 Abstract

The intestinal epithelium is exposed to the external environment and therefore undergoes rapid turnover. To maintain the integrity of the gastrointestinal system, multiple cellular events such as cell proliferation, differentiation, and programmed cell death must be tightly regulated. Recently, several partial loss-of-function studies have suggested that LRH-1 is involved in intestinal cell renewal via crosstalk with the β-catenin/Tcf4 signaling pathway, which is critical for cell proliferation and differentiation (Botrugno et al., 2004). To gain further insights into LRH-1 function in intestine, we generated transgenic mice expressing a constitutively active form of LRH-1 (VP16LRH-1) under the control of the villin promoter. As expected, VP16-LRH-1 transgenic mice have enlarged small intestines due to a marked increase in the number of crypts and longer villi. BrdU labeling in the intestine revealed increased proliferation in VP16-LRH-1 transgenic animals. To investigate the molecular basis of this phenotype, microarray analysis was performed using RNA prepared from duodenum and ileum of either VP16-LRH-1 transgenic or wild type mice. The results revealed a number of established LRH-1 target genes including small heterodimer partner (SHP), steroidogenic acute regulatory protein (StAR), and cytochrome P450 family17 (CYP17), and also identified new potential target genes that are upregulated including retinol dehydrogenase 1 (RDH1), telomerase reverse transcriptase (TERT), pituitary tumor-transforming 1 (PTTG1), and

lymphocyte antigen 6 complex D (LY6D), which are all involved in either cell differentiation, proliferation, or tumor formation. Moreover, genes such as apoptotic peptidase activating factor 1 (APAF1), caspase 3, and granzyme B, which are important for apoptosis and immune response, were down-regulated. Taken together, these data indicate that LRH-1 plays a central role in promoting growth in the small intestine.

4.2 Introduction

Intestinal epithelium consists of a single layer of epithelial cells which function as a barrier between the inside of the body and the external environment, like the epidermis of the skin. The intestinal epithelium is challenged by a variety of foreign molecules every day. In order to fulfill its protective function, the intestine is comprised of four differentiated cell types that execute divergent biological tasks. The most abundant cell type is the enterocyte, which is mainly involved in nutrient absorption. Enteroendocrine cells secrete hormones and goblet cells secrete mucus. These cell types continuously differentiate from progenitor cells and migrate into the villi. By contrast, paneth cells reside in the bottom of crypts, where they protect intestinal stem cells by secreting antimicrobial peptides and enzymes (Porter et al., 2002).

The development of intestine is a multi-step process. A single-layered epithelium is converted from pseudostratified layers of endodermal origin around E14.5 followed by villus formation (Sancho et al., 2004). Much later during development, the crypts of Lieberkühn, proliferative pockets of bottle-shaped invaginations, are formed to complete the intestinal architecture. Intestine homeostasis is maintained by elaborate and orchestrated cellular mechanisms which control cell renewal, cell lineage fate, and cell

positioning. Intestinal stem cells located at the bottom of crypts continuously produce progenitor cells to maintaining the structural integrity of the intestine. This proliferative capacity of stem cells resembles that of tumors. Therefore, tight control of cellular processes in stem cells is required.

Numerous cellular signaling pathways are involved in intestinal stem cell and cancer biology. The Wnt signaling pathway in stem cells has been extensively studied. This is a key pathway to maintain crypt cell proliferation and thus, obstruction of this pathway leads to tumorigenesis. Many different mutations in adenomatous polyposis coli (APC), which binds to β–catenin to block its nuclear translocation, were found in familial adnomatous polyposis (FAP) and sporadic colorectal cancers (Sancho et al., 2004). Wnt signaling also controls the arrangement of cell types along the villus-crypt axis by regulating Eph/Ephrin signals (Batlle et al., 2002). Juvenile polyposis syndrome (JPS) is caused by loss of intestinal bone morphogenic protein (BMP), which is a member of the transforming growth factor-β (TGFβ) superfamily (Howe et al., 2001; Howe et al., 1998). Blocking BMP signaling by overexpression of noggin causes an increase in the number of crypts throughout the epithelium (Haramis et al., 2004). Communication between epithelial and mesenchymal cells is also important for normal development of intestine. Hedgehog signaling is a good example: mice lacking hedgehog interacting protein (HHIP), which inhibits hedgehog signaling, lack villi and have high rates of intestinal cell proliferation (Madison et al., 2005).

Studies with *Lrh-1*^{+/-} mice showed that LRH-1 is involved in intestinal stem cell renewal through effects on β-catenin/TCF signaling, and *Lrh-1*^{+/-} mice were susceptible to chemical-induced intestinal tumorigenesis (Botrugno et al., 2004; Schoonjans et al.,

2005). In this study, we describe a significant intestine mucosal phenotype in mice overexpressing a constitutively active form of LRH-1. In addition, we identified potential LRH-1 target genes and LRH-1-regulated pathways using microarrays. The results suggest that LRH-1 contributes to intestinal cell growth by regulating genes involved in cell proliferation and apoptosis via several signaling pathways.

4.3 Materials and Methods

Animal Procedures

All animal experiments were approved by the Institutional Animal Care and Research Advisory Committee of the University of Texas Southwestern Medical Center. Animals were housed in a temperature-controlled conventional environment with 12 hour light/dark cycles and fed with standard rodent chow (TD2016, Harlan Teklad, Madison, WI) and water *ad libitum*. All animal experiments were done with 8 to 12 week-old male and female mice killed at starting 2 pm. For detection of crypt fission, 4 week-old mice were used. For the intestinal proliferation study, BrdU (100 mg/kg in phosphate-buffered saline) was injected intraperiotoneally 2 hours prior to sacrifice. Small intestine length was measured from the pyloric end to the ileocecal border. Small intestine was weighed without flushing and normalized to body weight.

Generation of mice overexpressing constitutively active LRH-1 in intestine

A 12.4 Kb villin promoter was kindly provided by Dr. Gumucio (University of Michigan). To generate a constitutively active LRH-1, the VP16 activation domain (78 amino acids) was fused to the N-terminus of full length LRH-1 by inserting a cDNA fragment encoding this region into the MluI and XhoI sites of the p12.4KVill plasmid

(Madison et al., 2002). Approximately 15 Kb of final construct was confirmed by restriction mapping and partial sequencing. DNA was linearilzed by PmeI digestion and purified for injection into the pronucleus of a fertilized egg. The hybrid of C57BL/6.SJL female was mated with C57BL/6 male mouse. Transgenic founder screening was done by Southern blot and PCR analysis. Genomic DNA was digested with BglII and NheI and a Southern probe (360bp) was prepared by PCR amplification using primers: villin forward, CCAATGGAGGGTTCTTTTTGTG; villin reverse, AAACTGGCTTCCTATGGGGGTC. Genotype analysis was done by multiplex PCR using the primers: VP16AD forward, GCTCGAGGCCACCATGGCCCCCCCG; TgLRH-1 reverse, CTGGTTCTCTATGCACGTGTAC. PCR results in a 360bp product from the wild type *Lrh-1* gene control and a 700 bp product from the transgene.

Morphometric Measurements

The small intestine was cut into three segments of equal length representing the duodenum, jejunum and ileum. Each section was cut transversely, fixed with 10% formalin, paraffin embedded, sectioned, and stained with hematoxylin and eosin. For villus and crypt measurements, duodenum sections were photographed using a Nikon Eclipse 80i camera at 2X, 10X and 20X magnifications. The number of crypts was counted around the perimeters of transverse sections photographed at 2X magnification. Crypt quantification was done blinded by Dr. Klementina Fon Tacer, a postdoctoral scientist, and by me. Five villi and crypts per mouse (n=7 mice/group) for Villin-VP16LRH-1 mice and ten villi and crypts per mouse (n=11-12 mice/group) for LRH-1 deficient mice were measured in duodenum using MetaVue software (Meta Imaging Series 6.1, Lewisville, TX).

Immunohistochemistry

To determine proliferation indices, BrdU incorporation was detected by immunohistochemistry. Sections were deparaffinized and rehydrated. DNA was denatured by 2N HCl for 1 hour at 37°C and then neutralized by immersing sections twice in 0.1 M borate buffer (pH8.5) for 5 min each. Sections were permeabilized in 0.3% Triton for 5 min, incubated in 1.5% horse serum for 30 min, and incubated with anti-mouse BrdU mouse antibody (Roche) at a 1:25 dilution overnight at 4°C. Biotinylated horse anti-mouse IgG was added at a dilution of 1:200 for 30 min at room temperature followed by FITC-conjugated streptavidin at a 1:50 dilution for 30 min at room temperature. Five crypts per mouse for Villin-VP16LRH-1 mice and ten crypts per mouse for LRH-1 deficient mice were analyzed for BrdU incorporation (n=4 mice/group).

Affymetrix Analysis

Total RNA was extracted from duodenum and ileum using RNA STAT-60 (Tel-Test, Inc.,Friendswood, TX) and cDNA was prepared (n=5, 12 week-old male mice/group). Preparation of *in vitro* transcription (IVT) products, oligonucleotide array hybridization and scanning were performed according to Affymetrix (Santa Clara, CA) protocols by Dr. Michael Downes, a staff scientist in the laboratory of Dr. Ronald Evans at the Salk Institute. In brief, 5 μg of total RNA from each sample and T7-linked oligo-dT primers were used for first-strand cDNA synthesis. IVT reactions were performed in batches to generate biotinylated cRNA targets, which were chemically fragmented at 94°C for 35 minutes. Fragmented biotinylated cRNA (15 μg) was hybridized at 45°C for 16 hours to Affymetrix® high density oligonucleotide array mouse genome 430A 2.0 chips, which contain probe sets representing more than 14,000 well-substantiated mouse

genes. The arrays were washed and stained with streptavidin-phycoerythrin (10 μg/ml).

Signal amplification was performed using a biotinylated anti-streptavidin antibody. The

array was scanned according to the manufacturer's instructions (Affymetrix Genechip

Technical Manual, 2004). Scanned images were inspected for obvious defects (artifacts

or scratches) on the array to exclude defective chips. To minimize discrepancies due to

variables, the raw expression data was scaled using Affymetrix Microarray Suite 5.0

software and pair-wise comparisons were performed. The trimmed mean signal of all

probe sets on the MG430A chip was adjusted to a user-specified target signal value (200)

for each array for global scaling. No specific exclusion criteria were applied. Additional

analysis was performed using the freeware program Bullfrog version 7 (http://Barlow

LockhartBrainMapNIMHGrant.org).

RT-qPCR Analysis

Total RNA was extracted from scraped intestine using RNA STAT-60 (Tel-Test,

Inc.) and RT-qPCR was carried out in triplicate using an Applied Biosystems Prism

7900HT instrument as described in Chapter 3. Primer sequences are shown in Table 4-1.

Relative mRNA levels were calculated using the comparative C_T methods normalize to

cyclophilin.

Immunoblot Analysis

Proteins were extracted from homogenized duodenum of WT and Villin-

VP16LRH-1 mice (n=3 mice/group) using lysis buffer (140 mM NaCl, 10 mM Tris/HCl

pH 8.10, 1 mM $MgCl_2$, 1 mM $CaCl_2$, 10 % Glycerol, 1% NP-40, Complete Protease

Inhibitor Cocktail (Roche Diagnostic)) following a standard procedure. Whole cell lysate

(40 μg) was resolved on a 10% SDS-polyacrylamide gel and transferred to a PVDF

Genes	Accession number	Forward Primer	Reverse Primer
APAF1	NM_009684	GTTCATGCGATTCAGCAGAAG	GCCTGCCATCCCATAGATG
BOK	NM_016778	CAGTCGGAGCCTGTGGTG	ACCTTGCCCCATGTGATACC
CASP3	NM_009810	CATAAGAGCACTGGAATGTCATCT	CCCATGAATGTCTCTCTGAGGTT
Cyclin	BC044841	GCCGAGAAGTTGTGCATCTACA	TGTTCACCAGAAGCAGTTCCATT
Cyclin	X75888	CCAAGATTGACAAGACTGTGAAAA	GGTCCACGCATGCTGAATTA
Cyclin	NM_007635	GGAGGCTACCCCGGAGAA	TTAAATCTTCCACTTTGGCATTTC
cMYC	NM_010849	CACCACCAGCAGCGACTCT	CCACAGACACCACATCAATTTCTT
GZMB	NM_013542	TGAAGATCCTCCTGCTACTGCT	GACTTCATGTCCCCCGATG
LRH-1	NM_030676	TGGGAAGGAAGGGACAATCTT	CGAGACTCAGGAGGTTGTTGAA
LY6D	NM_010742	CGTCCAACTTCTACTTCTGCAAA	TCCTCACCAGGTTCCCATTC
REG2	NM_009043	GAGTGGTACTACAGCTTCCAATGT	CAGTGCCAACGACGGTTACT
RDH1	NM_080436	CAAGGCCAGCTCGGAAGT	GTCCAATTCGTTTAGGTTTTTCAG
PTTG1	NM_013917	CGACCTTGACTGGGAAAAAGA	CAGGAGCAGGAACAGAACTTTG
SMAD4	NM_008540	TGAGCTTGCATTCCAGCC	GGAGCACCAGTACTCAGGAGC
TERT	NM_009453	TTTCGGAGACATGGAGAACAA	AGTCATCAACAAAACGTAAAAGC
VP16AD		CCCTACGGCGCTCTGGATA	TTCCAAGGGCATCGGTAAAC

Table 4-1. RT-qPCR primer sequences (The primers not included here are listed in Table 3-1)

membrane (Amersham). The membrane was probed with following antibodies; Cyclin A (sc-751), Cyclin B1 (sc-7393), Cyclin D1 (sc450), Cyclin G2 (sc 7266), and PCNA (sc-56) from Santa Cruz Biotechnology, Musashi-1 (AB5977) from Chemicon International, and PTEN (9511), phospho-PTEN (9552), Akt (9272), Pathscan Multiplex Western Cocktail I (7100) from Cell Signaling. PCNA antibody was used at a dilution of 1:1000 and the rest of antibodies used at a 1:500 dilution. Incubation with the primary antibody was done at 4 °C overnight, and incubation with secondary horseradish peroxidase-conjugated antibodies was done at a dilution of 1:5,000 at room temperature for 1h. The membrane was reprobed with antibody against βActin (A5316, Sigma) at a dilution of 1:5000 as loading controls. Proteins were detected by a LumiLight Western blot substrate (Roche) chemiluminescense kit.

Statistical analyses

Minitab Release 14 software (Minitab Inc, State College, PA) was used. Values are expressed as mean ± SEM. Significant differences of two groups were evaluated using a two-tailed, unpaired Student's T-test.

4.4 Results

Generation of intestine-specific Villin-VP16LRH-1 mice. For intestine-specific overexpression, 12.4 Kb of the villin promoter was fused to a constitutively active form of LRH-1 as shown Figure 4-1A. From three independent injections, two lines of Villin-VP16LRH-1 mice were generated and designated as the Line 1 and Line 2. Line 1 animals express high levels of transgene and SHP, a downstream target gene of LRH-1, along the length of the small and large intestine (Figure 4-1B). Line 2 expresses
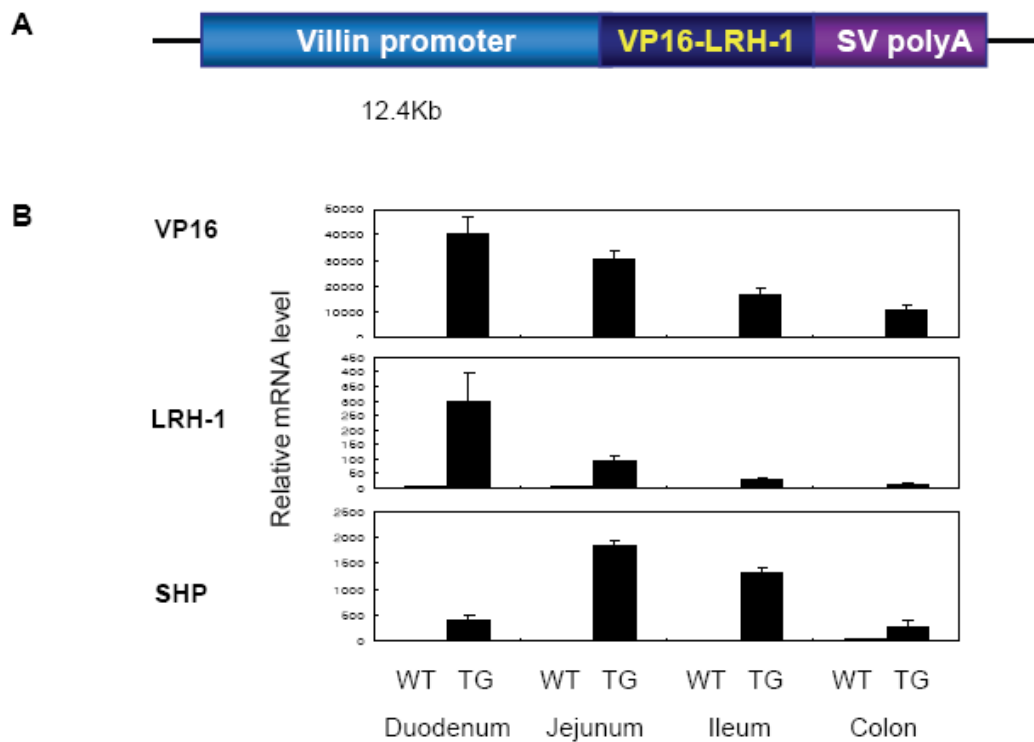
Figure 4-1. Generation of mice overexpressing VP16LRH-1 in intestine

(A) Construct map of LRH-1 transgenic mice. VP16 activation domain was fused to N-terminus of full-length LRH-1 cDNA. 12.4 Kb villin promoter was used for intestine-specific overexpression. (B) RT-qPCR analysis for VP16, LRH-1, SHP expression in each section of intestine in the first line of transgenic mice.

very low level of transgene. Line 2 transgenic animals were bred for transgene homozygosity. Homozygote animals showed increased transgene expression, but it was not associated with the strong intestinal phenotype seen in Line 1 mice as early as 6 to 8 weeks of age (data not shown). Line 1 was used for the rest of experiments in this study.

The villin promoter drove VP16-LRH-1 transgene expression at highest levels in the proximal part of the small intestine and expression gradually decreased distally (Figure 4-1B). This expression pattern suggested that the effects of the transgene were likely to be strongest in duodenum and thus, analysis of Villin-VP16LRH-1 mice focused on duodenum. SHP, a target gene of LRH-1, is also highly expressed in transgenic animals. Based on these data, we conclude that Villin-VP16LRH-1 mice overexpress active LRH-1 in intestine as expected.

Enlarged small intestine in Villin-VP16LRH-1 mice. LRH-1 is implicated in promoting intestinal cell proliferation by regulating cell cyclin D1 and cyclin E1 (Botrugno et al., 2004). As expected, mice overexpressing VP16LRH-1 in intestine exhibited enlarged small intestine compared to wild type littermates (Figure 4-2). Phenotypic data, including body weight and intestine weight and length were measured. There were no significant differences in body weight and length of small intestine (Figure 4-3A and C). However, the wet weight of small intestine in Villin-VP16LRH-1 mice was much heavier than in wild type mice (Figure 4-3B). These data raised the possibility of increased intestinal cell growth in transgenic mice. To examine this possibility more closely, each segment of small intestine was cut, fixed, and stained with hematoxyln and eosin, and villi length and crypt number were measured as indices of mucosal cell growth (Figure 4-4A). In duodenum, overexpression of VP16LRH-1 resulted in significant
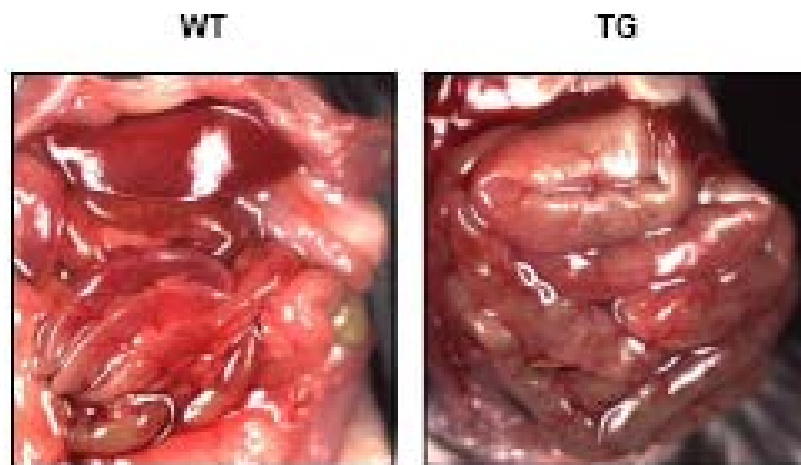
Figure 4-2. Abdominal anatomy of Villin-VP16LRH-1 mice

Enlarged small intestine was observed in Villin-VP16 LRH-1 transgenic mice (right panel) compared to wild type littermate (left panel). Pictures were taken by John Shelton in Hitology Core Facility.

Figure 4-3. Phenotypical analysis of Villin-VP16LRH-1 mice

(A-C) Body weight **(A)**, wet small intestine weight **(B)**, and length of small intestine **(C)** were measured from 12 week-old WT and Villin-VP16LRH-1 mice (male, n=5/group). Data are the mean ± SEM. *, P<0.05.

increases in villus length and crypt number but did not alter crypt depth (Figure 4-4B-D).
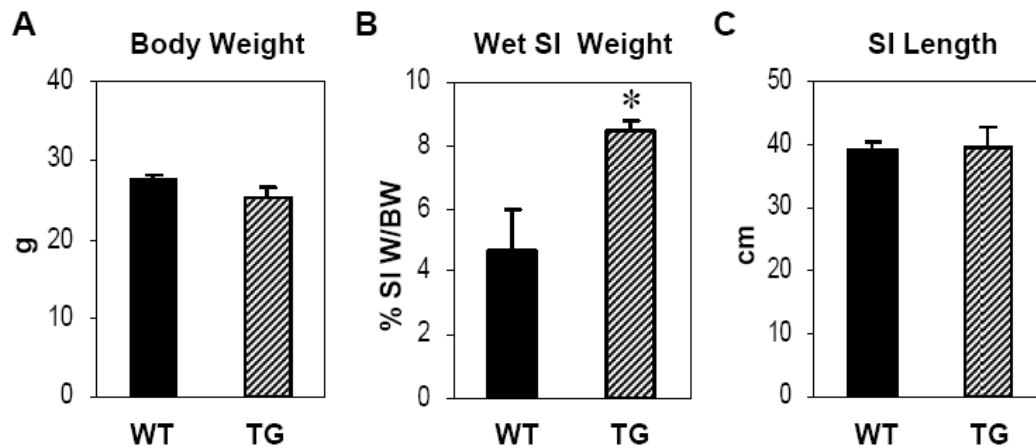
Increased intestinal proliferation and decreased apoptosis in Villin-VP16LRH-1 mice. Increase crypt numbers and villus length of Villin-VP16LRH-1 mice could be due to either increased cell proliferation or reduced apoptosis, or both. To investigate these possibilities, we performed BrdU-labeling analysis in duodenum of wild type and Villin-VP16LRH-1 mice at 2 h after BrdU administration. There were more BrdU-positive crypts in Villin-VP16LRH-1 mice than wild type (Figure 4-5A and B) indicating increased crypt cell proliferation. TUNEL staining was performed to quantify apoptotic cells in villus epithelium of wild type and Villin-VP16LRH-1 mice (Data not shown). There was no significant difference due to the difficulty of interpretation of results.

In *Lrh-1$^{+/-}$* mice, cyclin E1, cyclin D1, and c-myc expression was reduced and TNFα expression was elevated (Botrugno et al., 2004). we evaluated mRNA expression of these genes in Villin-VP16LRH-1 mice. Surprisingly, expression of cyclins and c-myc was unaffected in Villin-VP16LRH-1 mice (Figure 4-6) indicating that other LRH-1-regulated processes are likely to be responsible for the observed phenotype.

We next used Affymetrix microarray technology to identify genes whose expression is changed in the Villin-VP16LRH-1 mice. RNAs were prepared from duodenum and ileum epithelium of wild type and Villin-VP16LRH-1 mice. Affymetrix gene expression data demonstrated that VP16LRH-1 led to up-regulation of genes encoding cell cycle progression, differentiation, and tumor formation, and down-regulation of genes implicated in apoptosis and immune response (Tables 4-2 and 3).
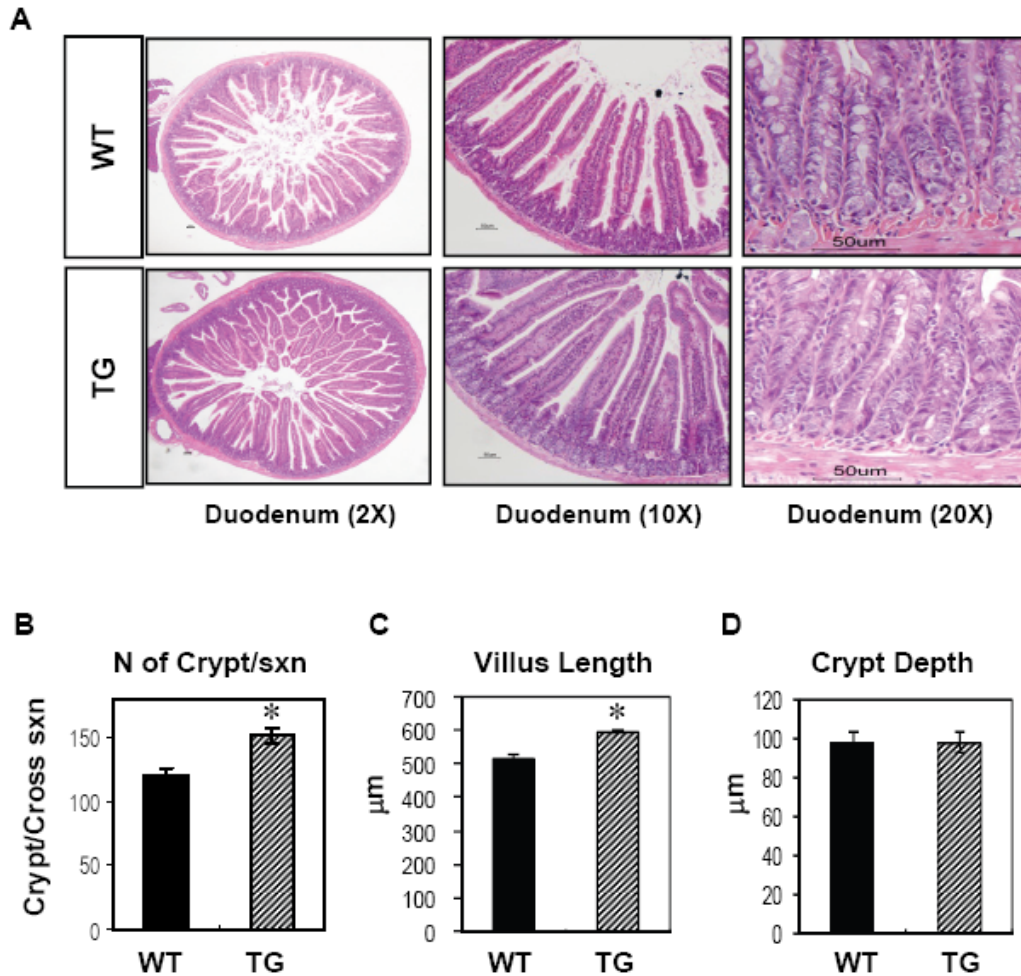
Figure 4-4. Morphometric data of Villin-VP16LRH-1 mice

(A) Hematoxylin and eosin (H&E) stained duodenums from wild-type and Villin-VP16LRH-1 mice at 4X, 10X, and 20X magnification. Scale bar=50 μm. **(B-D)** Microscopic measurements were done from wild type and Villin-VP16LRH-1 mice (12 week-old, n=7/group). **(B)** Number of well-oriented crypts per cross section was counted. **(C and D)** The length of villi and crypts were measured by Metavue program. Data are the mean ± SEM. *, P<0.05.
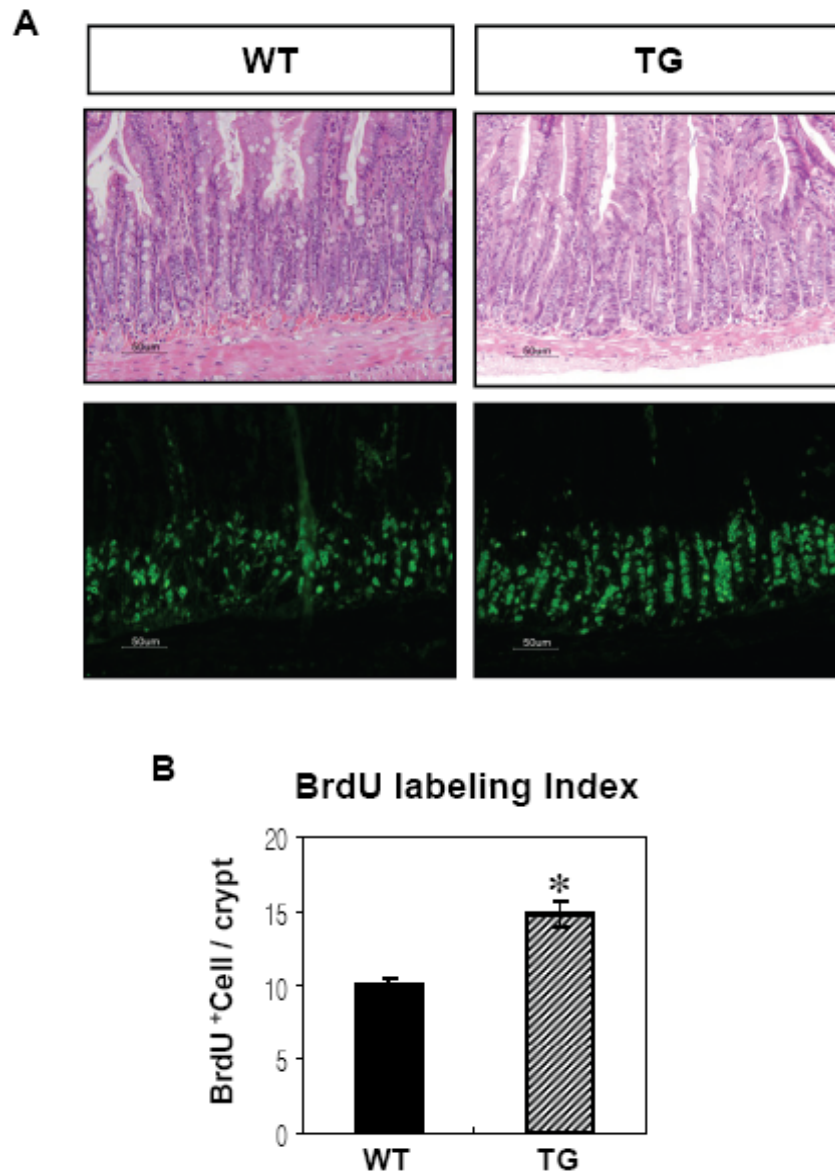
Figure 4-5. Increased proliferation in Villin-VP16 LRH-1 mice

(A) Upper panel showed H&E stained duodenum sections of WT and Villin-VP16LRH-1 mice. BrdU immunohistochemistry assay was performed. Highly proliferative cells were represented as green in lower panel. 20X magnification. **(B)** Quantification of BrdU-positive cells per crypt were measured. (12 week-old mice, n=4/group). Data are the mean ± SEM. *, P<0.05.

Figure 4-6. Expression of genes regulated by LRH-1 in intestine

mRNA levels of the indicated genes were analyzed by RT-qPCR using intestinal epithelium derived from duodenum of wild type and Villin-VP16LRH-1 mice. (n=5 male mice/group) *;P<0.05.

Previously-known LRH-1 target genes such as SHP and StAR were also identified. The regulation of a subset of these genes was further confirmed by RT-qPCR. LY6D, RDH1, and PTTG1 were more highly expressed in both duodenum and ileum of Villin-VP16LRH-1 mice, whereas cyclin G2 and SMAD4 were expressed at lower l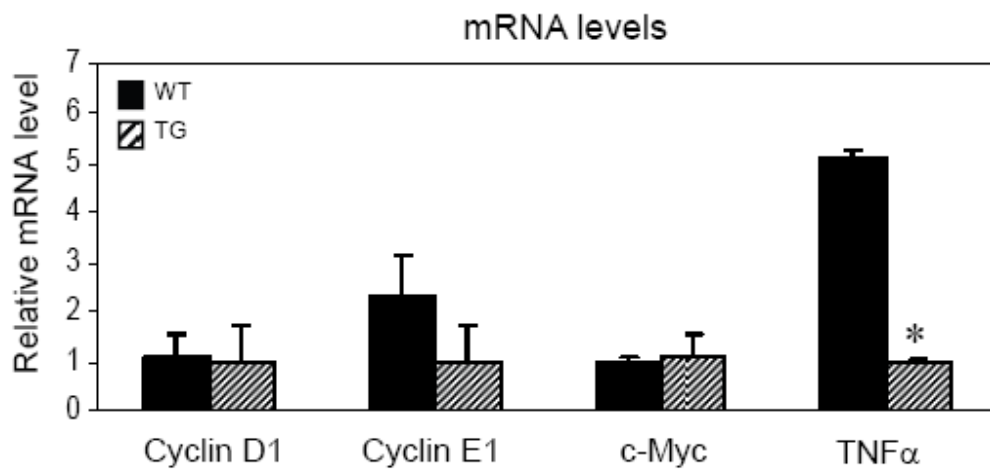evels compared to wild type mice (Figure 4-7A and B). REG2, TERT, and PCNA were upregulated only in duodenum of transgenic mice (Figure 4-7A). APAF1, BOK, caspase3, and granzyme B which are involved in cell apoptosis and inflammatory response were all downregulated (Figure 4-8A and B). BrdU labeling and gene expression experiments indicated that intestinal cell proliferation was increased and programmed cell death was reduced in Villin-VP16LRH-1 mice, consistent with the observed morphological changes.

The expression of PCNA, cyclin G2 and other cell cyclins was further characterized by immunoblot analysis (Figure 4-9). PCNA is a cell proliferation marker and cyclin G2 plays a negative role for cell cycle progression (Martinez-Gac et al., 2004b) Consistent with the mRNA data, their protein levels were reduced in Villin-VP16LRH-1 mice. Other cyclins such as cyclin A and B1, which are involved in control of cell entry into mitosis, were increased whereas cyclin D1 levels were unchanged. These data suggest that LRH-1 may promote cell cycle progression.

Morphological and gene expression changes in *Lrh-1$^{fl/f}$;Vil-Cre* mice. LRH-1 is abundant in the crypts of both the small and large intestine, and *Lrh-1$^{+/-}$* mice display reduced intestinal proliferation, decreased crypt depth, and decreased mRNA levels of cyclin D1, cyclin E1 and c-myc (Botrugno et al., 2004). Consistent with this previous study, c-myc mRNA levels were decreased in duodenum of *Lrh-1$^{flox/flox}$;Vil-Cre* mice and cyclin E1 mRNA levels trended lower (Figure 4-10A). However, there were no

Ave Ratio	Unigene Accession	Gene Title
176.285	Mm.293314	**Steroidogenic acute regulatory protein**
88.72	Mm.235814	Retinol dehydrogenase 1 (all trans)
71.445	Mm.46360	**Regenerating islet-derived 2**
57.724	Mm.346759	**Nuclear receptor subfamily 0, group B, member 2**
51.525	Mm.10109	**Telomerase reverse transcriptase**
47.676	Mm.878	Lymphocyte antigen 6 complex, locus D
31.538	Mm.1262	**Cytochrome P450, family 17, subfamily a, polypeptide1**
3.526	Mm.6856	Pituitary tumor-transforming 1
1.758	Mm.378980	**Proliferating cell nuclear antigen**
-1.87	Mm.34405	Caspase 3
-1.9	Mm.220289	Apoptotic peptidase activacting factor 1
-2.18	Mm.100399	MAD homolog 4
-2.46	Mm.3295	Bcl-2-related ovarian killer protein
-4.92	Mm.3527	Cyclin G2
-15.73	Mm.14874	Granzyme B

Table 4-2. List of target genes from Affymetrix analysis in duodenum

Total RNA was extracted from duodenum epithelium of transgenic and littermate controls, converted to cRNA, and hybridized to Affymetrix chips (n=5 male mice/group, 12 week old of age). Average ratio (fold change between WT and TG), gene ID, and names are listed. Genes in bold characters are known LRH-1 target genes and in blue are candidates specific in duodenum.

Ave Ratio	Unigene Accession	Gene Title
218.466	Mm.293314	**Steroidogenic acute regulatory protein**
106.548	Mm.329582	**Betaine-homocysteine methyltransferase**
104.33	Mm.346759	**Nuclear receptor subfamily 0, group B, member 2**
61.934	Mm.878	Lymphocyte antigen 6 complex, locus D
41.541	Mm.235814	Retinol dehydrogenase 1 (all trans)
37.281	Mm.1262	**Cytochrome P450, family 17, subfamily a, polypeptide1**
4.44	Mm.6856	Pituitary tumor-transforming 1
-1.65	Mm.34405	Caspase 3
-2.56	Mm.220289	Apoptotic peptidase activacting factor 1
-2	Mm.100399	MAD homolog 4
-3.86	Mm.3295	Bcl-2-related ovarian killer protein
-4.84	Mm.3527	Cyclin G2
-15.73	Mm.14874	Granzyme B

Table 4-3. List of target genes from Affymetrix analysis in ileum

Total RNA was extracted from ileum epithelium of transgenic and littermate controls, converted to cRNA, and hybridized to Affymetrix chips (n=5 male mice/group, 12 week old of age). Average ratio (fold change between WT and Tg), gene ID, and names are listed. Genes in bold characters are known LRH-1 target genes and in blue are candidates specific in ileum.

Figure 4-7. Expression of genes involved in cell proliferation and differentiation. RNA were prepared from duodenum (A) and ileum (B) of WT and Tg mice. RT-qPCR was used to measure mRNA levels of target genes. Data are the mean ± SEM (n=5 male mice/group). *, P<0.05; **, P<0.01.
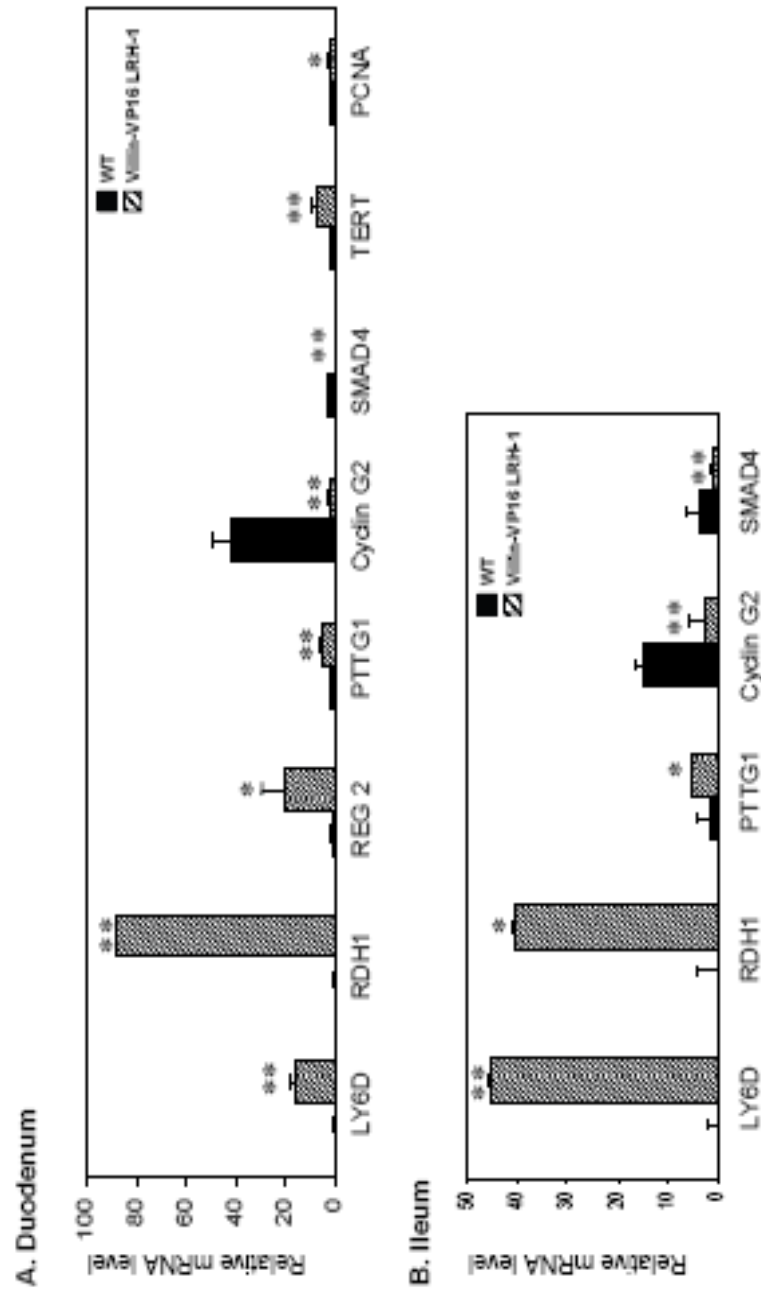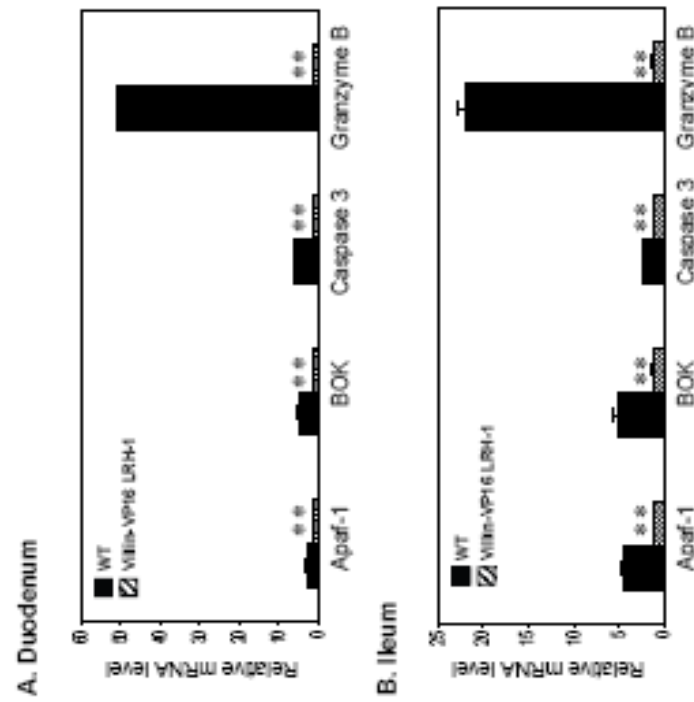
Figure 4-8. Expression of genes involved in cell apoptosis and immune response RNA were prepared from duodenum (A) and ileum (B) of WT and Tg mice. RT-qPCR was used to measure mRNA levels of target genes. Data are the mean ± SEM (n=5 male mice/group). **, P<0.01.
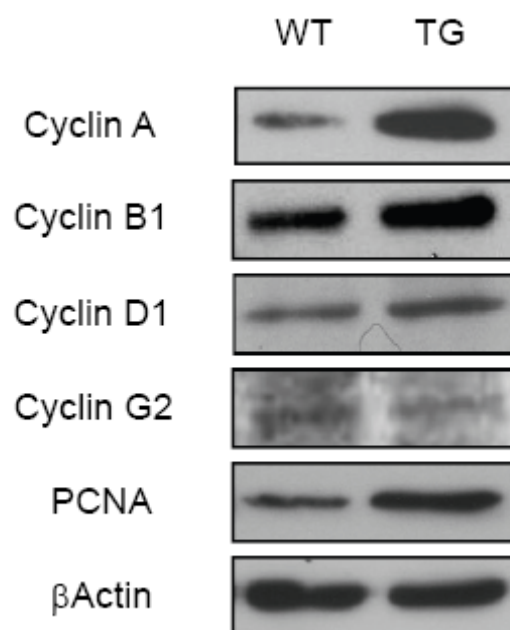
Figure 4-9. Protein expression profile in Villin-VP16LRH-1 intestine

Immunoblot analysis of cell cycle relative proteins; cyclin A, cyclin B1, cyclin D1, and cyclin G2, and PCNA. Whole cell lysates were prepared from duodenum of WT and Villin-VP16LRH-1 mice (n=3, pooled). βActin was used as a loading control.

significant changes in villus length, crypt depth, crypt number, BrdU labeling index or mRNA levels of cyclin D1 in the duodenum of *Lrh-1^{flox/flox};Vil-Cre* mice (Figures 4-10A-E). These data raise the possibility that decreased LRH-1 expression in both the epithelial and stromal compartments is required to blunt proliferation in the intestine. Alternatively, there may a compensatory proliferative response in the intestinal epithelium of *Lrh-1^{flox/flox};Vil-Cre* mice.
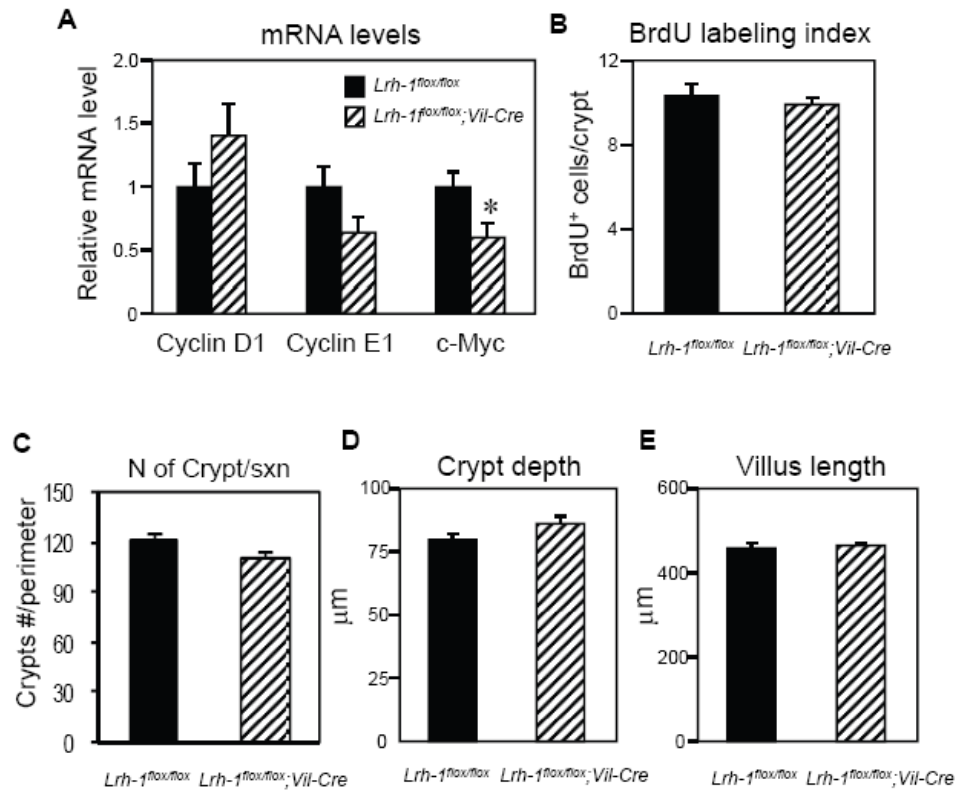
Figure 4-10. Analysis of mice deficient LRH-1 in intestine

(A) mRNA levels of the indicated genes were analyzed by RT-qPCR using intestinal epithelium derived from $Lrh-1^{flox/flox}$ and $Lrh-1^{flox/flox};Vil-Cre$ mice. n=7-8 mice/group. *, P<0.05. (B-E) BrdU labeling index (B), Number of crypts along with cross section (C), villus length (D), and crypt depth (E) were measured in duodenum of $Lrh-1^{flox/flox}$ and $Lrh-1^{flox/flox};Vil-Cre$ mice.

4.5 Discussion

In Villin-VP16LRH-1 mice, the small intestine was enlarged due to increased proliferation and decreased apoptosis. The phenotype was clearly evident in microscopic analysis of small intestine. It has been shown that LRH-1 stimulates intestinal crypt cell renewal via crosstalk with the β-catenin/TCF signaling pathway (Botrugno et al., 2004). Subsequent characterization of LRH-1 function in intestinal tumorigenesis using either the $Apc^{Min/+}$ mouse model or carcinogen treatment revealed that aberrant crypt foci formation was blunted in Lrh-$1^{+/-}$ mice (Schoonjans et al., 2005). Based on these results, it was anticipated that overexpression of LRH-1 would promote cell proliferation. Consistent with this hypothesis, we observed intestinal enlargement in Villin-VP16LRH-1 mice in this study. However, surprisingly, there was no change in the mRNA levels of cyclin E1 or cyclin D1 in either intestine-specific LRH-1 transgenic mice or the intestine-specific LRH-1 knockout mice. This prompted us to search for other potential LRH-1 target genes using microarray analysis. There were significant increases in the mRNA levels of LY6D, RDH1, and PTTG1 and decreases in the mRNA levels of SMAD4 and cyclin G2 in both duodenum and ileum. LY6D is a GPI-linked cell surface glycoprotein (Brakenhoff et al., 1995) that has been used as a diagnostic marker for head and neck cancer (Wang et al., 2003). High levels of LY6D are also found in murine gastrointestinal adenomas (Reichling et al., 2005). RDH1 catalyzes a step in the synthesis of all-trans retinoic acid (Zhang et al., 2001b). A recent study suggested that retinoic acid can inhibit apoptosis and stimulate crypt cell proliferation after resection (Wang et al., 2007). The *Pttg1* gene (Pei and Melmed, 1997) regulates sister chromatid separation during cell division. Pttg1 knockout mice showed testicular, splenic, thymic, pancreatic β-cell and

pituitary hypoplasia due to impaired cell cycle progression (Chesnokova et al., 2005; Wang et al., 2003; Wang et al., 2001). In contrast to Pttg1 knockout mice, overexpression of Pttg1 induces cell transformation and contributes to colon cancer metastasis (Heaney et al., 2000). SMAD4 mutant mice phenocopy human juvenile polyposis syndrome (Howe et al., 1998), and SMAD4 has been shown to have anti-proliferative functions (Levy and Hill, 2005). Cyclin G2 is an unconventional cyclin that is highly expressed in quiescent cells (Martinez-Gac et al., 2004a; Martinez-Gac et al., 2004b). Expression of both SMAD4 and cyclin G2 was downregulated in Villin-VP16LRH-1 mice. The change in expression of these genes is consistent with the increased intestinal proliferation seen in VP16-LRH-1 transgenic mice. In addition, PCNA, which is a cell proliferation marker, TERT, which is a catalytic subunit of telomerase, and REG2, which has mitogenic and antiapoptotic properties (Lieu et al., 2006) were all up-regulated in duodenum of Villin-VP16LRH-1.

Genes involved in apoptosis, including Apaf1 and caspase3, and in inflammatory responses, including granzyme B, were significantly reduced in Villin-VP16LRH-1 mice. Granzyme B targets caspase3 to initiate programmed cell death in virus-infected cells (Trapani and Smyth, 2002). Thus, the enlarged size of the small intestine in Villin-VP16LRH-1 mice appears to be due not only to increased cell proliferation but also to decreased apoptosis. A role for LRH-1 in apoptosis has previously been shown in LRH-1 RNA interference studies in BEL-7402 human hepatocellular carcinoma cells (Wang et al., 2005a). Knockdown of human LRH-1 in BEL-7402 cells induced apoptosis.

There are two mechanisms for crypt expansion and formation: crypt fission and crypt budding (Edwards and Chapman, 2007; Preston et al., 2003; Satoh et al., 1985; Wasan et al., 1998). Our studies showed that overexpression of LRH-1 leads to an increase in the number of crypts per transverse section. H&E staining revealed the presence of repopulating crypts (Figure 4-11). A number of studies have elucidated the molecular mechanism of crypt formation. Among them, He *et al.,* showed that excess intestinal stem cells in PTEN-deficient mice initiate *de novo* crypt formation and crypt fission via the PTEN-Akt pathway, which enhances β-catenin activity and inactivates the cycle-dependent kinase inhibitor, p27^{kip1}. To determine the involvement of the PTEN-Akt pathway in Villin-VP16LRH-1 mice, we performed immunoblot analysis. Preliminary results from profiling of signaling proteins revealed that there is a subtle increase in phosphorylated PTEN in Villin-VP16LRH-1 mice (Figure 4-12). Phosphorylated PTEN no longer efficiently inhibits Akt activity, and thus phosphorylated Akt is increased. The Akt signaling pathway has well-established effects on cell survival. One of the molecular mechanisms for this is the control of cell cycle entry by modulating the activity of the forkhead transcription factor, FoxO3a (Martinez-Gac et al., 2004b). Active Akt phosphorylates FoxO3a, which blocks its transcriptional activity by blocking its nuclear translocation. Among the genes regulated by FoxO3a is cyclin G2. The level of cyclin G2 expression is reciprocally related to cell cycle progression (Bennin et al., 2002; Horne et al., 1997). The low mRNA and protein level of cyclin G2 in Villin-VP16LRH-1 mice suggests that Akt signaling is active, although it still remains to be tested whether LRH-1 regulates cyclin G2 directly.
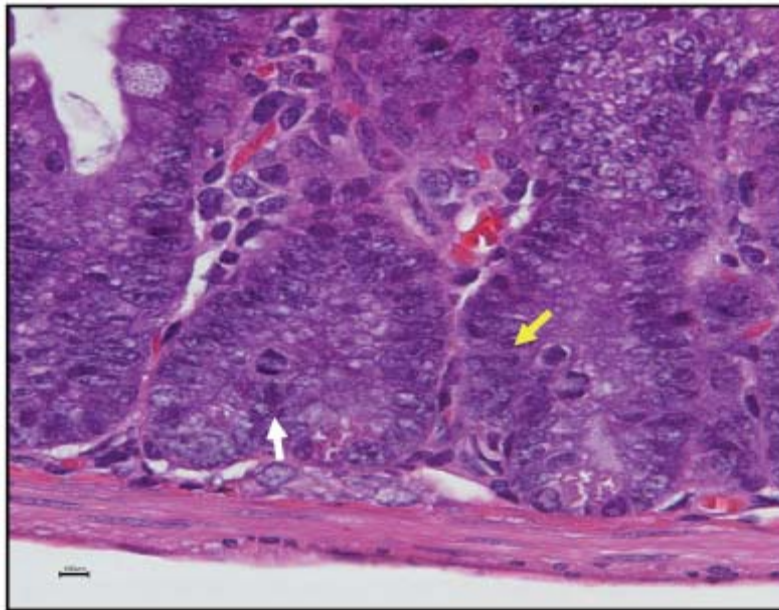
Figure 4-11. *De novo* **crypts formation in Villin-VP16LRH-1 intestine**

H&E stained section from duodenum of 4 week-old Villin-VP16LRH-1 mice. Crypt fission and budding were found; white arrow indicates apex of bifurcation and yellow arrow indicates initiation point of crypt budding. 20X magnification.
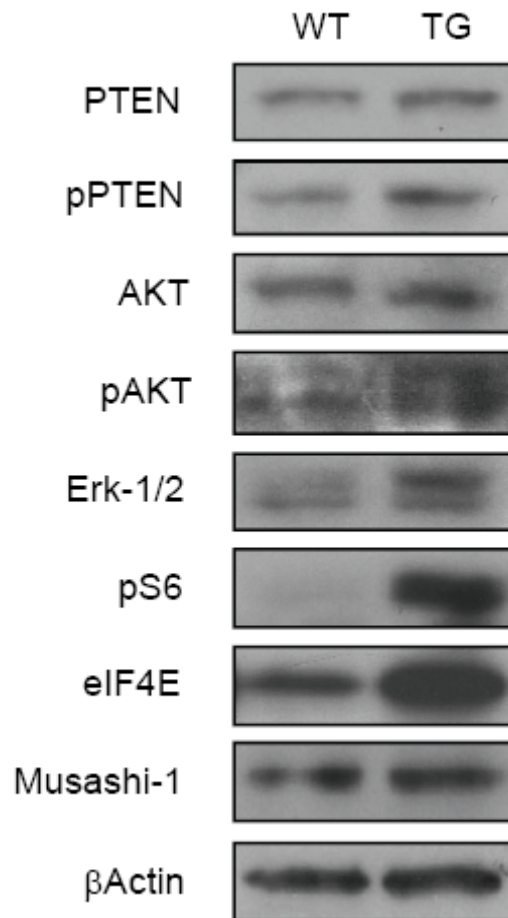
Figure 4-12. Profile of signaling proteins in Villin-VP16LRH-1 intestine

Immunoblot analysis of singaling pathways which involved in cell proliferation and growth. Whole cell lysates were prepared from duodenum of WT and Villin-VP16LRH-1 mice (n=3, pooled). βActin was used as a loading control.

An unanticipated finding from these studies was that phosphorylated ribosomal protein, S6 (rpS6), and eukaryotic initiation factor, eIF4E, were significantly elevated in Villin-VP16LRH-1 mice. Both of these proteins are well established downstream effectors of target of rapamycin (mTOR) signaling. RpS6 is phosphorylated by ribosomal protein S6 kinases (S6K) and has been shown to regulate cell and body size, protein synthesis, and glucose homeostasis (Montagne et al., 1999; Ohanna et al., 2005; Pende et al., 2000). Direct evidence that rpS6 controls cell size and glucose homeostasis was provided using mice in which a non-phosphorylatable rpS6 derivative was knocked into mice (Ruvinsky et al., 2005). The mouse embryo fibroblasts (MEF) of mutant mice exhibited a small cell phenotype and mutant mice suffered from hypoinsulinemia and impaired glucose tolerance. Overexpression of eIF4E leads to oncogenic transformation of cell lines and induces tumor formation in mice (Culjkovic et al., 2007). eIF4E regulates the nuclear export of specific mRNAs such as cyclin D1. It is speculated that LRH-1 regulates cyclin D1 at a post-transcriptional level via eIF4E rather than at a transcriptional level. Additional studies will be needed to determine the role of LRH-1 and its relationship with the mTOR and Akt signaling pathways.

Crypts are flask-shaped invaginations of intestinal epithelium where stem cells reside and continuously produce progenitor cells. Musashi-1 is a RNA-binding protein that has been proposed as a marker of proliferating neural precursor cells and epithelial stem cells including intestinal and mammary gland stem cells (Kaneko et al., 2000; Okano et al., 2005; Potten et al., 2003). However, immunoblotting showed that there was no difference in Musashi-1 protein levels between wild type and Villin-VP16LRH-1 mice (Figure 4-12). Additional experiments such as immunostaining with anti-Musashi-1

antibody will be useful to determine whether there is any difference in the intestinal stem cells between wild type and Villin-VP16LRH-1 mice.

In summary, this study demonstrates a role for LRH-1 in promoting crypt cell proliferation and crypt formation and reducing apoptosis.

4.5 References

Batlle, E., Henderson, J.T., Beghtel, H., van den Born, M.M., Sancho, E., Huls, G., Meeldijk, J., Robertson, J., van de Wetering, M., Pawson, T., *et al.* (2002). Beta-catenin and TCF mediate cell positioning in the intestinal epithelium by controlling the expression of EphB/ephrinB. Cell *111*, 251-263.

Bennin, D.A., Don, A.S., Brake, T., McKenzie, J.L., Rosenbaum, H., Ortiz, L., DePaoli-Roach, A.A., and Horne, M.C. (2002). Cyclin G2 associates with protein phosphatase 2A catalytic and regulatory B' subunits in active complexes and induces nuclear aberrations and a G1/S phase cell cycle arrest. J Biol Chem *277*, 27449-27467.

Botrugno, O.A., Fayard, E., Annicotte, J.S., Haby, C., Brennan, T., Wendling, O., Tanaka, T., Kodama, T., Thomas, W., Auwerx, J., *et al.* (2004). Synergy between LRH-1 and beta-catenin induces G1 cyclin-mediated cell proliferation. Mol Cell *15*, 499-509.

Brakenhoff, R.H., Gerretsen, M., Knippels, E.M., van Dijk, M., van Essen, H., Weghuis, D.O., Sinke, R.J., Snow, G.B., and van Dongen, G.A. (1995). The human E48 antigen, highly homologous to the murine Ly-6 antigen ThB, is a GPI-anchored molecule apparently involved in keratinocyte cell-cell adhesion. J Cell Biol *129*, 1677-1689.

Chesnokova, V., Kovacs, K., Castro, A.V., Zonis, S., and Melmed, S. (2005). Pituitary hypoplasia in Pttg-/- mice is protective for Rb+/- pituitary tumorigenesis. Mol Endocrinol *19*, 2371-2379.

Culjkovic, B., Topisirovic, I., and Borden, K.L. (2007). Controlling gene expression through RNA regulons: the role of the eukaryotic translation initiation factor eIF4E. Cell Cycle *6*, 65-69.

Edwards, C.M., and Chapman, S.J. (2007). Biomechanical modelling of colorectal crypt budding and fission. Bull Math Biol *69*, 1927-1942.

Haramis, A.P., Begthel, H., van den Born, M., van Es, J., Jonkheer, S., Offerhaus, G.J., and Clevers, H. (2004). De novo crypt formation and juvenile polyposis on BMP inhibition in mouse intestine. Science *303*, 1684-1686.

Heaney, A.P., Singson, R., McCabe, C.J., Nelson, V., Nakashima, M., and Melmed, S. (2000). Expression of pituitary-tumour transforming gene in colorectal tumours. Lancet *355*, 716-719.

Horne, M.C., Donaldson, K.L., Goolsby, G.L., Tran, D., Mulheisen, M., Hell, J.W., and Wahl, A.F. (1997). Cyclin G2 is up-regulated during growth inhibition and B cell antigen receptor-mediated cell cycle arrest. J Biol Chem *272*, 12650-12661.

Howe, J.R., Bair, J.L., Sayed, M.G., Anderson, M.E., Mitros, F.A., Petersen, G.M., Velculescu, V.E., Traverso, G., and Vogelstein, B. (2001). Germline mutations of the gene encoding bone morphogenetic protein receptor 1A in juvenile polyposis. Nat Genet *28*, 184-187.

Howe, J.R., Roth, S., Ringold, J.C., Summers, R.W., Jarvinen, H.J., Sistonen, P., Tomlinson, I.P., Houlston, R.S., Bevan, S., Mitros, F.A.*, et al.* (1998). Mutations in the SMAD4/DPC4 gene in juvenile polyposis. Science *280*, 1086-1088.

Kaneko, Y., Sakakibara, S., Imai, T., Suzuki, A., Nakamura, Y., Sawamoto, K., Ogawa, Y., Toyama, Y., Miyata, T., and Okano, H. (2000). Musashi1: an evolutionarily conserved marker for CNS progenitor cells including neural stem cells. Dev Neurosci *22*, 139-153.

Levy, L., and Hill, C.S. (2005). Smad4 dependency defines two classes of transforming growth factor {beta} (TGF-{beta}) target genes and distinguishes TGF-{beta}-induced epithelial-mesenchymal transition from its antiproliferative and migratory responses. Mol Cell Biol *25*, 8108-8125.

Lieu, H.T., Simon, M.T., Nguyen-Khoa, T., Kebede, M., Cortes, A., Tebar, L., Smith, A.J., Bayne, R., Hunt, S.P., Brechot, C.*, et al.* (2006). Reg2 inactivation increases sensitivity to Fas hepatotoxicity and delays liver regeneration post-hepatectomy in mice. Hepatology *44*, 1452-1464.

Madison, B.B., Braunstein, K., Kuizon, E., Portman, K., Qiao, X.T., and Gumucio, D.L. (2005). Epithelial hedgehog signals pattern the intestinal crypt-villus axis. Development *132*, 279-289.

Madison, B.B., Dunbar, L., Qiao, X.T., Braunstein, K., Braunstein, E., and Gumucio, D.L. (2002). Cis elements of the villin gene control expression in restricted domains of the vertical (crypt) and horizontal (duodenum, cecum) axes of the intestine. J Biol Chem *277*, 33275-33283.

Martinez-Gac, L., Alvarez, B., Garcia, Z., Marques, M., Arrizabalaga, M., and Carrera, A.C. (2004a). Phosphoinositide 3-kinase and Forkhead, a switch for cell division. Biochem Soc Trans *32*, 360-361.

Martinez-Gac, L., Marques, M., Garcia, Z., Campanero, M.R., and Carrera, A.C. (2004b). Control of cyclin G2 mRNA expression by forkhead transcription factors: novel

mechanism for cell cycle control by phosphoinositide 3-kinase and forkhead. Mol Cell Biol *24*, 2181-2189.

Montagne, J., Stewart, M.J., Stocker, H., Hafen, E., Kozma, S.C., and Thomas, G. (1999). Drosophila S6 kinase: a regulator of cell size. Science *285*, 2126-2129.

Ohanna, M., Sobering, A.K., Lapointe, T., Lorenzo, L., Praud, C., Petroulakis, E., Sonenberg, N., Kelly, P.A., Sotiropoulos, A., and Pende, M. (2005). Atrophy of S6K1(-/-) skeletal muscle cells reveals distinct mTOR effectors for cell cycle and size control. Nat Cell Biol *7*, 286-294.

Okano, H., Kawahara, H., Toriya, M., Nakao, K., Shibata, S., and Imai, T. (2005). Function of RNA-binding protein Musashi-1 in stem cells. Exp Cell Res *306*, 349-356.

Pei, L., and Melmed, S. (1997). Isolation and characterization of a pituitary tumor-transforming gene (PTTG). Mol Endocrinol *11*, 433-441.

Pende, M., Kozma, S.C., Jaquet, M., Oorschot, V., Burcelin, R., Le Marchand-Brustel, Y., Klumperman, J., Thorens, B., and Thomas, G. (2000). Hypoinsulinaemia, glucose intolerance and diminished beta-cell size in S6K1-deficient mice. Nature *408*, 994-997.

Porter, E.M., Bevins, C.L., Ghosh, D., and Ganz, T. (2002). The multifaceted Paneth cell. Cell Mol Life Sci *59*, 156-170.

Potten, C.S., Booth, C., Tudor, G.L., Booth, D., Brady, G., Hurley, P., Ashton, G., Clarke, R., Sakakibara, S., and Okano, H. (2003). Identification of a putative intestinal stem cell and early lineage marker; musashi-1. Differentiation *71*, 28-41.

Preston, S.L., Wong, W.M., Chan, A.O., Poulsom, R., Jeffery, R., Goodlad, R.A., Mandir, N., Elia, G., Novelli, M., Bodmer, W.F.*, et al.* (2003). Bottom-up histogenesis of colorectal adenomas: origin in the monocryptal adenoma and initial expansion by crypt fission. Cancer Res *63*, 3819-3825.

Reichling, T., Goss, K.H., Carson, D.J., Holdcraft, R.W., Ley-Ebert, C., Witte, D., Aronow, B.J., and Groden, J. (2005). Transcriptional profiles of intestinal tumors in Apc(Min) mice are unique from those of embryonic intestine and identify novel gene targets dysregulated in human colorectal tumors. Cancer Res *65*, 166-176.

Ruvinsky, I., Sharon, N., Lerer, T., Cohen, H., Stolovich-Rain, M., Nir, T., Dor, Y., Zisman, P., and Meyuhas, O. (2005). Ribosomal protein S6 phosphorylation is a determinant of cell size and glucose homeostasis. Genes Dev *19*, 2199-2211.

Sancho, E., Batlle, E., and Clevers, H. (2004). Signaling pathways in intestinal development and cancer. Annu Rev Cell Dev Biol *20*, 695-723.

Satoh, Y., Nagashima, Y., Oomori, Y., Ishikawa, K., Matoba, M., and Ono, K. (1985). Scanning electron microscopical observation on the isolated mucosa of rat small intestine: with special reference to the intestinal crypt. Anat Anz *159*, 305-309.

Schoonjans, K., Dubuquoy, L., Mebis, J., Fayard, E., Wendling, O., Haby, C., Geboes, K., and Auwerx, J. (2005). Liver receptor homolog 1 contributes to intestinal tumor formation through effects on cell cycle and inflammation. Proc Natl Acad Sci U S A *102*, 2058-2062.

Trapani, J.A., and Smyth, M.J. (2002). Functional significance of the perforin/granzyme cell death pathway. Nat Rev Immunol *2*, 735-747.

Wang, L., Tang, Y., Rubin, D.C., and Levin, M.S. (2007). Chronically administered retinoic acid has trophic effects in the rat small intestine and promotes adaptation in a resection model of short bowel syndrome. Am J Physiol Gastrointest Liver Physiol *292*, G1559-1569.

Wang, S., Lan, F., Huang, L., Dong, L., Zhu, Z., Li, Z., Xie, Y., and Fu, J. (2005). Suppression of hLRH-1 mediated by a DNA vector-based RNA interference results in cell cycle arrest and induction of apoptosis in hepatocellular carcinoma cell BEL-7402. Biochem Biophys Res Commun *333*, 917-924.

Wang, Z., Moro, E., Kovacs, K., Yu, R., and Melmed, S. (2003). Pituitary tumor transforming gene-null male mice exhibit impaired pancreatic beta cell proliferation and diabetes. Proc Natl Acad Sci U S A *100*, 3428-3432.

Wang, Z., Yu, R., and Melmed, S. (2001). Mice lacking pituitary tumor transforming gene show testicular and splenic hypoplasia, thymic hyperplasia, thrombocytopenia, aberrant cell cycle progression, and premature centromere division. Mol Endocrinol *15*, 1870-1879.

Wasan, H.S., Park, H.S., Liu, K.C., Mandir, N.K., Winnett, A., Sasieni, P., Bodmer, W.F., Goodlad, R.A., and Wright, N.A. (1998). APC in the regulation of intestinal crypt fission. J Pathol *185*, 246-255.

Zhang, M., Chen, W., Smith, S.M., and Napoli, J.L. (2001). Molecular characterization of a mouse short chain dehydrogenase/reductase active with all-trans-retinol in intact cells, mRDH1. J Biol Chem *276*, 44083-44090.

CHAPTER 5

LRH-1 IN EARLY ENDODERM DEVELOPMENT

5.1 Abstract

LRH-1 is highly expressed in developing endoderm and adult tissues of endodermal origin and regulates transcription factors involved in early endoderm development (Pare et al., 2001; Rausa et al., 1999). Studies of embryonic stem cells that harbor a disrupted *Lrh-1* locus show that LRH-1 regulates expression of many transcription factors involved in early development including the POU homeodomain transcription factor, OCT4, fibroblast growth factor 4 (FGF4), Sry-related high mobility group box transcription factor 2 (SOX2), undifferentiated embryonic cell transcription factor 1 (UTF1), and the zinc-finger transcription factor, REX1 (Gu et al., 2005). To test whether LRH-1 influences endoderm development, we expressed either mouse LRH-1 or its frog ortholog, xFF1rA, in animal caps of *Xenopus laevis* and measured markers of endoderm differentiation. Ectopic expression of LRH-1 or xFF1rA induced endoderm markers including xSox17α, xSox17β, liver fatty acid binding protein (LFABP), and intestinal fatty acid binding protein (IFABP) in animal cap explants. These data support a central role for LRH-1 in the transcriptional cascades that govern endoderm development.

5.2 Introduction

LRH-1 was originally defined by its binding to the promoter of α1-fetoprotein (AFP), a key marker of endoderm differentiation (Galarneau et al., 1996). Its frog

ortholog, xFF1rA, is expressed in the embryo from gastrula to late tailbud stage (Figure 5-1) (Ellinger-Ziegelbauer et al., 1995; Ellinger-Ziegelbauer et al., 1994). Several lines of evidence indicate that LRH-1 plays a prominent role in early development. First, LRH-1 is expressed in developing endoderm: LRH-1 expression segregates with the visceral endoderm in the egg cylinder, persists in the endodermal layers through gastrulation, and is abundant in the forgut endoderm during liver and pancreas morphogenesis (Pare et al., 2004a; Rausa et al., 1999). Annicotte *et al.* reported that LRH-1 is coexpressed with pancreatic-duodenal homeobox 1 (PDX1) in both endocrine and exocrine pancreas until E17 and PDX1 controls LRH-1 transcription in developing pancreas (Annicotte et al., 2003). At a later stage, LRH-1 expression is restricted to exocrine pancreas. Furthermore, LRH-1 binding sites have been identified in the promoters of the transcription factors OCT4, which plays a central role in the self renewal of ES cells and also the differentiation of totipotent inner cell mass cells into mesendoderm (Gu et al., 2005). LRH-1 also regulates the expression of HNF1α, HNF3β, and HNF4α, which are involved in endoderm differentiation (Pare et al., 2001). Finally, *Lrh-1 -/-* embryos die prior to gastrulation with defects of disorganized endoderm (Pare et al., 2004). These studies highlight a pivotal role for LRH-1 in early embryogenesis.
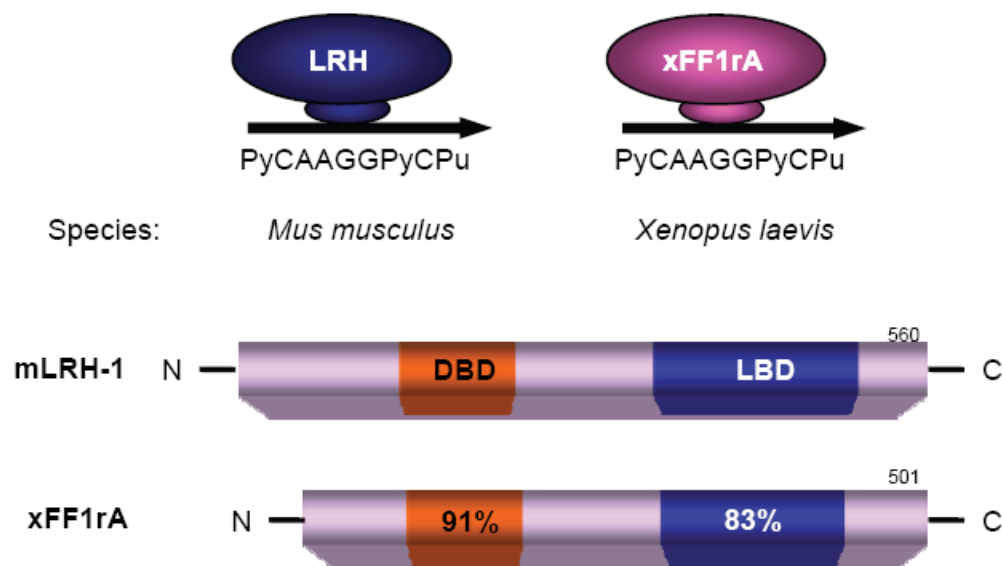
Figure 5-1. Schematic representation of mLRH-1 and xFF1r

Conserved DNA binding sequence for mouse and frog LRH-1 is illustrated (upper panel). Percent amino acid identities to mouse LRH-1 are indicated in *Xenopus* xFF1rA subdomains. DBD; DNA binding domain, LBD; ligand binding domain.

5.3 Materials and Methods

Subcloning and in vitro transcription

DNAs encoding full-length mLRH-1 and xFF1rA were cloned into the BamHI and EcoRI sites of the pCS2+ expression vector. To generate a dominant negative form of mLRH-1, arginine 380 was mutated to glycine, the transactivating domain (AF2) was deleted, and the engrailed repressor domain was fused to its carboxyl terminus. All constructs were evaluated in standard transient transfection/luciferase assays as described in Chapter 3 (Figure 5-2). For *in vitro* transcription, plasmids were linearized with either SnaBI or NotI, and 5'capped mRNAs were synthesized using the SP6 Megascript kit (Ambion).

Embryos and Microinjection

Female frogs were injected with 600 units of human chorionic gonadotrophin (HCG;Sigma) 12 hours prior to obtaining eggs. *In vitro* fertilization was carried out by mixing eggs and testis extracts, and the eggs subsequently cultured in 0.1X MMR (10X MMR contains 1 M NaCl, 20 mM KCl, 10 mM $MgSO_4 \bullet 7H_2O$, 50 mM HEPES, 20 mM $CaCl_2 \bullet 2H_2O$, and 1 mM EDTA, pH 8.0). After removal of the jelly with 2% cysteine (pH8.0), embryos were washed and cultured in 0.1X MMR and 3% ficoll before injection. Microinjection into embryos was done by Ed Fortuno in Dr. Jonathan Graff's laboratory. Two ng of mLRH-1, 4 ng of xFF1rA, 4 ng of mLRH-1Enr, and 500 pg of VegT mRNAs were injected into one-cell stage embryos. Embryos were either processed for the animal cap assay or incubated until they reached the tailbud stages. Animal caps were cut at stage 8 blastulae and incubated with 0.5X MMR at 18°C.
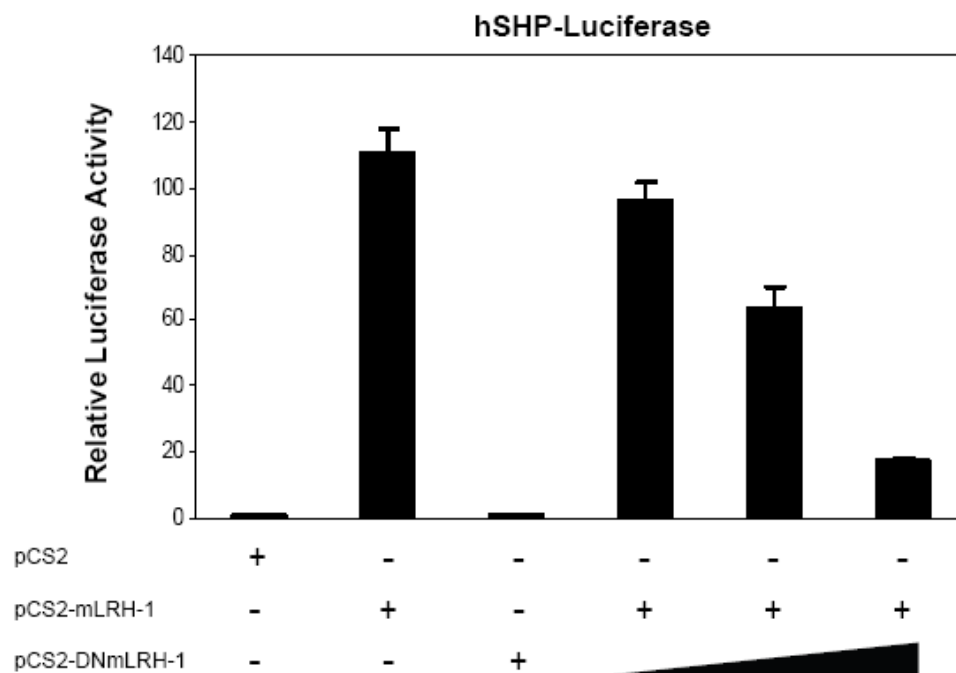
Figure 5-2. Luciferase assay with constructs for *Xenopus* embryo microinjection

Indicated constructs were transiently co-transfected into HEK293 cells with human SHP-luciferase reporter. pCS2 vector was used as a negative control. Dominant-negative LRH-1 (DN-mLRH-1) was co-transfected with mouse LRH-1in a dose-dependent manner.

RNA extraction and RT-PCR

RNA extraction from embryos at stage 28, cDNA synthesis, and RT-PCR were performed as described previously (LeSueur and Graff, 1999). RT-PCR was performed using 20 cycles for EF1α and α-cardiac actin, 25 cycles for xSox17α, xSox17β, and EDD, and 30 cycles for IFABP and LFABP. Sequences of gene specific primers are shown in Table 5-1. Radioactive-labeled PCR products were resolved on 5% non-denaturing polyacrylamide gels.

Gene	Forward Primer	Reverse Primer	Reference
xSox17α	GGCATCACCAGCTCCAC	CAGCAGTACTGGCATCG	Hudson et al.,1997
xSox17β	CAGGTGAAGAGGATGAAGAG	CATTGAGTTGTGGCCCTCAA	Engleka et al.,2001
EF1α	CCTGAACCACCCAGGCCAGATTGGTG	GAGGGTAGTCAGAGAAGCTCTCCACG	Agius et al.,2000
EDD	AGCAGAAAATGGCAAACACAC	GGTCTTTTAATGGCAACAGGT	Sasai et al.,1996
α cardiac actin	TCCCTGTACGCTTCTGGTCGTA	TCTCAAAGTCCAAAGCCACATA	Stutz et al., 1986
IFABP	CGTGTTCCTACAGGAC	GTATGCCCAATGTGCC	Shi, 1994
LFABP	ACCGAGATTGAACAGAATGG	CCTCCATGTTTACCACGGAC	Henry et al.,1998

Table 5-1. RT-PCR primer sequences

5.4 Results & Discussion

LRH-1 induces endoderm markers in *Xenopus* animal caps. Loss-of-function studies performed using either LRH-1 -/- mice or differentiated LRH-1 -/- ES cells show dysregulated expression of many transcription factors including HNF3β, HNF4α, OCT4, and SOX2, suggesting that LRH-1 plays a prominent role in endoderm development. To study this role of LRH-1, we examined whether ectopic expression of LRH-1 or its *Xenopus* homolog, xFF1rA, is sufficient to promote endoderm formation in *Xenopus* animal caps, which is a well established assay for testing whether affect early differentiation events (Ang et al., 1993). Mouse LRH-1 and xFF1rA share 91% and 83% amino acid identity in their DNA and ligand binding domains, respectively (Figure 5-1) (Ellinger-Ziegelbauer et al., 1994). Like LRH-1, xFF1rA is expressed in the embryo during early development (Ellinger-Ziegelbauer et al., 1994). LRH-1 and xFF1rA were transcribed *in vitro* and injected into the animal pole of embryos at the one-cell stage, and then caps were taken at stage 8 and cultured to stage 28. RNA encoding the T-box transcription factor, VegT, which induces both endoderm and mesoderm (Horb and Thomsen, 1997; Lustig et al., 1996; Stennard et al., 1996; Zhang et al., 1998), was injected as a positive control. As expected, VegT efficiently induced expression of the endoderm markers xSox17α, xSox17β, LFABP, IFABP, and endodermin, and the mesoderm marker α-cardiac actin (Figure 5-3). Both LRH-1 and xFF1rA induced xSox17α, LFABP, and IFABP, and also weakly induced xSox17β and endodermin (Figure 5-3). SOX17 mutant mouse embryos have profound defects in gut and endoderm formation (Kanai-Azuma et al., 2002), and *Xenopus* SOX17 homologs, xSOX17α and β,
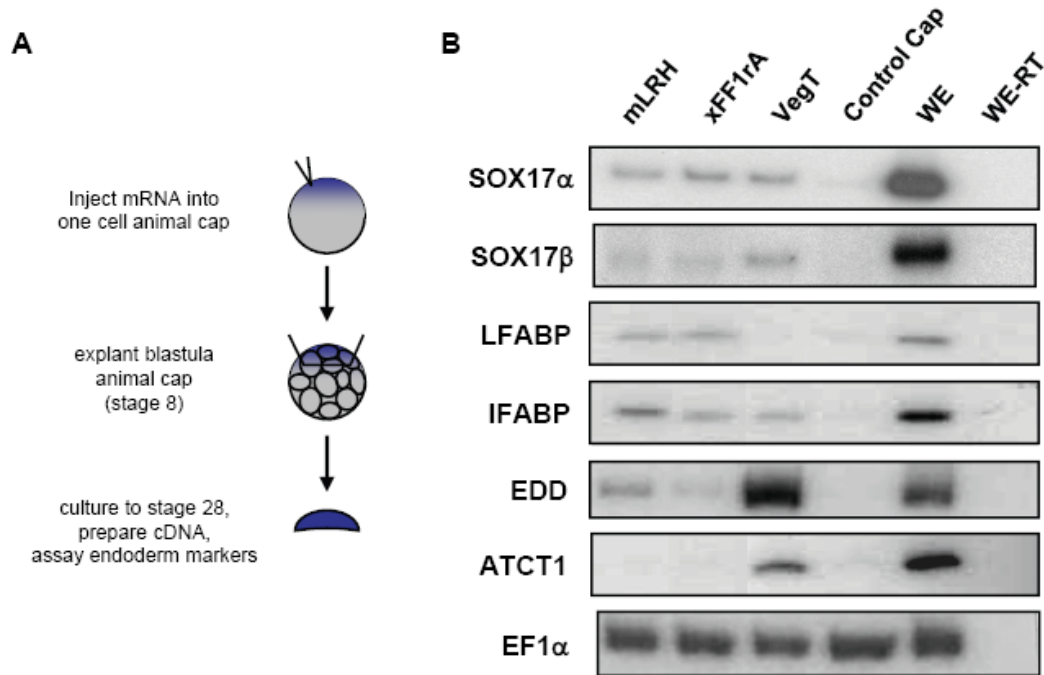
Figure 5-3. LRH-1 induces endoderm markers in animal cap explants.

(**A**) mRNA encoding LRH-1, its *Xenopus* homolog xFF1rA, and VegT was microinjected into one cell stage *Xenopus* embryos and then animal caps were dissected from blastula stage embryos. At stage 28, total RNAs were harvested from a pool of five animal caps. (**B**) RT-PCR for induction of the indicated markers. RNA was also analyzed from animal caps derived from embryos that were not microinjected (Control Cap). RNA from uninjected whole embryos (WE) serves as a positive control. The negative control (no RT) is identical to the WE lane except that reverse transcriptase was omitted. LFABP, liver fatty acid binding protein; IFABP, intestinal fatty acid binding protein; EDD, endodermin; ACTC1, α-cardiac actin 1. Elongation factor 1α (EF-1α) serves as a loading control.

promote endoderm formation in *Xenopus* animal explants (Hudson et al., 1997). Neither LRH-1 nor xFF1rA induced expression of the mesoderm marker cardiac actin (Figure 5-3). Thus, LRH-1 and its *Xenopus* homolog can induce endoderm markers in animal cap explants.

Dominant negative LRH-1 disrupts normal endoderm formation. To further examine the actions of LRH-1 during early development, whole embryos were injected with either dominant negative LRH-1 (DN-LRH-1) or xFF1rA and allowed to develop to stage 45 (Figure 5-4). As shown at Figure 5-4B, animals injected with dominant negative LRH-1 exhibited loss of head structures as well as defective gut development compared to wild type animals (Figure 5-4A). This is similar to the phenotype seen in embryos injected with a dominant negative form of Mixer, which is required to maintain expression of both Sox17α and Sox17β (Henry and Melton, 1998). Based on animal cap assays, LRH-1 can induce Sox17α as well as other endodermal markers. The similar phenotype observed in animals injected with DN-LRH-1 may be due to the blockage of the expression of genes important for endoderm lineage including Sox17. However, additional experiments such as LRH-1 morpholino or rescue experiments are required to determine whether the gut phenotype is LRH-1 specific. Notably, animals over-expressing xFF1rA showed severe defects in gut looping and shortening of the anteroposterior axis (Figure 5-4D). In summary, these abnormal phenotypes suggest that LRH-1 plays a critical role in early *Xenopus* gut development.
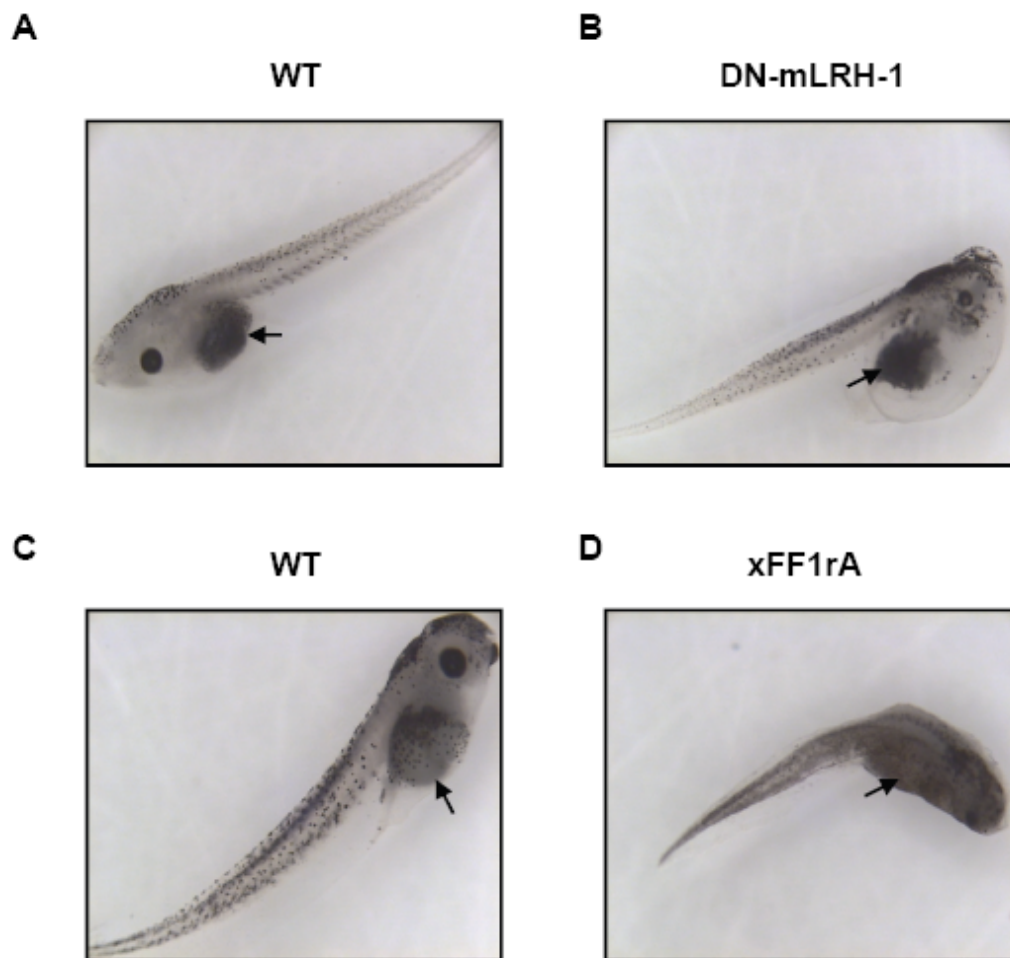
Figure 5-4. Effects of LRH-1 on early development of *Xenopus* embryos.

Animals microinjected with dominant negative mouse LRH-1 (DN-mLRH-1) **(B),** xFF1rA **(D)**, and their pairs of control (WT, **A and C**) are shown. Each was microinjected into one cell stage *Xenopus* embryos and allow to develop to stage 45. DN-mLRH-1 injected animal shows mild defects on gut size and craniofacial development compared to WT, while xFF1rA injected animal exhibits severe phenotype on gut coiling. Arrow indicates *Xenopus* gut.

5.5 References

Agius, E., Oelgeschläger, M., Wessely, O., Kemp, C., and De Robertis, E.M. (2000). Endodermal Nodal-related signals and mesoderm induction in Xenopus. Development *127*, 1173-1183.

Ang, S.L., Wierda, A., Wong, D., Stevens, K.A., Cascio, S., Rossant, J., and Zaret, K.S. (1993). The formation and maintenance of the definitive endoderm lineage in the mouse: involvement of HNF3/forkhead proteins. Development *119*, 1301-1315.

Annicotte, J.S., Fayard, E., Swift, G.H., Selander, L., Edlund, H., Tanaka, T., Kodama, T., Schoonjans, K., and Auwerx, J. (2003). Pancreatic-duodenal homeobox 1 regulates expression of liver receptor homolog 1 during pancreas development. Mol Cell Biol *23*, 6713-6724.

Ellinger-Ziegelbauer, H., Glaser, B., and Dreyer, C. (1995). A naturally occurring short variant of the FTZ-F1-related nuclear orphan receptor xFF1rA and interactions between domains of xFF1rA. Mol Endocrinol *9*, 872-886.

Ellinger-Ziegelbauer, H., Hihi, A.K., Laudet, V., Keller, H., Wahli, W., and Dreyer, C. (1994). FTZ-F1-related orphan receptors in Xenopus laevis: transcriptional regulators differentially expressed during early embryogenesis. Mol Cell Biol *14*, 2786-2797.

Engleka, M.J., Craig, E.J., and Kessler, D.S. (2001). VegT activation of Sox17 at the midblastula transition alters the response to nodal signals in the vegetal endoderm domain. Dev Biol *237*, 159-172.

Galarneau, L., Pare, J.F., Allard, D., Hamel, D., Levesque, L., Tugwood, J.D., Green, S., and Belanger, L. (1996). The alpha1-fetoprotein locus is activated by a nuclear receptor of the Drosophila FTZ-F1 family. Mol Cell Biol *16*, 3853-3865.

Gu, P., Goodwin, B., Chung, A.C., Xu, X., Wheeler, D.A., Price, R.R., Galardi, C., Peng, L., Latour, A.M., Koller, B.H.*, et al.* (2005). Orphan nuclear receptor LRH-1 is required to maintain Oct4 expression at the epiblast stage of embryonic development. Mol Cell Biol *25*, 3492-3505.

Henry, G.L., and Melton, D.A. (1998). Mixer, a homeobox gene required for endoderm development. Science *281*, 91-96.

Horb, M.E., and Thomsen, G.H. (1997). A vegetally localized T-box transcription factor in Xenopus eggs specifies mesoderm and endoderm and is essential for embryonic mesoderm formation. Development *124*, 1689-1698.

Hudson, C., Clements, D., Friday, R.V., Stott, D., and Woodland, H.R. (1997). Xsox17alpha and -beta mediate endoderm formation in Xenopus. Cell *91*, 397-405.

Kanai-Azuma, M., Kanai, Y., Gad, J.M., Tajima, Y., Taya, C., Kurohmaru, M., Sanai, Y., Yonekawa, H., Yazaki, K., Tam, P.P*., et al.* (2002). Depletion of definitive gut endoderm in Sox17-null mutant mice. Development *129*, 2367-2379.

LeSueur, J.A., and Graff, J.M. (1999). Spemann organizer activity of Smad10. Development *126*, 137-146.

Lustig, K.D., Kroll, K.L., Sun, E.E., and Kirschner, M.W. (1996). Expression cloning of a Xenopus T-related gene (Xombi) involved in mesodermal patterning and blastopore lip formation. Development *122*, 4001-4012.

Pare, J.F., Malenfant, D., Courtemanche, C., Jacob-Wagner, M., Roy, S., Allard, D., and Belanger, L. (2004). The fetoprotein transcription factor (FTF) gene is essential to embryogenesis and cholesterol homeostasis and is regulated by a DR4 element. J Biol Chem *279*, 21206-21216.

Pare, J.F., Roy, S., Galarneau, L., and Belanger, L. (2001). The mouse fetoprotein transcription factor (FTF) gene promoter is regulated by three GATA elements with tandem E box and Nkx motifs, and FTF in turn activates the Hnf3beta, Hnf4alpha, and Hnf1alpha gene promoters. J Biol Chem *276*, 13136-13144.

Rausa, F.M., Galarneau, L., Belanger, L., and Costa, R.H. (1999). The nuclear receptor fetoprotein transcription factor is coexpressed with its target gene HNF-3beta in the developing murine liver, intestine and pancreas. Mech Dev *89*, 185-188.

Sasai, Y., Lu, B., Piccolo, S., and De Robertis, E.M. (1996). Endoderm induction by the organizer-secreted factors chordin and noggin in Xenopus animal caps. EMBO J *15*, 4547-4555.

Shi, Y.B. and Hayes, W.P. (1994). Thyroid hormone-dependent regulation of the intestinal fatty acid-binding protein gene during amphibian metamorphosis. Dev Biol *161*, 48-58.

Stennard, F., Carnac, G., and Gurdon, J.B. (1996). The Xenopus T-box gene, Antipodean, encodes a vegetally localised maternal mRNA and can trigger mesoderm formation. Development *122*, 4179-4188.

Stutz, F. and Spohr, G. (1986). Isolation and characterization of sarcomeric actin genes expressed in Xenopus laevis embryos. J Mol Biol *187*, 349-361.

Zhang, J., Houston, D.W., King, M.L., Payne, C., Wylie, C., and Heasman, J. (1998). The role of maternal VegT in establishing the primary germ layers in Xenopus embryos. Cell *94*, 515-524.

CHAPTER 6

ANTIBACTERIAL DEFENSE BY FXR

∗ In this study, I contributed to the gene profiling studies and mouse procedures.

6.1 Abstract

Obstruction of bile flow results in bacterial proliferation and mucosal injury in small intestine that can lead to the translocation of bacteria across the epithelial barrier and systemic infection. These adverse effects of biliary obstruction can be inhibited by administration of bile acids. Here, we show that the farnesoid X receptor (FXR), a nuclear receptor for bile acids, induces genes involved in enteroprotection and inhibits bacterial overgrowth and mucosal injury caused by blockage of bile flow. Mice lacking FXR have an increase in intestinal bacteria and a compromised epithelial barrier function. These findings reveal a central role for FXR in protecting the small intestine and, furthermore, suggest that FXR agonists may prevent epithelial deterioration and bacterial translocation in patients with impaired bile flow.

6.2 Introduction

Bile acids are polar cholesterol metabolites that are synthesized in the liver, stored in the gallbladder, and released in response to feeding into the small intestine, where they are crucial for the absorption of lipids and lipid-soluble vitamins (Russell, 2003). In addition to their role in digestion, bile acids affect the microflora and integrity of the small intestine. Obstruction of bile flow in humans or rodents causes proliferation

130

of intestinal bacteria and mucosal injury, which can lead to bacterial translocation across the mucosal barrier and systemic infection (Berg, 1995). Oral administration of bile acids inhibits the bacterial overgrowth and translocation caused by biliary obstruction in rodents (Ding et al., 1993; Lorenzo-Zuniga et al., 2003). Moreover, preoperative oral administration of bile acids blocks endotoxemia in patients with obstructive jaundice (Cahill, 1983; Cahill et al., 1987; Evans et al., 1982). The mechanisms underlying the beneficial actions of bile acids are not known.

The farnesoid X receptor (FXR) is a member of the steroid/thyroid hormone receptor family of ligand-activated transcription factors that is activated by bile acids including cholic acid and chenodeoxycholic acid (Edwards et al., 2002; Makishima et al., 1999). FXR is much studied in liver, where it regulates a program of genes involved in maintaining bile acid homeostasis (Edwards et al., 2002; Makishima et al., 1999). FXR is also expressed in the intestine, where it regulates several genes including the ileal bile acid binding protein and fibroblast growth factor 15 (Forman et al., 1995; Grober et al., 1999; Inagaki et al., 2005). However, little is known about the overarching function of FXR in the gut.

In this report we have examined the role of FXR in the ileum. We demonstrate that it plays a crucial role in maintaining the integrity of the intestinal epithelium and in preventing bacterial overgrowth and translocation across the epithelial barrier.

6.3 Materials and Methods

Animal Procedures

All experiments were performed on age matched, male mice. WT mice, CYP27-KO mice (a gift from Eran Leitersdorf, Hadassah University Hospital, Jerusalem), and FXR-KO mice (a gift from Frank Gonzalez, National Institutes of Health, Bethesda) were maintained on a mixedstrain background (C57BL/6:129Sv). For transcriptional profiling studies, 3- to 4-month-old mice received a first dose of GW4064 (100 mg/kg in 1% Tween 80/1% methylcellulose) or vehicle by oral gavage followed by a second dose 12 h later. The mice were killed 14 h after the first dose, and the small intestine was removed, flushed with ice-cold saline, and cut into three segments of equal length representing the duodenum, jejunum, and ileum. The three segments were cut open longitudinally, and the mucosa were gently scraped and flash-frozen in liquid nitrogen. For BDL experiments, 8- to 10-month-old WT and FXR-KO mice were treated daily with GW4064 (100 mg/kg per day in 1% Tween 80/1% methylcellulose) or vehicle by gavage for 2 days before surgery and 5 days after. Animals treated with GW4064 or vehicle for 2 days were randomly assigned to BDL or sham-operated groups. Surgery was performed under general anesthesia through an upper midline abdominal incision. The common bile duct was mobilized and ligated by using 4/0 silk for the BDL group. Sham-operated mice had the same incision followed by mobilization of the common bile duct without ligation. All experiments were approved by the Institutional Animal Care and Research Advisory Committee at the University of Texas Southwestern Medical Center.

Affymetrix Analysis

Total RNA was extracted from tissues by using RNA STAT-60 (Tel-Test, Friendswood,

TX), and cDNA was prepared. Affymetrix analysis was done as described in Chapter 4.

RT-qPCR Analysis

Primer sequences are listed in Table 6-1. RT-qPCR performed as described in Chapter 3.

Genes	Accession Number	Forward Primer	Reverse Primer
ANG1	NM_007447	AGCGAATGGAAGCCCTTACA	CTCATCGAAGTGGACCGGCA
CAR12	NM_178396	CTCAGACCTGTACCCTGACTTCA	GAGCCTATCTCAATAAGAACAGCAA
IL18	NM_008360	CCGCCTCAAACCTTCCAA	TCTGACATGGCAGCCATTGT
iNOS	U43428	CAGGAGGAGAGAGATCCGATTTA	GCATTAGCATGGAAGCAAAGA

Table 6-1. RT-qPCR primer sequences (The primers not included here are listed in Table 3-1)

Serum Total Bilirubin Concentrations and Bacterial Counts

At the end of the BDL experiment, the mice were killed by halothane inhalation, blood

was obtained from the inferior vena cava, and the ileum, cecum, and mesenteric lymph

node complex were removed. The lumen of the ileum was washed with 1.5 ml of tryptic

soy broth (Becton Dickinson), and the contents were collected. The cecum and

mesenteric lymph node complex were weighed and homogenized in 1.5 ml of tryptic soy

broth. Serial dilutions of ileal contents and cecal and mesenteric lymph node complex

extracts were cultured on trypticase soy agar with 5% sheep blood plates (Becton

Dickinson) under aerobic or anaerobic conditions. The numbers of colonyforming units

were counted after incubation for 20 h at 37°C. Serum total bilirubin concentrations were

measured by variation of the diazo method by using an Olympus Chemistry

ImmunoAnalyzer in the Aston Pathology Laboratory at the University of Texas Southwestern Medical Center.

In Situ Hybridization

In situ hybridization was performed on paraffin sections of ileum by using ^{35}S-labeled sense and antisense riboprobes against the FXR ligand binding domain (nucleotides 921-1380; GenBank accession no. U09416). Slides were exposed at 4°C for 14 days. In all cases, sections hybridized with the sense probe resulted in the absence of signal (data not shown).

Immunohistochemistry

Immunostaining was performed on deparaffinized transverse sections of ileum. Endogenous peroxidase activity was quenched with 0.3% H_2O_2. Nonspecific binding was blocked by incubating the sections for 30 min in 3% normal goat serum. The sections were incubated overnight with rabbit anti-occludin antisera (Zymed) at a dilution of 1:800 at 4°C. The bound anti-occludin was detected by sequential incubation with a biotinylated goat anti-rabbit F(ab')2 (Vector Laboratories) diluted at 1:200 followed by horseradish peroxidase-conjugated streptavidin (Vector Laboratories) at 1:500 dilution. Bound horseradish peroxidase–streptavidin was detected by addition of diaminobenzidine (DAKO).

Transmission Electron Microscopy

A 2- to 3-cm length of distal ileum was harvested, and the lumen was rinsed. The lumen was gently inflated with 2% glutaraldehyde in 0.1 M cacodylate buffer, and both ends were tied off with a suture. Further fixation was carried out at 4°C overnight. The tissues were postfixed in 1% osmium tetroxide in 0.1 M cacodylate buffer for 1 h, dehydrated in

ethanol, and embedded in 812 resin. Onemicrometer-thick survey sections were stained with 0.5% toluidine blue, and ultrathin sections were prepared from selected areas.

Statistical Analyses

All results are expressed as mean ± SEM. Statistical analyses were performed by using MINITAB RELEASE 13.3 software (Minitab, State College, PA). Multiple groups were tested by one-way ANOVA, followed by Fisher's leastsignificant- difference test for unpaired data, followed by the Mann–Whitney *U* test where appropriate. Comparisons of two groups were performed by using a Student *t* test. In cases where

there was unequal variance (Bartlett's test) among groups, data were reevaluated after logarithmic transformation. A *P* value<0.05 was considered to be significant.

6.4 Results

Expression pattern of FXR in intestine. Real-time quantitative PCR was used to measure FXR mRNA concentrations in duodenum, jejunum, ileum, colon, and liver. FXR was expressed in each of these tissues, with highest mRNA levels in ileum (Figure 6-1A). A previous study showed that FXR is expressed in the villus epithelium in late-stage mouse embryos (Forman et al., 1995). Consistent with this finding, *in situ* hybridization analysis with ileum sections revealed that FXR is expressed in the villus epithelium in adult mouse ileum, with highest expression in the intervillus regions (Figure 6-1B). Little or no FXR mRNA was detected in the crypts of Lieberkühn, lamina propria, and tunica muscularis.

Transcriptional profiling in distal small intestine. To gain insight into the function of FXR in the small intestine, transcriptional profiling experiments were done by
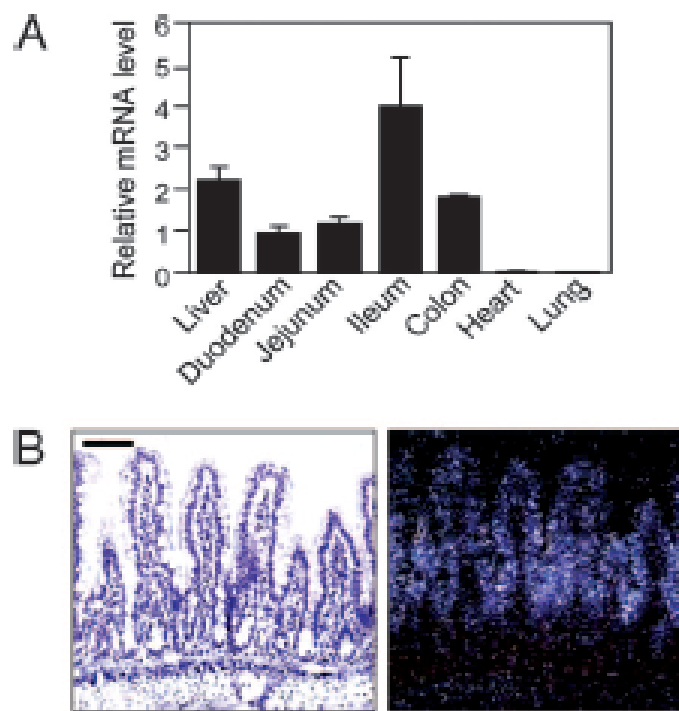
Figure 6-1. FXR is expressed in the intestine.

(A) TotalRNAwas prepared from the indicated tissues of WT mice (n=5), and FXR mRNA concentrations were measured by RTQ-PCR by using cyclophilin as the internal control.Data represent the mean ±SEM and are plotted as fold change relative to mRNA levels in duodenum. **(B)** *In situ* hybridization analysis was performed with an ^{35}S-labeled FXR antisense riboprobe and transverse sections of distal ileum from WT mice. Bright-field (Left) and dark-field (Right) images are shown. (Scale bar: 50 μm)

using mice lacking the gene encoding sterol 27-hydroxylase (CYP27), a key enzyme for

bile acid synthesis. The CYP27-knockout (KO) mice produce only low levels of bile

acids and thus are essentially devoid of endogenous FXR agonists (Rosen et al., 1998).

RNA was prepared from ileal mucosa of CYP27-KO mice administered either the potent,

synthetic FXR agonist GW4064 (Maloney et al., 2000) or vehicle for 14 h. Microarray

analysis yielded a list of 15 genes whose expression was changed ≥2-fold by GW4064

administration (Table 6-2). Among these were the established FXR target genes small

heterodimer partner (Rosen et al.), fibroblast growth factor 15 (*Fgf15*), and ileal bile acid

binding protein (*Ibabp*), which encode proteins involved in bile acid homeostasis

(Goodwin et al., 2000; Grober et al., 1999; Li et al., 2005a; Lu et al., 2000; Makishima et

al., 1999). Interestingly, several of the other genes in Table 6-2 have established roles in

mucosal defense in the intestine. NO, the product of inducible NO synthase (iNOS), has

direct antimicrobial effects and regulates many different aspects of the innate immune

response, including mucus secretion, vascular tone, and epithelial barrier function

(Nathan, 1997; Wallace and Miller, 2000). The proinflammatory cytokine IL18

stimulates resistance to an array of pathogens, including intracellular and extracellular

bacteria and mycobacteria, and appears to have a protective role during the early, acute

phase of mucosal immune response (Biet et al., 2002; Reuter and Pizarro, 2004).

Angiogenin (ANG1) and RNase A family member 4 (RNASE4) are closely related

proteins that arise by differential splicing from a common gene locus (Dyer and

Rosenberg, 2005). Although the function of RNASE4 is not established, ANG1 is part of

the acute phase response to infection and has potent antibacterial and antimycotic actions

(Hooper et al., 2003). Carbonic anhydrase 12 (CAR12) is a member of a family of

Avg Ratio	Unigene Accession #	Gene Title
83	Mm.3904	fibroblast growth factor 15
43	Mm.34209	small heterodimer partner
11	Mm.140210	ubiquitin D
4.0	Mm.2893	inducible nitric oxide synthase
2.8	Mm.175173	RNase A family 4
2.8	Mm.215171	transient receptor potential cation channel
2.6	Mm.12914	ubiquitin specific protease 2
2.3	Mm.202665	angiogenin
2.3	Mm.21397	carbonic anhydrase 12
2.2	Mm.1410	interleukin 18
2.1	Mm.142716	ileal bile acid binding protein
2.0	Mm.116904	solute carrier family 26, member 3
2.0	Mm.33987	dual adaptor for phosphotyrosine
2.0	Mm.29988	peroxisomal trans-2-enoyl-CoA reductase
-3.7	Mm.34289	histocompatibility 2, blastocyst (H2-Q10)

Table 6-2. Genes regulated by FXR agonist GW4064 in ileum.

CYP27-KO mice were treated for 14 hrs with vehicle or GW4064. RNA was prepared from ileum and used in transcriptional profiling studies. Average ratio represents the fold regulation in RNA prepared from GW4064-treated mice relative to vehicle-treated mice.

proteins involved in the maintenance of pH and ion balance (Halmi et al., 2004). The regulation of all of these genes by FXR was confirmed by RT-qPCR by using WT, CYP27-KO, and FXR-KO mice administered either GW4064 or vehicle (Figure 6-2). Notably, FXR had different effects on different genes. For example, activation of FXR had little or no effect on *Ibabp* or *iNos* expression in WT mice, but its elimination caused a marked decrease in the basal expression of these genes (Figure 6-2). In contrast, FXR activation induced *Il18* but did not contribute to its basal expression (Figure 6-2). Based on these data, the possibility that *Il18* induction by FXR is pharmacological rather than physiological cannot be excluded.

Effects on BDL and GW4064 in FXR-KO mice. Decreased bile secretion in rodents by either ligation of the common bile duct or induction of cirrhosis causes changes in the small intestine, including bacterial overgrowth and translocation across the mucosal barrier (Clements et al., 1996; Deitch et al., 1990; Ding et al., 1992; Ding et al., 1993, 1994; Kalambaheti et al., 1994; Lorenzo-Zuniga et al., 2003; Slocum et al., 1992). Oral administration of bile acids inhibits these effects (Ding et al., 1993; Lorenzo-Zuniga et al., 2003). The genes regulated by FXR in ileum suggested that it might contribute to the enteroprotective actions of bile acids. To test this hypothesis, groups of WT and FXR-KO mice (Sinal et al., 2000) were administered either GW4064 or vehicle for 2 days and then subjected to bile duct ligation (BDL) or sham operation. After 5 days, during which GW4064 or vehicle treatment was continued, the mice were killed and their intestines were analyzed for FXR target gene expression and bacterial content.

As expected, BDL caused jaundice manifested by increased total serum bilirubin concentrations in both WT and FXR-KO mice (Figure 6-3A). GW4064 administration
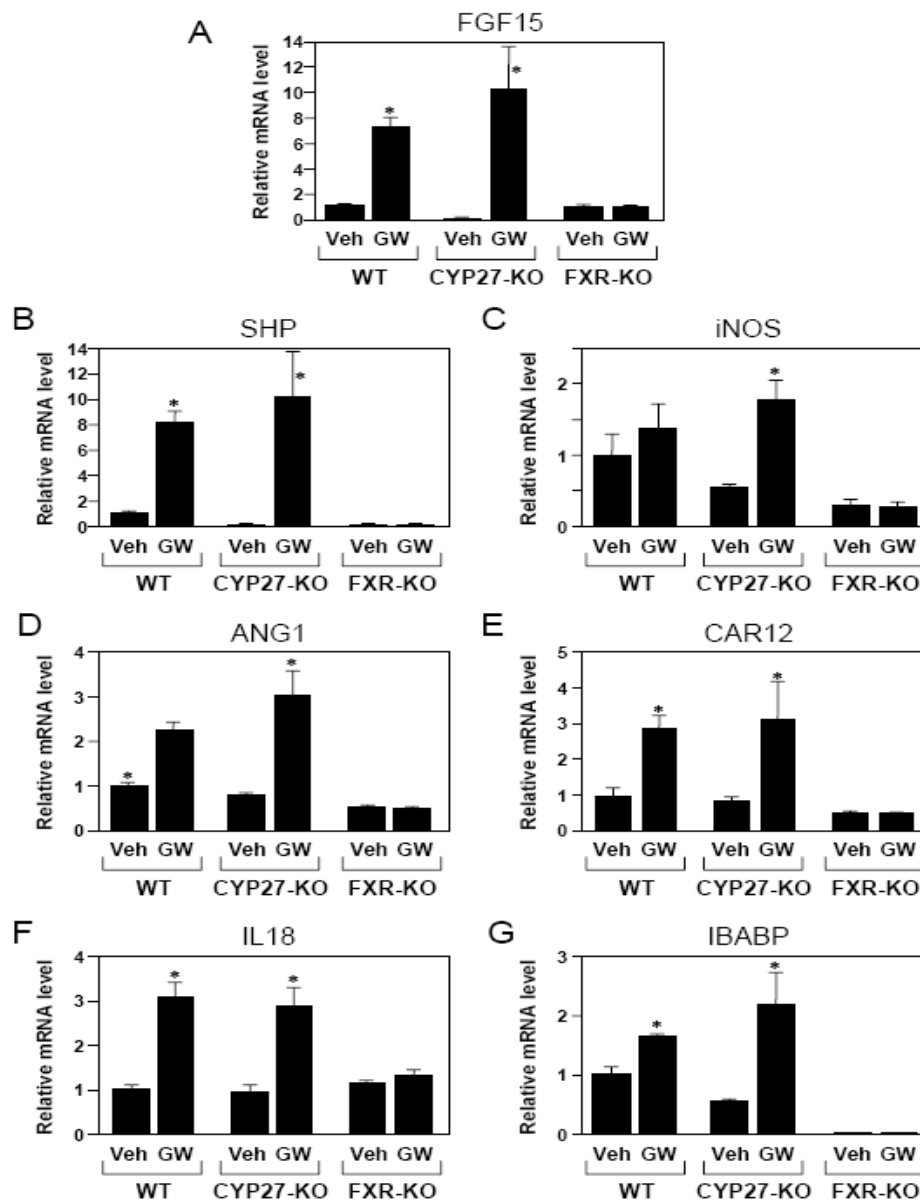
Figure 6-2. Confirmation of genes regulated by FXR in ileum.

Total RNA was prepared from ileum of WT, CYP27-KO, and FXR-KO (n=5) mice treated for 14 h with GW4064 (GW) or vehicle (Veh). Expression of the indicated genes was measured by RTQ-PCR by using cyclophilin as the internal control. Data represent the mean±SEM and are plotted as fold change relative to mRNA levels in WT mice treated with vehicle. *, $P<0.05$ (GW4064 treatment versus vehicle treatment for each strain).

had no effect on total serum bilirubin concentrations in BDL mice. BDL also had marked effects on genes regulated by FXR in ileum. In WT mice, expression of *Fgf15*, *Shp*, *Ang1*, *Car12*, and *Ibabp* was reduced by BDL (Figure 6-3). GW4064 administration increased expression of these genes in BDL mice to levels above those seen in sham operated animals. None of these genes was induced by GW4064 in FXR-KO mice. In contrast, the *iNos* and *Il18* genes showed a more complex expression pattern (Figure 6-3D and G). Although both genes are induced by FXR (Figure 6-2), there was a trend toward increased expression in BDL mice that occurred in an FXR independent fashion (Figure 6-3D and G). Because both *iNos* and *Il18* are induced by proinflammatory stimuli, including lipopolysaccharide and various cytokines (Kleinert et al., 2003; Manigold et al., 2000), this likely reflects regulation of these genes by additional signaling pathways that are activated by BDL.

FXR activation blocks bacterial overgrowth and translocation. The effect of BDL and GW4064 treatment on the bacterial content of ileum and cecum was assessed. As expected, BDL increased the number of aerobic and anaerobic bacteria in the ileum and cecum of WT mice (Figure 6-4A–D). The increase was particularly pronounced for aerobic bacteria (Figure 6-4A and C). Notably, bacterial overgrowth in the lumen of both tissues was completely blocked by administration of GW4064 to BDL mice (Figure 6-4A–D).

To determine whether FXR is required for the antibacterial actions of GW4064, the same set of experiments was performed in FXR-KO mice. Two important differences were seen between WT and FXR-KO mice. First, GW4064 did not decrease aerobic or anaerobic bacteria counts in the ileum or cecum of FXR-KO mice (Figure 6-4A–D). The
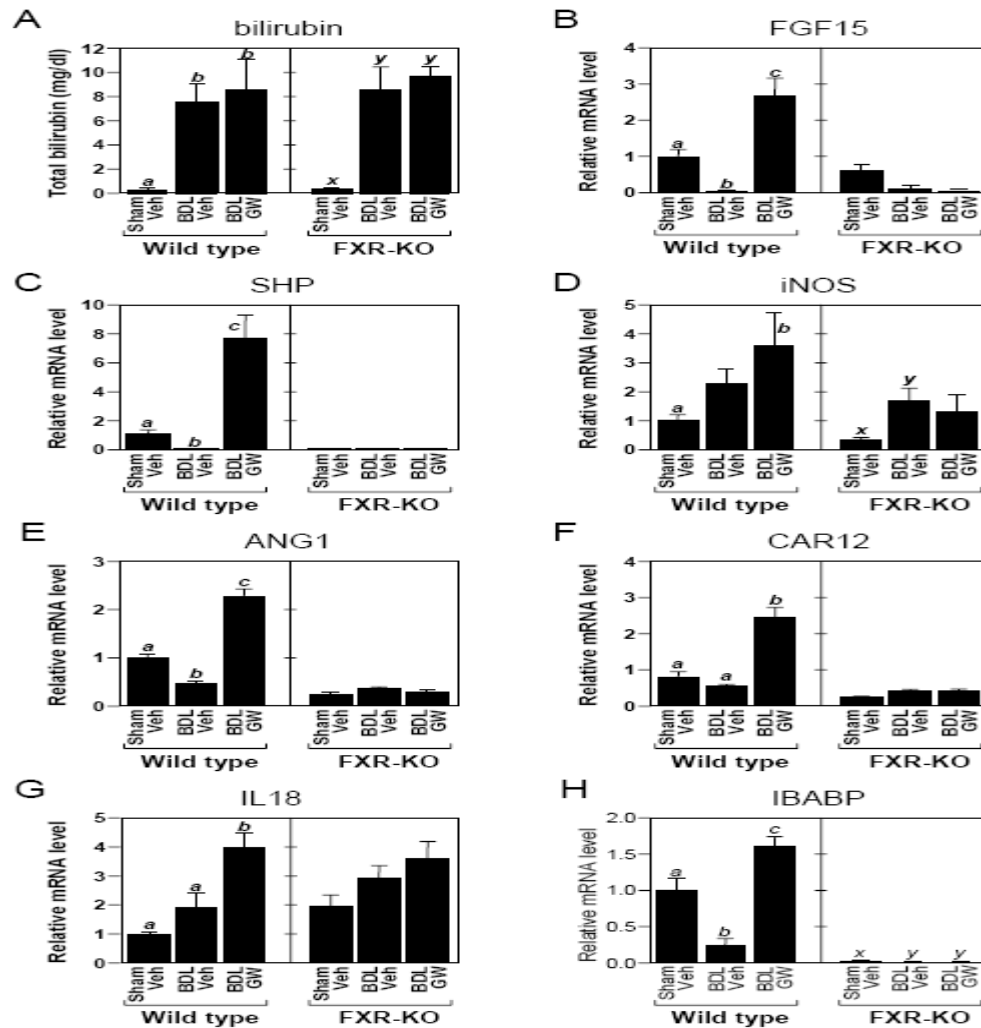
25

Figure 6-3. Effects of BDL and GW4064 on serum bilirubin concentrations and FXR-regulated genes. (A) Total bilirubin was measured in serum from WT and FXR-KO mice (n=5–9) subjected to sham operation and vehicle (Veh) treatment, BDL and vehicle treatment, or BDL and GW4064 (GW) treatment. The presence of different lowercase letters indicates statistical significance (P<0.01) within each strain. **(B–H)** Total RNA was prepared from ileum of WT and FXR-KO mice (n=5–9) subjected to sham operation and vehicle (Veh) treatment, BDL and vehicle treatment, or BDL and GW4064 (GW) treatment. Expression of the indicated genes was measured by RT-qPCR by using cyclophilin as the internal control. Data represent the mean ±SEM and are plotted as fold change relative to mRNA levels in sham-operated mice treated with vehicle. The presence of different lowercase letters indicates statistical significance (P<0.05) within each strain.

reason for the marked variability in the bacterial counts in BDL FXR-KO mice is not known. Nevertheless, these data demonstrate that the antibacterial actions of GW4064 require FXR. Second, sham-operated FXR-KO mice had significantly higher aerobic bacteria counts than sham-operated, WT mice (Figure 6-4A and C). These data support a role for FXR in suppressing bacterial proliferation under normal physiologic conditions. Because FXR-KO mice have reduced hepatic bile salt export pump (ABCB11) expression (Sinal et al., 2000), decreased bile acid concentrations in the intestinal lumen of these animals may contribute to the bacterial overgrowth. In complementary *in vitro* experiments, GW4064 had no bacteriostatic effects in aerobic cultures of ileal contents even at 10 µM concentrations (data not shown), demonstrating that GW4064 itself does not have direct antibacterial activity. As a measure of bacterial translocation across the mucosal barrier, bacteria were also quantified in the mesenteric lymph node complex for each of the treatment groups (Figure 6-4E and F). The pattern for the bacterial counts was similar to that seen for bacterial overgrowth in the ileum and cecum. In WT mice, BDL resulted in an increase in bacterial number in the mesenteric lymph node complex, and GW4064 treatment completely inhibited this effect. The effect was particularly pronounced for aerobic bacteria (Figure 6-4E). FXR-KO mice had ≈10-fold higher levels of aerobic bacteria in mesenteric lymph nodes as compared with WT animals (Figure 6-4E; note differences in scales for WT and FXR-KO mice), and BDL caused a trend toward increased bacterial counts (Figure 6-4E and F). This trend was not reversed by GW4064 administration (Figure 6-4E and F).
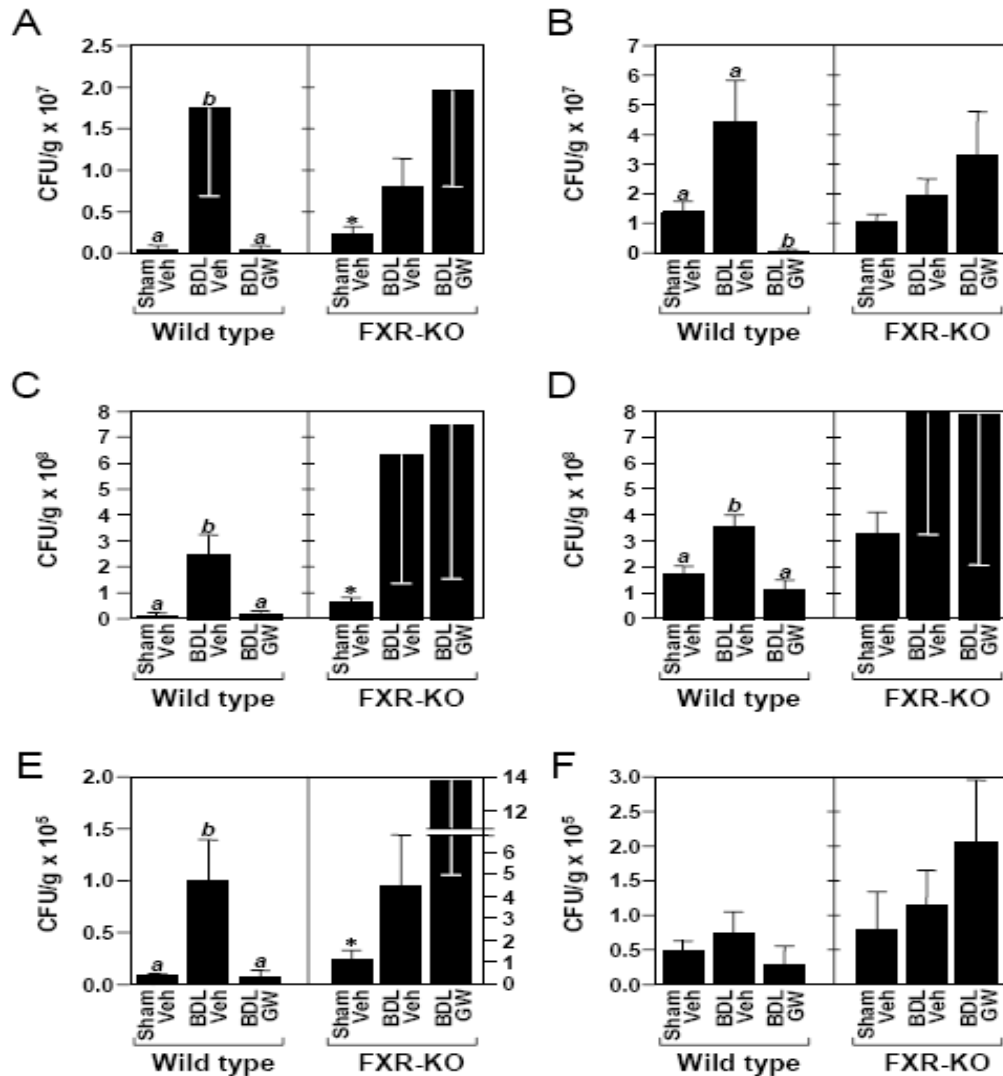
Figure 6-4. FXR activation blocks bacterial overgrowth and translocation.
Aerobic **(A, C, and E)** and anaerobic **(B, D, and F)** bacteria were quantified in
Ileum **(A and B),** cecum **(C and D)**, and mesenteric lymph node complexes **(E
and F)** of WT and FXR-KO mice (n=5–9) subjected to sham operation and
vehicle(Veh) treatment, BDL and vehicle treatment, or BDL and GW4064
(GW) treatment. Data represent the mean ±SEM. The presence of different
lowercase letters indicates statistical significance (P<0.05) within each strain.
Asterisks indicate statistical significance (P<0.05) between sham-operated,
vehicle-treated FXR-KO mice and sham-operated, vehicle-treated WT mice.
CFU, colony-forming units.

FXR activation blocks mucosal injury. The increase in *in vivo* bacterial translocation suggested that BDL causes a disruption of the intestinal barrier function that is inhibited by FXR. To examine barrier integrity, immunostaining was done for occludin, a component of the epithelial tight junctions. In the villus epithelium of WT mice, occludin staining was continuous except where interrupted by the normal presence of mucus-secreting goblet cells (Figure 6-5A). In contrast, many enterocytes in the BDL mice expressed little or no occludin (Figure 6-5A). Consistent with these data, transmission electron microscopy revealed large ruptures in the mucosal surface of BDL WT mice, with bacteria penetrating deep into the epithelium (Figure 6-5C and D). Hematoxylin and eosin staining revealed that the breakdown in barrier function was accompanied by dilated lymphatics and a pronounced interstitial edema, as previously described (Figure 6-5B) (Deitch et al., 1990; Ding et al., 1993; Parks et al., 2000; Slocum et al., 1992). In many villi, the severity of the edema caused separation of the villus epithelium from the underlying lamina propria (Figure 6-5B). Bacteria were seen within edematous areas by electron microscopy (Figure 6-5D). Consistent with the edema resulting from an inflammatory response, there was a marked increase in the number of neutrophils infiltrating the villi of BDL mice (Figure 6-5G). Neutrophils are known to contribute to epithelial permeability in inflammatory diseases of the intestine (Yu et al., 2004).

GW4064 prevented the pathological effects caused by BDL. Ilea from BDL mice administered GW4064 showed a more continuous pattern of occludin immunostaining (Figure 6-5A), little or no edema (Figure 6-5B), and a reduction in the

number of neutrophils to the level seen in sham-operated mice (Figure 6-5G). Virtually no mucosal damage was detected in electron microscopy studies done by using tissue from GW4064-treated mice (data not shown). Thus, activation of FXR prevents deterioration of the epithelial barrier and the accompanying inflammation caused by biliary obstruction. No changes were seen in ileal rates of cell proliferation (assessed by immunostaining with Ki67 antibody) or apoptosis (assessed by TUNEL assays) in the different treatment groups (data not shown). Thus, FXR blocks the changes caused by BDL in WT mice without affecting cell proliferation or programmed cell death.

In marked contrast to the continuous occludin immunostaining seen in sham-operated WT mice, occludin staining was discontinuous and weak in FXR-KO mice, indicating adeterioration in the epithelial barrier even without BDL (Figure 6-5A). Consistent with this result and the higher incidence of bacterial translocation in FXR-KO mice (Figure 6-4E), bacteria and edema were present in the junctions between epithelial cells in FXR-KO animals (Figure 6-5E). Bacteria were also present in the dilated lymphatic vessels (Figure 6-5F). These data demonstrate that the lack of FXR leads to mucosal injury and bacterial translocation even in the absence of additional insult. BDL did not exacerbate the edema (data not shown) or further increase the elevated neutrophil numbers (Figure 6-5G) in the FXR-KO mice. Moreover, GW4064 administration had no effect on any of these parameters in FXR-KO mice (Figure 6-5G and data not shown).
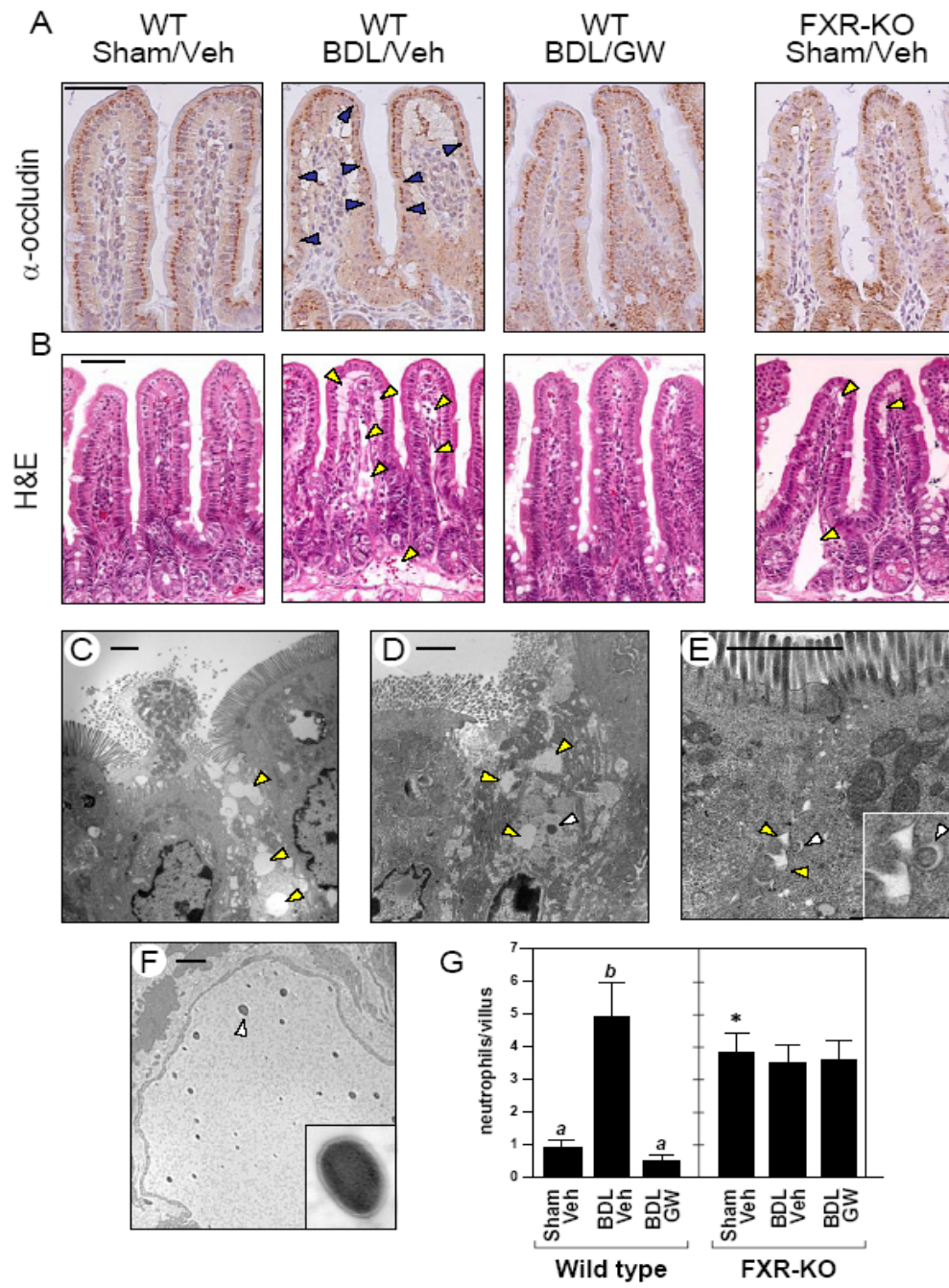
Figure 6-5. FXRactivation blocks mucosal injury.

(AandB) Transverse sections of terminal ileum areshownforWTmice subjected toshamoperationandvehicle treatment (WTShamVeh), BDL and vehicle treatment (WTBDLVeh), or BDL and GW4064 treatment (WTBDLGW) and FXR-KO mice subject to sham operation and vehicle treatment (FXR-KOShamVeh). The sections were immunostained with anti-occludin antisera **(A)** or stained with hematoxylin and eosin (H&E) **(B)**. Occludin immunostaining (dark brown) is detected in the enterocytes of the villus epithelium. Notable examples of diminished occludin immunostaining are indicated by blue arrowheads in the WTBDLVeh section. Occludin immunostaining is drastically reduced in ileum from the FXR-KOShamVeh mice. Edema and dilated lymphatic vessels are indicated by yellow arrowheads in hematoxylin and eosin (H&E)-stained sections. (Scale bars: 50 m.) **(C–F)** Electron microscopy performed with sections of terminal ileum prepared from BDL WT mice **(C and D)** and sham-operated FXR-KO mice **(E and F). C–E** are oriented with the epithelial brush border at the top. Edema is indicated in C–E by yellow arrowheads. Bacteria in the mucosa are indicated in *D* and *E* by white arrowheads. **(E Inset)** A higher magnification of the bacterium andthe surrounding edema. **(F)** Bacteria in the lymphatic vessels of a sham-operated FXR-KO mouse. (*Inset*) A higher magnification view of the bacterium indicated by the white arrowhead. (Scale bars: 2 μm) **(G)** Neutrophils were quantified in transverse sections of terminal ileum prepared from WT and FXR-KO mice subjected to sham operation and vehicle treatment (Veh), BDL and vehicle treatment, or BDL and GW4064 (GW) treatment. Neutrophils were counted in 10 randomly chosen villi from four mice in each treatment group. The presence of different lowercase letters indicates statistical significance (P<0.05) within each strain. The asterisk indicates statistical significance (P<0.01) between sham-operated, vehicle-treated FXR-KO mice and sham-operated, vehicle-treated WT mice.

6.5 Discussion

Biliary obstruction causes bacterial overgrowth and translocation in the small intestine that can be reversed by administration of bile acids (Clements et al., 1996; Deitch et al., 1990; Ding et al., 1992; Ding et al., 1993, 1994; Kalambaheti et al., 1994; Lorenzo-Zuniga et al., 2003; Slocum et al., 1992). It has been proposed that the detergent properties of bile acids are responsible for their enteroprotective actions. Although bile acids were not assessed for direct antibacterial actions in this study, our data suggest a more sophisticated mechanism wherein activation of the bile acid receptor FXR protects against bacterial proliferation and its detrimental effects in the distal small intestine. The products of several genes regulated by FXR in ileum, including *Ang1*, *iNos*, and *Il18*, have established antimicrobial actions. It is not possible to tell from our data whether these genes are regulated by FXR in enterocytes or other cell types, including resident immune cells. The expression profile of *Ang1* as well as *Fgf15*, *Shp*, *Car12*, and *Ibabp* correlate well with FXR-mediated enteroprotection in the BDL model (Figure 6-3), suggesting that the protective actions of FXR are likely to involve multiple downstream genes. Expression of *iNos* and *Il18* is more complex in that their expression is increased by BDL in both WT and FXR-KO mice (Figure 6-3), which likely reflects their regulation by proinflammatory signaling cascades that are activated by BDL. Nevertheless, iNOS and IL18 may contribute to FXR-induced enteroprotection under physiologic or other pathophysiologic conditions. Notably, elevated concentrations of iNOS and IL18 are associated with mucosal damage and inflammatory bowel disease (Alican and Kubes, 1996; Reuter and Pizarro, 2004). Regulation of these genes by bile acids, which are released from the gallbladder into the small intestine during feeding,

may ensure an adequate level of enteroprotection during periods of increased microbial exposure while preventing the overproduction of proteins that can cause inflammation and intestinal disease.

In summary, our results demonstrate that FXR plays a crucial role in protecting the distal small intestine against bacterial overgrowth and the resulting disruption of the epithelial barrier. These findings raise the intriguing possibility that potent, synthetic FXR agonists may have therapeutic utility in patients with obstructed or reduced bile flow, including those on total parenteral nutrition, who are susceptible to bacterial overgrowth and translocation (Garcia-Tsao, 2004; Holman et al., 1979).

6.6 References

Alican, I., and Kubes, P. (1996). A critical role for nitric oxide in intestinal barrier function and dysfunction. Am J Physiol *270*, G225-237.

Berg, R.D. (1995). Bacterial translocation from the gastrointestinal tract. Trends Microbiol *3*, 149-154.

Biet, F., Locht, C., and Kremer, L. (2002). Immunoregulatory functions of interleukin 18 and its role in defense against bacterial pathogens. J Mol Med *80*, 147-162.

Cahill, C.J. (1983). Prevention of postoperative renal failure in patients with obstructive jaundice--the role of bile salts. Br J Surg *70*, 590-595.

Cahill, C.J., Pain, J.A., and Bailey, M.E. (1987). Bile salts, endotoxin and renal function in obstructive jaundice. Surg Gynecol Obstet *165*, 519-522.

Clements, W.D., Parks, R., Erwin, P., Halliday, M.I., Barr, J., and Rowlands, B.J. (1996). Role of the gut in the pathophysiology of extrahepatic biliary obstruction. Gut *39*, 587-593.

Deitch, E.A., Sittig, K., Li, M., Berg, R., and Specian, R.D. (1990). Obstructive jaundice promotes bacterial translocation from the gut. Am J Surg *159*, 79-84.

Ding, J.W., Andersson, R., Norgren, L., Stenram, U., and Bengmark, S. (1992). The influence of biliary obstruction and sepsis on reticuloendothelial function in rats. Eur J Surg *158*, 157-164.

Ding, J.W., Andersson, R., Soltesz, V., Willen, R., and Bengmark, S. (1993). The role of bile and bile acids in bacterial translocation in obstructive jaundice in rats. Eur Surg Res *25*, 11-19.

Ding, J.W., Andersson, R., Soltesz, V., Willen, R., and Bengmark, S. (1994). Obstructive jaundice impairs reticuloendothelial function and promotes bacterial translocation in the rat. J Surg Res *57*, 238-245.

Dyer, K.D., and Rosenberg, H.F. (2005). The mouse RNase 4 and RNase 5/ang 1 locus utilizes dual promoters for tissue-specific expression. Nucleic Acids Res *33*, 1077-1086.

Edwards, P.A., Kast, H.R., and Anisfeld, A.M. (2002). BAREing it all: the adoption of LXR and FXR and their roles in lipid homeostasis. J Lipid Res *43*, 2-12.

Evans, H.J., Torrealba, V., Hudd, C., and Knight, M. (1982). The effect of preoperative bile salt administration on postoperative renal function in patients with obstructive jaundice. Br J Surg *69*, 706-708.

Forman, B.M., Goode, E., Chen, J., Oro, A.E., Bradley, D.J., Perlmann, T., Noonan, D.J., Burka, L.T., McMorris, T., Lamph, W.W., *et al.* (1995). Identification of a nuclear receptor that is activated by farnesol metabolites. Cell *81*, 687-693.

Garcia-Tsao, G. (2004). Bacterial infections in cirrhosis. Can J Gastroenterol *18*, 405-406.

Goodwin, B., Jones, S.A., Price, R.R., Watson, M.A., McKee, D.D., Moore, L.B., Galardi, C., Wilson, J.G., Lewis, M.C., Roth, M.E., *et al.* (2000). A regulatory cascade of the nuclear receptors FXR, SHP-1, and LRH-1 represses bile acid biosynthesis. Mol Cell *6*, 517-526.

Grober, J., Zaghini, I., Fujii, H., Jones, S.A., Kliewer, S.A., Willson, T.M., Ono, T., and Besnard, P. (1999). Identification of a bile acid-responsive element in the human ileal bile acid-binding protein gene. Involvement of the farnesoid X receptor/9-cis-retinoic acid receptor heterodimer. J Biol Chem *274*, 29749-29754.

Halmi, P., Lehtonen, J., Waheed, A., Sly, W.S., and Parkkila, S. (2004). Expression of hypoxia-inducible, membrane-bound carbonic anhydrase isozyme XII in mouse tissues. Anat Rec A Discov Mol Cell Evol Biol *277*, 171-177.

Holman, J.M., Jr., Rikkers, L.F., and Moody, F.G. (1979). Sepsis in the management of complicated biliary disorders. Am J Surg *138*, 809-813.

Hooper, L.V., Stappenbeck, T.S., Hong, C.V., and Gordon, J.I. (2003). Angiogenins: a new class of microbicidal proteins involved in innate immunity. Nat Immunol *4*, 269-273.

Inagaki, T., Choi, M., Moschetta, A., Peng, L., Cummins, C.L., McDonald, J.G., Luo, G., Jones, S.A., Goodwin, B., Richardson, J.A.*, et al.* (2005). Fibroblast growth factor 15 functions as an enterohepatic signal to regulate bile acid homeostasis. Cell Metab *2*, 217-225.

Kalambaheti, T., Cooper, G.N., and Jackson, G.D. (1994). Role of bile in non-specific defence mechanisms of the gut. Gut *35*, 1047-1052.

Kleinert, H., Schwarz, P.M., and Forstermann, U. (2003). Regulation of the expression of inducible nitric oxide synthase. Biol Chem *384*, 1343-1364.

Li, J., Pircher, P.C., Schulman, I.G., and Westin, S.K. (2005). Regulation of complement C3 expression by the bile acid receptor FXR. J Biol Chem *280*, 7427-7434.

Lorenzo-Zuniga, V., Bartoli, R., Planas, R., Hofmann, A.F., Vinado, B., Hagey, L.R., Hernandez, J.M., Mane, J., Alvarez, M.A., Ausina, V.*, et al.* (2003). Oral bile acids reduce bacterial overgrowth, bacterial translocation, and endotoxemia in cirrhotic rats. Hepatology *37*, 551-557.

Lu, T.T., Makishima, M., Repa, J.J., Schoonjans, K., Kerr, T.A., Auwerx, J., and Mangelsdorf, D.J. (2000). Molecular basis for feedback regulation of bile acid synthesis by nuclear receptors. Mol Cell *6*, 507-515.

Makishima, M., Okamoto, A.Y., Repa, J.J., Tu, H., Learned, R.M., Luk, A., Hull, M.V., Lustig, K.D., Mangelsdorf, D.J., and Shan, B. (1999). Identification of a nuclear receptor for bile acids. Science *284*, 1362-1365.

Maloney, P.R., Parks, D.J., Haffner, C.D., Fivush, A.M., Chandra, G., Plunket, K.D., Creech, K.L., Moore, L.B., Wilson, J.G., Lewis, M.C.*, et al.* (2000). Identification of a chemical tool for the orphan nuclear receptor FXR. J Med Chem *43*, 2971-2974.

Manigold, T., Bocker, U., Traber, P., Dong-Si, T., Kurimoto, M., Hanck, C., Singer, M.V., and Rossol, S. (2000). Lipopolysaccharide/endotoxin induces IL-18 via CD14 in human peripheral blood mononuclear cells in vitro. Cytokine *12*, 1788-1792.

Nathan, C. (1997). Inducible nitric oxide synthase: what difference does it make? J Clin Invest *100*, 2417-2423.

Parks, R.W., Stuart Cameron, C.H., Gannon, C.D., Pope, C., Diamond, T., and Rowlands, B.J. (2000). Changes in gastrointestinal morphology associated with obstructive jaundice. J Pathol *192*, 526-532.

Reuter, B.K., and Pizarro, T.T. (2004). Commentary: the role of the IL-18 system and other members of the IL-1R/TLR superfamily in innate mucosal immunity and the pathogenesis of inflammatory bowel disease: friend or foe? Eur J Immunol *34*, 2347-2355.

Rosen, H., Reshef, A., Maeda, N., Lippoldt, A., Shpizen, S., Triger, L., Eggertsen, G., Bjorkhem, I., and Leitersdorf, E. (1998). Markedly reduced bile acid synthesis but maintained levels of cholesterol and vitamin D metabolites in mice with disrupted sterol 27-hydroxylase gene. J Biol Chem *273*, 14805-14812.

Russell, D.W. (2003). The enzymes, regulation, and genetics of bile acid synthesis. Annu Rev Biochem *72*, 137-174.

Sinal, C.J., Tohkin, M., Miyata, M., Ward, J.M., Lambert, G., and Gonzalez, F.J. (2000). Targeted disruption of the nuclear receptor FXR/BAR impairs bile acid and lipid homeostasis. Cell *102*, 731-744.

Slocum, M.M., Sittig, K.M., Specian, R.D., and Deitch, E.A. (1992). Absence of intestinal bile promotes bacterial translocation. Am Surg *58*, 305-310.

Wallace, J.L., and Miller, M.J. (2000). Nitric oxide in mucosal defense: a little goes a long way. Gastroenterology *119*, 512-520.

Yu, Y., Sitaraman, S., and Gewirtz, A.T. (2004). Intestinal epithelial cell regulation of mucosal inflammation. Immunol Res *29*, 55-68.

CHAPTER 7

CONCLUSIONS AND FUTURE PERSPECTIVES

The field of bile acid biology has been an area of intense research due to its importance in metabolism including cholesterol homeostasis. As a consequence, many genetic and pharmacological tools have been developed to manipulate bile acid biosynthesis and circulation. A molecular mechanism for the negative feedback regulation of bile acid biosynthesis was proposed based on *in vitro* studies using cultured cells (Goodwin et al., 2000; Lu et al., 2000). In this model, activation of FXR by bile acids induces hepatic expression of SHP, which interacts with LRH-1 bound to the CYP7A1 promoter to suppress gene transcription. While the importance of FXR and SHP in this feedback loop has been demonstrated using knockout mice, the LRH-1 part of this model had not been tested in an *in vivo*, complete loss-of-function model because *Lrh-1*$^{-/-}$ mice die during early embryogenesis (Pare et al., 2004). Using gene targeting in a tissue-specific manner, we tested the importance of LRH-1 in the FXR-SHP-LRH-1 signaling cascade *in vivo*. Much to our surprise, basal CYP7A1 expression and its repression by FXR were not altered in either *Lrh-1*$^{flox/flox}$*;Alb-Cre* or *Lrh-1*$^{flox/flox}$*;Vil-Cre* mice. We conclude that LRH-1 is not essential for CYP7A1 regulation. As suggested in Chapter 3, one might speculate that there are compensatory factors which maintain CYP7A1 regulation in the absence of LRH-1. HNF4α is a plausible candidate because it regulates CYP7A1 expression through the same binding site on the CYP7A1 promoter as LRH-1, and it is repressed by SHP *in vitro* (Lee et al., 2000). In this respect, it will be

154

informative to test whether HNF4α is required for FXR-mediated repression of CYP7A1 by administering GW4064 to HNF4α-deficient mice. Creation of double knockout mice for HNF4α and LRH-1 in liver will also be useful for determining the contributions of these factors to the repression of CYP7A1. A limitation of our study is that all of the analyses, including the gene profiling studies, were performed at a single time point. Interestingly, the effects of HNF4 deficiency on CYP7A1 mRNA and protein levels varied in a circadian manner. Thus, RT-qPCR should be performed to elucidate the temporal effects of LRH-1 deficiency on CYP7A1 expression. It has been proposed that LRH-1 acts as a competency factor for LXR on the CYP7A1 promoter (Lu et al., 2000; Shang et al., 2006). LRH-1 was also shown to be required for maximal LXR responsiveness to endogenous FAS or CETP (Luo et al., 2001; Matsukuma et al., 2007). Therefore, it will also be worthwhile to investigate the effect of LRH-1 deficiency under different dietary conditions such as high cholesterol, fat, or carbohydrate to test how this affects bile acids biology. It has also been reported that there are species-specific differences in LRH-1 activity. For example, the three-dimensional structures of mouse and human LRH-1 LBDs purified from bacteria demonstrated that the human LRH-1 was bound to ligands while the mouse LRH-1 was not (Ortlund et al., 2005; Sablin et al., 2003). Additional studies are required to determine whether LRH-1 is indeed involved in the feedback control mechanisms in other species, including humans.

In Chapter 4, we demonstrated that a constitutively active form of LRH-1 induces proliferation and reduces apoptosis in intestine by regulating genes involved in these processes. However, mice lacking LRH-1 show normal intestinal morphology. There are many issues to be addressed regarding this apparent discrepancy. First, it needs

to be determined whether the genes identified by microarray analysis in the villin-VP16LRH-1 mice are regulated by LRH-1 directly or indirectly. *In vivo* analysis of these genes in *Lrh-1$^{flox/flox}$;Vil-Cre* mice showed only a partial overlap in the gain-of-function and loss-of-function models. The lack of dysregulation of these genes in the *Lrh-1$^{flox/flox}$;Vil-Cre* mice might explain the lack of morphological changes in intestine. Many important signaling pathways contribute to intestine development and homeostasis and have been linked to diseases such as cancer. It is possible that these other signaling pathways compensate for LRH-1 function in its absence. One possible candidate is the signaling molecule Wnt, which controls intestinal stem cell renewal and contributes to tumorigenesis when perturbed. It has been reported that β-catenin, which is a downstream effector of Wnt, directly interacts with LRH-1 and stimulates its transcriptional activity (Botrugno et al., 2004). In this regard, we did not see changes in cyclin D1 and cyclin E1 mRNA levels in either the VP16LRH-1-transgenic mice or the *Lrh-1$^{flox/flox}$;Vil-Cre* mice, suggesting that the Wnt pathway may not be regulated by LRH-1. However, we did observe a potential connection between LRH-1 and the mTOR and Akt signaling pathways in our gain-of-function studies. For example, downstream effectors of mTOR, rpS6 and eIF4E are significantly elevated by overexpression of LRH-1. Studies into the possible relationship between LRH-1 and these pathways in intestine may provide a better understanding of how LRH-1 impacts intestinal physiology.

In Chapter 5, we presented data supporting a conserved role for LRH-1 in endoderm development in frog and mouse. Several important LRH-1 target genes involved in embryogenesis and endoderm development have been identified including OCT4, SOX2, HNF1α, HNF3β, and HNF4α. However, the precise role of LRH-1 in

endoderm formation has not been well defined. The availability of the floxed LRH-1 allele will permit endoderm-specific deletion of LRH-1. For example, the *Lrh-1*^{flox/flox} mice can be crossed with mice expressing cre under the control of the FOXA3, endoderm-specific enhancer (Lee et al., 2005). The availability of these mice will also provide an important tool for the identification of genes and pathways that are regulated by LRH-1 during the early stages of endoderm differentiation.

In Chapter 6 we showed that FXR protects against bacterial overgrowth in the small intestine. While FXR regulates genes that are involved in enteroprotection including angiogenin, carbonic anhydrase 12, interleukin 18, and inducible nitric oxide synthase, it is still not clear whether FXR-mediated activation of these particular genes conveys the beneficial effects of bile acid on small intestine. Additional studies are required to understand the molecular pathways that are regulated by FXR in small intestine.

References

Botrugno, O.A., Fayard, E., Annicotte, J.S., Haby, C., Brennan, T., Wendling, O., Tanaka, T., Kodama, T., Thomas, W., Auwerx, J.*, et al.* (2004). Synergy between LRH-1 and beta-catenin induces G1 cyclin-mediated cell proliferation. Mol Cell *15*, 499-509.

Goodwin, B., Jones, S.A., Price, R.R., Watson, M.A., McKee, D.D., Moore, L.B., Galardi, C., Wilson, J.G., Lewis, M.C., Roth, M.E.*, et al.* (2000). A regulatory cascade of the nuclear receptors FXR, SHP-1, and LRH-1 represses bile acid biosynthesis. Mol Cell *6*, 517-526.

Lee, C.S., Sund, N.J., Behr, R., Herrera, P.L., and Kaestner, K.H. (2005). Foxa2 is required for the differentiation of pancreatic alpha-cells. Dev Biol *278*, 484-495.

Lee, Y.K., Dell, H., Dowhan, D.H., Hadzopoulou-Cladaras, M., and Moore, D.D. (2000). The orphan nuclear receptor SHP inhibits hepatocyte nuclear factor 4 and retinoid X receptor transactivation: two mechanisms for repression. Mol Cell Biol *20*, 187-195.

Lu, T.T., Makishima, M., Repa, J.J., Schoonjans, K., Kerr, T.A., Auwerx, J., and Mangelsdorf, D.J. (2000). Molecular basis for feedback regulation of bile acid synthesis by nuclear receptors. Mol Cell *6*, 507-515.

Luo, Y., Liang, C.P., and Tall, A.R. (2001). The orphan nuclear receptor LRH-1 potentiates the sterol-mediated induction of the human CETP gene by liver X receptor. J Biol Chem *276*, 24767-24773.

Matsukuma, K.E., Wang, L., Bennett, M.K., and Osborne, T.F. (2007). A key role for orphan nuclear receptor liver receptor homologue-1 in activation of fatty acid synthase promoter by liver X receptor. J Biol Chem *282*, 20164-20171.

Ortlund, E.A., Lee, Y., Solomon, I.H., Hager, J.M., Safi, R., Choi, Y., Guan, Z., Tripathy, A., Raetz, C.R., McDonnell, D.P.*, et al.* (2005). Modulation of human nuclear receptor LRH-1 activity by phospholipids and SHP. Nat Struct Mol Biol *12*, 357-363.

Pare, J.F., Malenfant, D., Courtemanche, C., Jacob-Wagner, M., Roy, S., Allard, D., and Belanger, L. (2004). The fetoprotein transcription factor (FTF) gene is essential to embryogenesis and cholesterol homeostasis and is regulated by a DR4 element. J Biol Chem *279*, 21206-21216.

Sablin, E.P., Krylova, I.N., Fletterick, R.J., and Ingraham, H.A. (2003). Structural basis for ligand-independent activation of the orphan nuclear receptor LRH-1. Mol Cell *11*, 1575-1585.

Shang, Q., Pan, L., Saumoy, M., Chiang, J.Y., Tint, G.S., Salen, G., and Xu, G. (2006). The stimulatory effect of LXRalpha is blocked by SHP despite the presence of a LXRalpha binding site in the rabbit CYP7A1 promoter. J Lipid Res *47*, 997-1004.

VITAE

Youn-Kyoung Lee was born in Seoul, Republic of Korea, on July 14, 1975, the daughter of Youn-Rak Lee and Bu-Ja Seo. After graduating from Hae-Won Girls High School, in Seoul, Korea in 1994, she entered Kon-Kuk University in Seoul, Korea. She received the degree of Bachelor of Science in Agricultural Chemistry in February, 1998, with academic excellence honors from Kon-Kuk University. In August of 2000 she entered the Biology department of the University of Nebraska at Omaha. After completing thesis work in the laboratory of Dr. Bruce A. Chase, she received the degree of Master of Art on May 2002. She entered the Graduate School of Biomedical Sciences at the University of Texas Southwestern Medical Center at Dallas on June 27, 2002 and began work in the laboratory of Dr. Steven A. Kliewer on June 2, 2003.

Permanent Address: 70-53 Myunmok-Dong
                   Jungrang-Gu, Seoul
                   Republic of Korea